Proceedings of the Mini-Workshop

# Exciting Hadrons

Bled, Slovenia, July 11–18, 2005

Edited by

**Bojan Golli**

**Mitja Rosina**

**Simon Širca**

*University of Ljubljana and Jožef Stefan Institute*

## The Mini-Workshop *Exciting Hadrons*

**List of participants**

*Ilija Bizjak, Ljubljana*, `ilija.bizjak@ijs.si`
*Veljko Dmitrašinović, Beograd*, `dmitrasin@yahoo.com`
*Harald Fritzsch, München*, `fritzsch@mppmu.mpg.de`
*Bojan Golli, Ljubljana*, `bojan.golli@ijs.si`
*Damijan Janc, Ljubljana*, `damijan.janc@telargo.com`
*Vladimir Kukulin, Moscow*, `kukulin@nucl-th.sinp.msu.ru`
*Norma Mankoč Borštnik, Ljubljana*, `Norma.Mankoc@ijs.si`
*Peter Minkowski, Bern*, `mink@itp.unibe.ch`
*Willibald Plessas, Graz*, `plessas@bkfug.kfunigraz.ac.at`
*Milan Potokar, Ljubljana*, `Milan.Potokar@ijs.si`
*Saša Prelovšek, Ljubljana*, `Sasa.Prelovsek@ijs.si`
*Ica Stancu, Liege*, `fstancu@ulg.ac.be`
*Mitja Rosina, Ljubljana*, `mitja.rosina@ijs.si`
*Simon Širca, Ljubljana*, `simon.sirca@fmf.uni-lj.si`
*Robert Wagenbrunn, Graz*, `robert.wagenbrunn@uni-graz.at`
*Herbert Weigel, Siegen*, `weigel@physik.uni-siegen.de`

# Contents

# Preface

The eight years of Bled Workshops in Physics have endowed them with a tradition and created their special flavour and colour. They have evolved into an interplay between a slow and steady progress in some topics and a lively display of puzzles and surprises in others.

The title of this Summer's Mini-Workshop, *Exciting Hadrons,* implies both, how experimentalist excited hadrons to new states, as well as how these excited and exciting hadrons excite theorists.

It was a pleasure to jointly propose solutions to puzzles as well as to technical difficulties in computation and experiment, with ample time for discussions and confrontations. Future will show which of our conclusions and suggestions were correct but we believe they were at least fruitful.

Multiquarks are still a controversial topic, or even more so. The third-millennium states $D_{s,J}$, two X, and Y which are reasonably well established call for an explanation of their puzzles: narrow widths and/or high production rates and/or branching ratios. The SELEX ccq baryons need reconfirmation and the pentaquark (non)sightings need an explanation before we can extrapolate to new multiquarks and guide experimentalists.

On the other hand, the *"light and low-energy"* hadronic physics continues at a slow pace of steady progress from qualitative to quantitative. Relativity brought the electromagnetic and weak form factors and some hadronic widths nearer to experiment, but not yet all; further understanding is needed. Electroexcitation of baryons remains a very promising tool to explore complicated states such as the Roper.

Ljubljana, November 2005

M. Rosina
B. Golli
S. Širca

**Workshops organized at Bled**

▷ *What Comes beyond the Standard Model* (June 29–July 9, 1998)
    Bled Workshops in Physics **0** (1999) No. 1
▷ *Hadrons as Solitons* (July 6–17, 1999)
▷ *What Comes beyond the Standard Model* (July 22–31, 1999)
▷ *Few-Quark Problems* (July 8–15, 2000)
    Bled Workshops in Physics **1** (2000) No. 1
▷ *What Comes beyond the Standard Model* (July 17–31, 2000)
▷ *Statistical Mechanics of Complex Systems* (August 27–September 2, 2000)
▷ *Selected Few-Body Problems in Hadronic and Atomic Physics* (July 7–14, 2001)
    Bled Workshops in Physics **2** (2001) No. 1
▷ *What Comes beyond the Standard Model* (July 17–27, 2001)
    Bled Workshops in Physics **2** (2001) No. 2
▷ *Studies of Elementary Steps of Radical Reactions in Atmospheric Chemistry*
▷ *Quarks and Hadrons* (July 6–13, 2002)
    Bled Workshops in Physics **3** (2002) No. 3
▷ *What Comes beyond the Standard Model* (July 15–25, 2002)
    Bled Workshops in Physics **3** (2002) No. 4
▷ *Effective Quark-Quark Interaction* (July 7–14, 2003)
    Bled Workshops in Physics **4** (2003) No. 1
▷ *What Comes beyond the Standard Model* (July 17–27, 2003)
    Bled Workshops in Physics **4** (2003) No. 2-3
▷ *Quark Dynamics* (July 12–19, 2004)
    Bled Workshops in Physics **5** (2004) No. 1
▷ *What Comes beyond the Standard Model* (July 19–29, 2004)
▷ *Exciting Hadrons* (July 11–18, 2005)
    Bled Workshops in Physics **6** (2005) No. 1
▷ *What Comes beyond the Standard Model* (July 18–28, 2005)


**Also published in this series**

▷ Book of Abstracts, *XVIII European Conference on Few-Body Problems in Physics*,
    Bled, Slovenia, September 8–14, 2002, Edited by Rajmund Krivec, Bojan Golli,
    Mitja Rosina, and Simon Širca
        Bled Workshops in Physics **3** (2002) No. 1–2

# The role of instantons in conventional light hadrons and multiquarks

V. Dmitrašinović

Vinča Institute (Lab 010), P.O.Box 522, 11001 Belgrade, Serbia

**Abstract.** I shall outline a unified approach to few-quark (including two, three, four and five quarks) states in a nonrelativistic constituent quark model. Particular attention will be paid to conventional mesons and baryons, which are basic decay products of multiquarks, such as tetra- and pentaquarks. We shall show that most of light mesons and baryons are readily reproduced with the flavour-dependent instanton-induced effective quark interaction. Exceptions to this rule will be discussed, time permitting.

The contents of this talk follow to a large degree the following papers: (1) the role of instanton-induced effective quark interaction in nonrelativistic light-flavoured mesons and baryons follows Ref. [1]; (2) instanton-induced interaction in charmed tetraquarks follows Ref. [2]; (3) instanton-induced interaction in light-flavoured pentaquarks follows Ref. [3].

## References

1. V. Dmitrašinović and H. Toki,"Light hadron spectra in the constituent quark model with the Kobayashi-Kondo-Maskawa-'t Hooft effective $U_A(1)$ symmetry breaking interaction", to appear in Ann. Phys. (N.Y.) (2005).
2. V. Dmitrašinović, Phys. Rev. **D 70**, 096011 (2004); Phys. Rev. Lett. **94**, 162002 (2005).
3. V. Dmitrašinović, Phys. Rev. **D 71**, 094003 (2005).

# The Spin Structure of the Constituent Quarks

Harald Fritzsch

Arnold Sommerfeld Center, University of Munich, Theresienstraße 37, D-8033 München

**Abstract.** We define a constituent quark within QCD. It is shown that the spin of such a quark and hence also the spin of the nucleon is reduced due to $\bar{q}q$–pairs, in agreement with experiment. A solution to the spin problem is given.

Experiments have revealed that the internal structure of the nucleon is more complicated than originally assumed[1]. In particular, the portion of the nucleon spin carried by the spins of the u- and d-quarks is not, as naively expected, about 75%, but much smaller[2]. This effect was discussed in connection with the effects of gluons, which can make a negative contribution to the net quark spins[3–5].

In this paper we study the situation by considering the internal spin structure of the constituent quarks. Often it is assumed that the nucleon consists of three constituent quarks, each of them having their own internal structure. However, in QCD the notion of a constituent quark has remained vague. Using a specific "gedankenexperiment" we first show how a constituent quark can be defined with all its dynamical properties. Then we apply our results to the nucleon. In order to simplify the task, we shall first neglect the s-quarks. Later we comment on what changes once s-quarks are introduced.

We relate the spin structure to the QCD anomaly[6]. A very specific picture emerges, giving an elegant solution of the spin problem.

For a proton being a system of three constituent quarks, i. e. (uud), it is difficult to disentangle the contributions of the three constituent quarks. Therefore we consider a heavy baryon of spin 3/2, e. g. one with a quark structure (bbu). The ground state of such a system is an isospin doublet, which we denote as U and D:

$$U \Uparrow = (b \Uparrow b \Uparrow u \Uparrow) \tag{1}$$
$$D \Uparrow = (b \Uparrow b \Uparrow d \Uparrow).$$

One expects that these states of spin 3/2 exist in reality, but will probably never be observed and studied in detail. We proceed to study the internal structure of these states, in particular the aspects related to the light quarks. Note that a state like (bbu) consists of a single light constituent quark.

The states U and D behave much like the proton–neutron system, if we turn off the weak interaction of the b–quarks. For example, the state D, being slightly heavier than U, would show a β-decay: $D \to U + e^- + \bar{\nu}_e$. This can be used to

define the associated vector and axialvector coupling constants, e. g. the matrix elements $< U|\bar{u}\gamma_\mu d|D >$ and $< U|\bar{u}\gamma_\mu\gamma_5 d|D >$.

The isospin doublet $U-D$ would exhibit a strong interaction with pions, e. g. there would be charge exchange reactions like $\pi^- U \to \pi^\circ D$. Relations analogous to the Goldberger–Treimann relations or the Adler–Weissberger relations would be valid.

Furthermore the $U$– or $D$–state can be used in a "gedankenexperiment" as target for lepton scattering experiments. This way the distribution functions of the light quarks $u$, $d$ can be studied. The heavy quark $b$ would constitute essentially a fixed portion of the momentum of the $U$– or $D$–state. The associated distribution function would essentially be a $\delta$–function in $x$–space. Thus the heavy quark contribution to the total momentum can be disregarded. What is left over, is the momentum distribution function of the constituent light quark, which we would like to investigate.

The light quark distribution functions are then given in terms of a scaling parameter $x$, defined to be the momentum of the quarks, divided by the total momentum of the constituent quark. Thus the variable $x$ varies as usual between zero and one.

The states $U$ and $D$ can be polarized. The simple $SU(6)$ type wave function is given by:

$$U \Uparrow = \frac{1}{\sqrt{3}} \left[ (b \Uparrow b \Uparrow u \Uparrow) + (b \Uparrow u \Uparrow b \Uparrow) + (u \Uparrow b \Uparrow b \Uparrow) \right]$$

In QCD the light quark distribution functions are given by the matrix elements of the bilocal densities $\bar{q}(x)\gamma_\mu q(y)$ or $\bar{q}(x)\gamma_\mu\gamma_5 q(y)$ at lightlike distances. Taking these matrix elements, one arrives at the distribution functions $u_+(x)$, $u_-(x)$, $d_+(x)$ and $d_-(x)$ of the $U$–state. The indices $+$ or $-$ denote the helicity $+$ or $-$ of the corresponding quark in a polarized $U$–state with positive helicity.

Let us first denote the sum rules following from the exact flavor conservation laws. The matrix element $< U|u^+u|U >$ is, of course, given by one, the matrix element $< U|d^+d|U >$ vanishes. Thus we have

$$\int_0^1 (u_+ + u_- - \bar{u}_+ - \bar{u}_-)\, dx = 1 \tag{2}$$

$$\int_0^1 \left(d_+ + d_- - \bar{d}_+ - \bar{d}_-\right) dx = 0$$

These rules above are the analog of the Adler sum rule in the case of nucleons. We proceed to discuss the analog of the Bjorken sum rule denoting the axial coupling constant of the $U - D$–system by $g_a$:

$$\int_0^1 \left\{ [(u_+ + \bar{u}_+) - (u_- + \bar{u}_-)] - \left[(d_+ + \bar{d}_+) - (d_- + \bar{d}_-)\right] \right\} dx = g_a \tag{3}$$

This sum rule concerns the isotriplet, i. e. the matrix element $< U|\bar{u}\gamma_\mu\gamma_5 u_- - \bar{d}\gamma_\mu\gamma_5 d|U >$. We can also consider the matrix element of the isosinglet current $\bar{u}\gamma_\mu\gamma_5 u + \bar{d}\gamma_\mu\gamma_5 d$. The associated sum rule

$$\int_0^1 \left[(u_+ + \bar{u}_+ - u_- - \bar{u}_-) + (d_+ + \bar{d}_+ - d_- - \bar{d})\right] dx = \Sigma \qquad (4)$$

gives a number $\Sigma$, which can be viewed as the contribution of the u– and d–quarks to the U–spin.

In a naive model the constituent u–quark inside the U–particle would be composed solely of a u–quark with positive helicity, i. e. all density functions vanish except for $u_+$:

$$\int_0^1 u_+ dx = 1, \qquad d_+ = d_- = \bar{d}_+ = \bar{d}_- = u_- = \bar{u}_+ = 0, \qquad g_a = \Sigma = 1 \qquad (5)$$

This relation would correspond to the $SU(6)$-result in the nucleon: $|G_A/G_V| = 5/3$. In reality we have $|G_A/G_V| = 1.26$, i. e. a reduction from 5/3 by nearly 25%. Taking the same reduction for U, D, as a guideline, we expect for the U/D–system: $g_a \cong 0.75$ instead of $g_a = 1$.

The axialvector coupling constant $g_a$ would fulfill a Goldberger–Treiman relation and would be related to the $\pi - U - D$-coupling constant. The associated axialvector current will be conserved in the limit $m_u = m_d = 0$.

However the singlet current $\bar{u}\gamma_\mu\gamma_5 u + \bar{d}\gamma_\mu\gamma_5 d$ is not conserved in this limit due to the gluon anomaly:

$$\partial^\mu \left(\bar{u}\gamma_\mu\gamma_5 U + \bar{d}\gamma_\mu\gamma_5 d\right) = 2 \cdot \left(g^2/8\pi^2\right) G_{\mu\nu} G^{\mu\nu} \qquad (6)$$

($G_a^{\mu\nu}$: Gluon field strength).

It is well–known that the gluonic anomaly leads to an abnormal mixing pattern for the $0^{-+}$–mesons, implying a strong violation of the Zweig rule in the $0^{-+}$–channel. We consider the anomaly as the reason why in the case of the nucleon the axial singlet charge deviates strongly from the naive quark model value[6].

As can be seen directly from the sum rules given above, we obtain immediately the naive result $g_a = \Sigma$, if all d–densities vanish. If we take as an example $g_a = 0.75$ and $\bar{u} = d = \bar{d} = 0$, we obtain:

$$\int_0^1 (u_+ - u_-) dx = 0.75, \qquad \int_0^1 (u_+ + u_-) dx = 1 \qquad (7)$$

$$\int_0^1 u_+ dx = 0.875, \qquad \int_0^1 u_- dx = 0.125$$

In this case 75% of the U–spin would be given by the spin of the u–quark, the remaining 25% are due to other effects like orbital effects and gluons.

However in the presence of the QCD anomaly the picture changes since $\Sigma \neq g_a$. We isolate the d–integral and obtain:

$$2 \int_0^1 \left( d_+ + \bar{d}_+ - d_- - \bar{d}_- \right) dx = \Sigma - g_a \tag{8}$$

The difference $\Sigma - g_a$ is given by the matrix element $< U|\bar{d}\gamma_\mu\gamma_5 d|U >$ which in a naive picture vanishes. We decompose this m. e. into an isosinglet and isotriplet term:

$$< U|\bar{d}\gamma_\mu\gamma_5 d|U >= \frac{1}{2} < U|\bar{d}\gamma_\mu\gamma_5 d - \bar{u}\gamma_\mu\gamma_5 d|U > + \frac{1}{2} < U|\bar{d}\gamma_\mu\gamma_5 d + \bar{u}\gamma_\mu\gamma_5 u|U > \tag{9}$$

The isospin triplet term is determined via a Goldberger–Treimann relation and related to PCAC and the associated pion pole.

Suppose, PCAC would also be valid for the singlet current. In this case there would be a Goldstone particle (the $\eta$–meson with quark composition $\frac{1}{\sqrt{2}} \left( \bar{u}u + \bar{d}d \right)$, and the $\pi^\circ$ and $\eta$–contribution would cancel. The matrix element vanishes, and we have $\Sigma = g_a$.

In reality this is not true. One finds, for example, for the nucleon $\Sigma \approx 0.30$. We set as an illustration $\Sigma = 0.30$ and obtain:

$$\int_0^1 dx \left( d_+ + \bar{d}_+ - d_- - \bar{d}_- \right) = \frac{1}{2} \left( \Sigma - g_a \right) \cong -0.22 \tag{10}$$

$$\int_0^1 dx \left( u_+ + \bar{u}_+ - u_- - \bar{u}_- \right) = \frac{1}{2} \left( \Sigma + g_a \right) \cong 0.53$$

We note that due to the QCD–anomaly $\bar{q}q$–pairs are generated inside the U–particle. Thus it is the QCD-anomaly, which leads to the $\bar{q}q$–pairs. This is a nonperturbative effect, like the QCD–anomaly itself. Furthermore the $\bar{q}q$–pairs are polarized, canceling partially the spin of the u–quark. Note that the sign of $(\Sigma - g_a)$ is negative.

The sum rule for the d–densities above implies that the sum $\left( d_- + \bar{d}_- \right)$ is nonzero, but it does not imply that the sum $\left( d_+ + \bar{d}_+ \right)$ is nonzero. Thus $\left( d_+ + \bar{d}_+ \right)$ can be zero or very small.

The $(\bar{q}q)$–pairs, generated by the QCD anomaly, e. g. by the gluonic dynamics, are not related to the constituent u–quark directly, and one therefore expects in particular $d_- = \bar{d}_-$. Thus one expects $d_+ = \bar{d}_+ = 0$, $d_- = \bar{d}_- = \bar{u}_-$.

In this case a polarized constituent u–quark is dominated by the $u_+$–function, accompanied by $\left( \bar{d}d \right)$– and $(\bar{u}u)$–pairs, which partially cancel the spin of the u–quark.

An interesting case, probably close to reality, is:

$$\bar{u}_+ = 0, \qquad d_+ = \bar{d}_+ = 0 \tag{11}$$

$$\int_0^1 \left( d_- + \bar{d}_- \right) dx = -\frac{1}{2} \left( \Sigma - g_a \right) \cong 0.22$$

$$\int_0^1 \bar{u}_- dx = - \left( \Sigma - g_a \right) \cong 0.11$$

$$\frac{1}{2} \left( \Sigma + g_a \right) = \int_0^1 dx \left( u_+ - u_- - \bar{u}_- \right) \cong 0.53 \,. \tag{12}$$

Now we include the s–quark. At first we consider the case of $SU(3)$–symmetry: $m_u = m_d = m_s$. The total spin sum is given by

$$\int_0^1 [u_+ + \bar{u}_+ - u_- - \bar{u}_- ) + \left( d_+ + \bar{d}_+ - d_- - \bar{d} \right) + \left( s_+ + \bar{s}_+ - s_- - \bar{s}_- \right)] \, dx = \Sigma$$

$$\tag{13}$$

We obtain:

$$\int_0^1 \left[ \left( d_+ + \bar{d}_+ - d_- - \bar{d}_- \right) 2 + \left( s_+ + \bar{s}_+ - s_- - \bar{s}_- \right) \right] dx = \Sigma - g_a \tag{14}$$

Again we set $s_+ = \bar{s}_+ = d_+ = \bar{d}_+ = 0$. Furthermore we have $d_- = \bar{d}_- = s_- = \bar{s}_-$, and obtain:

$$\int \left( d_- + \bar{d}_- \right) dx = \int \left( s_- + \bar{s}_- \right) dx \cong 0.15$$

$$\int \bar{u}_- dx \cong 0.075 \tag{15}$$

Again the spin is partially canceled by the $\bar{q}q$–pairs, this time including $\bar{s}s$–pairs.

Now we consider the realistic case with $SU(3)$–braking. It is well–known that the physical wave function of the $\eta$–meson and the $\eta'$–meson are approximately given by

$$\eta = \frac{1}{2} \left( \bar{u}u + \bar{d}d - \sqrt{2}\bar{s}s \right), \quad \eta' = \frac{1}{2} \left( \bar{u}u + \bar{d}d + \sqrt{2}\bar{s}s \right) \,. \tag{16}$$

Thus in reality we are between the two cases discussed above. As an example, which is probably close to reality, we take the strange cloud to be half as big as the nonstrange cloud, as suggested by (17).

$$\int \left( d_- + \bar{d}_- \right) dx \cong 0.18$$

$$\int \bar{u}_- dx \cong 0.09$$

$$\int \left( s_- + \bar{s}_- \right) dx \cong 0.09 \,. \tag{17}$$

Again we see that the QCD anomaly is the reason why the spin is partially canceled by the $\bar{q}q$-pairs, although the $\bar{s}s$–pairs are less relevant than the $\bar{d}d$– and $\bar{u}u$–pairs.

We think that we have found in the QCD anomaly the reason why the spin of the nucleon is a rather complicated object. The spin is reduced by $\bar{q}q$–pairs, which partially cancel the spin of the constituent quarks. The $\bar{q}q$–pairs are polarized.

Finally we make some comments about the nucleon. The quark-antiquark-pairs in each constituent quark diminish the spin, and one finds that the spin, provided by the quarks, is only about 30% of the total spin. The question arises who carries the remaining part of the spin. The departure of $|G_A/G_V|$ from 5/3 indicates that orbital effects are there. They make up about 25% of the spin of the nucleon. The remaining part of about 45% is related to the QCD–anomaly. Since the latter is a $\bar{q}q$–effect, caused by gluons, we conclude that about 45% of the nucleon spin is carried by gluons.

We summarize: 30% of the spin is carried by the valence quarks and the $\bar{q}q$–pairs, 25% by orbital effects, and 45% by gluons.

The polarized $\bar{q}q$–pairs should be searched for in the experiments. Also the gluonic contribution can be observed in the experiments, especially by studying the $\bar{c}c$–production in lepton–nucleon–scattering, as done in the Compass experiment[7].

I would like to thank Prof. Rosina for the arrangement of this meeting.

# References

1. For review, see e. g.: J. R. Ellis and M. Karliner, *hep–ph/9601280*
2. See e. g.: B. Adeva et. al., *Phys. Rev.* **D70** 012002 (2004)
3. AV Efremow and OV Teryaev, JINR-E2-88-287, *Proc. Symposium on Hadron Interactions - Theory and Phenomenology*, Bechyne, Czechoslovakia, Jun. 28- Jul. 1, 1988; eds. J Fischer et al., publ. by Inst. Phys., Czech. Acad. Sci.
4. G Altarelli and GG Ross, *Phys. Lett.* **B212** 391 (1988)
5. RD Carlitz, JC Collins and AH Mueller, *Phys. Lett.* **B214** 229 (1988)
6. H Fritzsch, *Phys. Lett.* **229B** 122 (1989)
   *Nucl. Phys.* **B15** 261 (1990)
   *Phys. Lett.* **B242** 451 (1990)
   *Phys. Lett.* **256B** 75 (1990)
7. G. Baum et. al., CERN.SPSLC – 96 – 14

# Dibaryons and Nuclear Force Models$^\star$

V. I. Kukulin

Institute of Nuclear Physics, Moscow State University, Moscow

**Abstract.** The numerous experimental works in which the dibaryon signals have been observed are analyzed critically A new concept of the dibaryon as six-quark bag dressed with strong meson fields, mainly with a scalar σ-field, is introduced and discussed. Novel concept for intermediate- and short-range nuclear force as driven by the dressed intermediate dibaryon generation is advocated. Various implications of the new force model in hadronic and nuclear physics are discussed.

First of all I would like to thank the workshop organizers for very fruitful and fully informal atmosphere on the workshop which stimulates the free discussions and debates among all participants during the workshop. It is especially important for presentation of the talk with non-orthodox content. The text below is strongly shortened version of the extended review-like oral talk presented to the workshop. However, for the reader's convenience, we include to the text the extended list of references.

## 1   Many facets of dibaryon

The idea of dibaryon is almost as old as that of quarks. Still in 70-ies, R.Jaffe et al., using the MIT-bag model, suggested the existence of low-lying specific multi-quark states which can be observed experimentally [1,2]. Jaffe has proposed the most probable candidate among the all low-lying six-quark states, viz. di-lambda dibaryon which should be seen as a bound state in ΛΛ-channel. Despite of the fact that the subsequent intensive searches of such a dibaryon for many years over the world gave the negative results, the activity of experimentalists and theoreticians in the field was extremely high up to 90ies [3–12]. The situation to the end of 80ies has been well summarized by Kamal Seth in his famous talk of 1988 *"Dibaryons in Theory and Practice"*:

*"Dibaryons have become a hot topic for intermediate-energy nuclear physicists during the last ten years. Rumours about their existence and discovery abound and hardly an international conference or annual review goes by without somebody expounding on*

*the subject with either a pro- or contra-bias. The debates between the believers and non-believers tend to be almost religious in their fervor and it is difficult to find objectivity in much of what is written or said. "*

A new renaissance in the field began a few years ago after the pentaquark became in the main focus of the interest of international QCD-community. There appeared for recent years some new experimental evidences [9–12] in favor of very narrow dibaryons with low mass. Some of these findings [12] have been criticized afterward and they look rather doubtful while the other ones [9,10] look to be more reliable and still wait for their confirmation in more accurate experiments with the higher statistics. However, it became much clearer in recent years there is completely different facet of dibaryon, i.e. its decisive role in intermediate- and short-range nuclear force and as an important component of nuclear wavefunctions [13–21] instead of its role as quark exotics as was assumed previously! Moreover, we have argued [20,21,32] the crucial contribution of the intermediate dibaryon in many hadronic processes, like two-pion or heavy-meson production in $pp$ collisions. Thus the present talk includes arguments the pros and cons dibaryon existence, and very short description of its role in nuclear force problem.

## 2    The contra arguments

As was conjectured still in early days of dibaryon physics there might be two forms of dibaryons: narrow multi-quark states and broad resonances. The first type must be uncoupled from the open NN channel or NN$\pi$ open channels, otherwise the state will be broad. Thus, the most attempts have been spent just for finding narrow dibaryon signals. We refer the reader to the review talk of Seth [22] for refs. to earlier works in the field and focus here on most recent predictions.

(i) On the experimental side, a few indications of the narrow dibaryon states below the NN$\pi$-threshold and uncoupled from the NNchannel have been found recently [7–10,12] in $pp \to pp\gamma\gamma$ and $pd$ collisions at intermediate energies. Some of the low-lying states have been studied afterward with higher statistics and no dibaryon signals have been found. The most probable candidates for the broad dibaryon states have been discovered in phase-shift analysis of $pp$ scattering in the $^1D_2$, $^3F_3$ etc. partial waves. In fact, the partial scattering amplitudes in these channels display some loops on the Argand plot. Later on, these loops have been ascribed to the near $N - \Delta$ threshold singularity. Also, many dedicated experiments with very good statistics have been done by Kamal Seth with coworkers, and they did not find any bumps or resonance-like behaviour in the respective reaction cross sections. All these experiments have been summarized as "there are NO experimental indications for both narrow and broad dibaryons".

(ii) On the theory side, numerous calculations made in terms of quark models (see e.g. [5,6]) resulted in rather high energies of six-quark states (in non-strange sector) $E(6q) \sim 400 \div 800$ MeV above the NN-threshold. So, these states lie high in the NN- or NN$\pi$-continuum and hardly can be visible in any experiments.

## 3    The pro arguments

However, more careful theoretical analysis of the existing data on deuteron fragmentation on hydrogen and other light targets [23,24], deuteron electro-disintegration, the numerous disagreements with experiments for few-nucleon systems [25] has revealed that the assumption of dibaryon degrees of freedom can give the best explanation for majority of the puzzles found up to date. Moreover, for the passed thirty years we did not find any arguments disproving the initial Jaffe's conjecture about the existence of dibaryons, i.e. which can forbid these objects. Thus, if they do not exist there should be some fundamental restrictions in QCD which forbid their existence. So we present here the pro arguments, both direct and indirect.

### 3.1    Direct arguments

There is a very broad class of processes in nuclear and hadronic physics, which are forbidden with a single-nucleon kinematics but quite feasible if two or more nucleons are involved simultaneously (the so-called cumulative processes). One of the most remarkable feature for such cumulative processes is a sub-threshold particle production. The distance from the threshold (on the energy scale) shows the mass of multi-nucleon cluster (multibaryon) on which the reaction proceeds. Experimentally it was registered the antiproton production in high-energy $p - A$ collisions on 2 GeV(!) below the normal threshold.

– Another almost direct manifestation of dibaryons in deuteron is the compilation by the Dubna group [26] about the nucleon momentum distribution in deuteron (see Fig. 1). The compilation includes many sorts of data, both for the deuteron electro-disintegration and purely hadronic fragmentation of deuteron on various targets. It is remarkable that all sorts of data are in a good agreement to each other. It is evident from Fig. 1 that there is a bump-like enhancement at nucleon momenta in deuteron between 0.3 and 0.6 GeV/c. The momentum range is very far from the average nucleon momenta typical for nuclear physics[1].

– There is very natural (but purely phenomenological) interpretation of the bump at $0.3\,\text{GeV} \lesssim k \lesssim 0.6\,\text{GeV}$ on Fig. 1. This explanation is based on the assumed non-coherent contribution of the 6q-bag [28] in deuteron with the structure $|s^6[6]L{=}0\rangle$.

– There is still another good example where the dibaryon contribution has been seen clearly. This is the pd backward scattering at intermediate energies $E_p \sim 0.4 - 2.8$ GeV [29] or $p + d \rightarrow (pp) + n$ process in the same kinematics [30,31].The latter process has been studied recently in a full detail at COSY [31]

---

[1] In conventional meson theory this enhancement can be explained only by the so-called $\Delta$-isobar current (IC). However, recent experiments done by the Novosibisk Electron-Deuteron Collaboration [27] on measurement of tensor observables in deuteron photo-disintegration at photon energy 40 - 500 MeV have demonstrated clearly that the IC in deuteron at the above range of nucleon momenta fail to explain the above polarization observables at $E_\gamma > 350$ MeV. So, the large contribution of IC assumed in the theoretical treatment of $d(e, e'p)$ process simply mimics the contribution of the dibaryon mode.
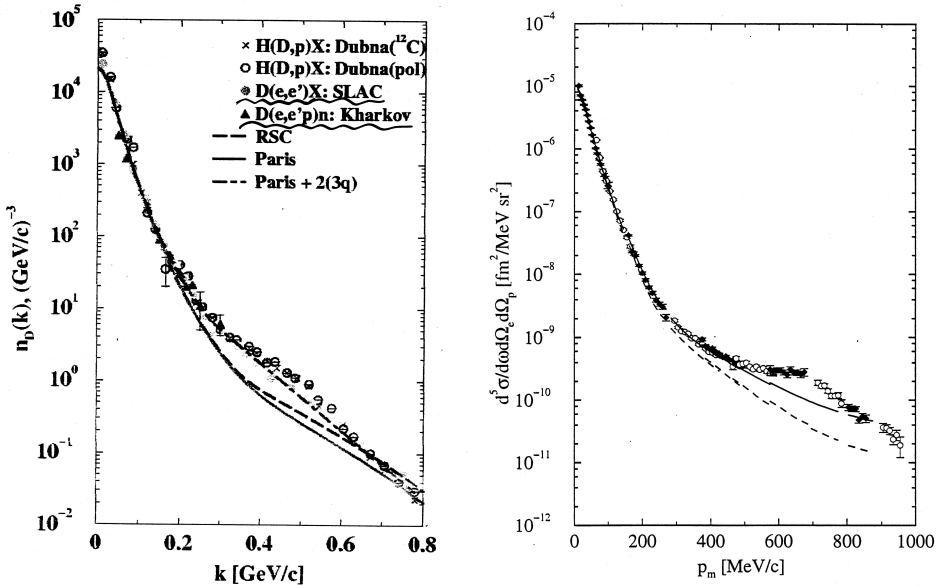
**Fig. 1.** Left: The nucleon distribution in the deuteron $n_d = |\psi_d(k)|^2$ extracted from $e - d$ scattering and $dp \to pX$ stripping data. The solid and dashed lines correspond to the calculations performed within the impulse approximation. The dash-doted line shows the effect of including of the non-nucleon component in the deuteron wavefunction [28]. Right: Comparison of the measured $d(e, e'p)n$ cross section to the calculation with Schiavilla's code with (solid curve) and without (dashed curve) MEC and IC.
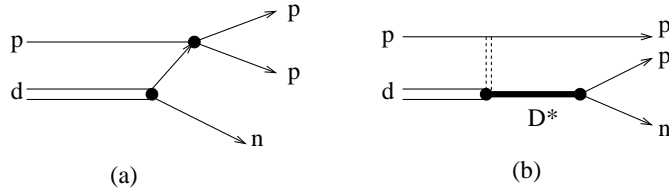


**Fig. 2.** Some graphs illustrating the conventional (a) and new (b) mechanisms for the $pd \to (pp) + n$ process at intermediate energies.

at very low $pp$ relative energy $E_{pp} < 3$ MeV. The authors have found in $p + d \to (pp) + n$ process that, at the incident proton energy $E_p < 400$ MeV, the FSI in $pp$-subsystem is seen clearly while at $E_p > 500$ MeV there is no FSI in the forwardly moving $pp$ system (at very low $pp$ relative energy!). The authors have suggested most plausible interpretation for this: at $E_p < 400$ MeV the process mechanism is represented by the pole diagram of proton exchange (see Fig. 2a) while at higher incident momentum of proton (when the probability of high momentum of proton inside deuteron gets much lower and the contribution of the exchange mechanism shown in Fig. 2a becomes much smaller) the leading mechanism is changed and can be presented by graph on Fig. 2b. In this graph $D^*$ means the exited intermediate dibaryon (in the authors' terminology it is a fire-

ball) the decay of which provides the second fast proton which does not interfere with the incident fast proton due to a time delay. Thus, the energy correlation of the two non-interacting moving forwardly protons measured in the experiment should not manifest any FSI effect.

## 3.2   Indirect arguments

There are many disagreements between the basic parameter values of the best current NN potential models and those derived from a consistent dynamical description and QCD. These concern e.g. with the coupling constant for the values $g_{\omega NN}$, $\varkappa_{\rho NN}$ and the values of cut-off parameters $\Lambda_{\pi NN}$, $\Lambda_{\pi N\Delta}$ etc. [15,16]. These disagreements with fundamental theory are well known more than 25 years but, even now, we have no real explanation for such contradictions. It is important to stress here all the above discrepancies are related only to the intermediate- and short-range components of nuclear force. However, it was demonstrated in our works [15–21] these discrepances could be removed if to incorporate an intermediate dibaryon into the fundamental NN interaction at intermediate and short ranges. So, this result can be considered as a good indirect argument in favor of crucial role of the dibaryons in NN interaction.
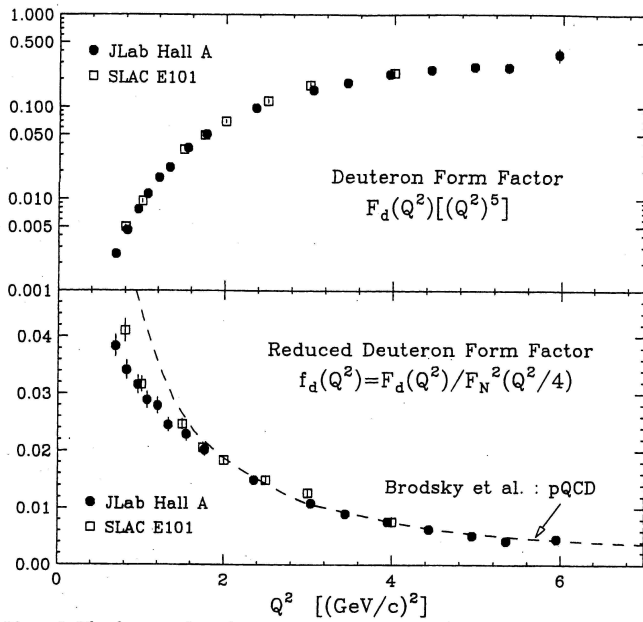


**Fig. 3.** The deuteron form factor $F_d(Q^2)$ multiplied by $(Q^2)^5$ (top) and the reduced form factor $f_d(Q^2)$ (bottom). The curve is an asymptotic pQCD prediction arbitrarily normalized to the data at $Q^2 = 4(GeV/c)^2$.

Another big portion of indirect arguments pros the dibaryons can be deduced from few-body physics. In fact, numerous calculations undertaken in last

years for $nd$, $nT$, $pd$ etc. elastic scattering at very low and intermediate energies have demonstrated clearly there are many evident disagreements between the best few-nucleon calculations and experimental data [14,15,25,29,30]. It is important to emphasize here that the processes under study were completely inside the scope of validity of the current force models and the theoretical models adopted have incorporated all the important components of the 2N and 3N forces. So the only thinkable reason for numerous disagreements observed is an incorrect off-energy-shell behaviour of the force, or, alternatively, highly incomplete underlying force models. To illustrate the point we present here only one such evident disagreement: the photo-disintegration cross section ratio for $^4$He $\eta = \sigma(^4\text{He}(\gamma, p))/\sigma(^4\text{He}(\gamma, n))$ at energies $E_\gamma \sim 15 - 25$ MeV measured experimentally reaches 1.5 - 1.7 while all traditional four-body calculations predict $\eta \sim 1.2 - 1.3$. So, in this reaction we observe some strong Coulomb effects which are absent in the conventional approach. However, recently it was found in our 3N calculations for the $^3$He Coulomb energy [18] the dibaryon model of nuclear force does predict strong additional Coulomb effects (which are fully absent in traditional force models): the Coulomb interaction between the charged dibaryon and external protons. This new three-body Coulomb interaction gives, as has been shown [18,19], full explanation for the Coulomb displacement energy between $^3$H and $^3$He.

There are also many very general, although indirect, arguments in favor of the dibaryon admixtures to nuclear wavefunctions. One of such arguments is an asymptotic behaviour of electromagnetic form factors of deuteron, $^3$H, $^4$He etc. at $Q^2 \rightarrow \infty$ (the so-called quark counting rules). This asymptotic behaviour have been observed experimentally at $Q^2 \sim 4 \div 8$ GeV$^2$ and points to the six-quark dominance at high $Q^2$ in deuteron (see Fig. 3). The similar arguments also can be applied to the high-energy photo-disintegration of deuteron measured recently in JLab.

Summarizing all the arguments together one can claim there are a lot of evidence (both direct and indirect) in favor of dibaryons in hadronic and nuclear physics.

## 4  Dibaryon as a carrier of basic nuclear force

In our previous works [13–19] we have proposed a new force model, in which the intermediate- and short-range NN-interaction proceeds through an intermediate dressed dibaryon, i.e. via an s-channel mechanism: NN $\rightarrow$ (6q + meson fields) $\rightarrow$ NN, where the meson dressing in the form of meson fields (mainly the $\sigma$-field) surrounding the dense six-quark core stabilises strongly the 6q-bag and shifts its self-energy down to the NN threshold (see Fig. 4). The physical pattern underlying this new s-channel mechanism can be shortly outlined as follows [15,16]. At the first step, the initial NN system, by gluon or quark exchange, gets confined in the excited six-quark configuration $|s^4p^2[42]LST\rangle$, i.e. it deals with the excited $C - C'$ channel with hidden color. On the second step, two p-shell quarks jump down to the s-shell and emit hereby two s-wave pions. The latter, in their turn, strongly interact in the field of six-quark core giving the scalar-isoscalar $\sigma$-meson
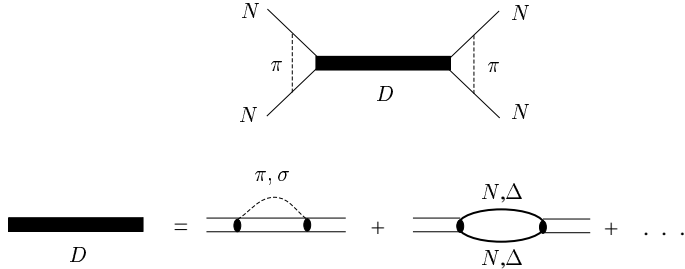
**Fig. 4.** The graph in the first row illustrates the s-channel NN interaction through the intermediate dressed dibaryon D; the peripheral exchanges are also shown for the one-pion case only. The graphs in the second row illustrate some possible diagrams for the dibaryon dressing.

with a reduced mass and width. Due to a strong attraction of the $\sigma$-meson to the quarks confined in the $|s^6[6]\rangle$ component and due to the spherical symmetry of the $s^6$ six-quark bag, the $\sigma$-field will compress the bag. This bag compression will induce scalar diquark correlations of very short range in the bag ($r_{qq} \sim 0.2$ fm) and will enhance further the quark-meson interaction. All these attractive effects will compensate completely the energy losses arising due to the intermediate $\sigma$-meson production and also from rather high kinetic energy of six quarks localized in the bag. Thus, the net result of this interplay has been estimated to be strongly attractive. Next, we employed the quark-meson microscopic model to estimate these effects and to construct the respective new model for the NN interaction at short ranges. Thus the following fundamental results have been obtained:

 (i) It was shown that the meson cloud of the symmetric six-quark bag (mainly the $\sigma$-field) should play a very important role in its dynamics [16,20,21], so that, instead of the bare six-quark bag, one should consider the novel object – the dressed dibaryon.
(ii) The above dressed dibaryon (with dominating $\sigma$-field) can be treated as a main carrier of nuclear force at intermediate- and short ranges, instead of the conventional t-channel heavy-meson exchange with artificially enhanced coupling constants and cut-off parameters).
(iii) The above dibaryon model of nuclear force leads inevitably to an appearance of scalar attractive many-body force and also new many-body Coulomb force in nuclei. This attractive many-body force may give a good dynamical basis (related intimately to the fundamental QCD theory) for relativistic Walecka-Serot hadrodynamical picture of nuclei. It was shown by direct three-body calculation that the above three-body scalar force contributes at least a half the total nuclear binding in $^3$H and $^3$He systems [18,19].
(iv) The intermediate dibaryons in nuclei must lead to new currents, according to general principle of quantum physics. These new specific currents have been shown to result in full explanation of deuteron magnetic form factor and magnetic moment, as well as the circular polarization of $\gamma$-quanta in $np \rightarrow d\gamma$ process for thermal neutrons [32]. It would be very interesting to test the new

force model in predictions of various cumulative processes. This work is in a progress now.

## References

1. R.L. Jaffe, Phys. Rev. Lett. **38**, 195 (1977); R.L. Jaffe, K. Johnson, Phys. Lett. **60**, 201 (1986).
2. E. Fahri, R.L. Jaffe, Phys. Rev. D **30**, 2379 (1984).
3. T. Goldman et al., Mod. Phys. Lett. **A13**, 59 (1997).
4. S.B. Gerasimov, nucl-th/9712064.
5. E.L. Lomon, J. Phys. Colloq. **51**, 363 (1990); Few-Body. Syst. Suppl. **7**,213 (1994); P. La France, E.L. Lomon, Phys. Rev. D **34**, 1341 (1986).
6. S.D. Paganis, T. Udagawa, G.W. Hoffmann, R.L. Ray, Phys. Rev. C **56**, 570 (1997).
7. S.B. Gerasimov, A.S. Khrykin, Mod. Phys. Lett. **A8**, 2457 (1993).
8. S.B. Gerasimov, S.N. Ershov, A.S. Khrykin, Yad. Fiz. **58**, 911 (1995).
9. A.S. Khrykin et al., Phys. Rev. C **64**, 03400 (2001).
10. A.S. Khrykin, nucl-ex/0211034; Nucl. Phys. **A721**, 625c (2003).
11. P.A. Zolnierczuk et al., Phys. Lett. B **549**,301 (2002); Acta Physica Polonica **B31**, 2349 (2000); nucl-ex/0007011.
12. L.V. Filkov, V.L. Kashevarov, nucl-th/0409009.
13. V.I. Kukulin, *Proceeds. of the V Winter School on Theoretical Physics PIYaF, Gatchina, S.-Petersburg, 8 – 14 Febr. 1999.*, p. 142.
14. V.I. Kukulin, I.T. Obukhovsky, V.N. Pomerantsev and A. Faessler, Physics of Atomic Nucl. **64**, 1748 (2001).
15. V.I. Kukulin, I.T. Obukhovsky, V.N. Pomerantsev and A. Faessler, J. Phys. G **27**, 1851 (2001).
16. V.I. Kukulin, I.T. Obukhovsky, V.N. Pomerantsev and A. Faessler, Int. Journ. of Mod. Phys. E **11**, 1 (2002).
17. M.M. Kaskulov, V.I. Kukulin, P. Grabmayr, Int. Journ. of Mod. Phys. E **12**, 449 (2003).
18. V.I. Kukulin, V.N. Pomerantsev M.M. Kaskulov and A. Faessler, J. Phys. G **30**, 287 (2004).
19. V.I. Kukulin, V.N. Pomerantsev and A. Faessler, J. Phys. G **30**, 309 (2004).
20. V.I. Kukulin and M.A. Shikhalev, Physics of Atomic Nucl. **67**, 1558 (2004).
21. A. Faessler, V.I. Kukulin and M.A. Shikhalev, Ann. Phys. **320**, 71 (2005).
22. K. Seth, Dibaryons in Theory and Practice, Talk at 1998 AIP meeting.
23. J. Napolitano et al., Phys. Rev. Lett. **81**, 4576 (1998).
24. C. Bochna et al., Phys. Rev. Lett. **61**, 2530 (1988).
25. H.O. Meyer, A talk at *Symposium on Current Topics in the Field of Light Nuclei, Cracow, Poland, 21–25 June 1999*, p. 858 (unpublished).
26. E.A. Strokovsky, Yad. Fiz. **62**, 1193 (1999).
27. D. Nikolenko (Novosibisk Electron-Deuteron Collaboration), Talk at 5-th Intern. Conference "Nuclear and Radiation Physics", Almaty, Sept. 26-29, 2005.
28. A.P. Kobushkin, Yad.Fiz. **62**, 1213 (1999).
29. P. Berthet et al., J. Phys. G **8**, L111 (1982); J. Arvieux et al., Phys. Rev. Lett. **50**, 19 (1983); Nucl. Phys. **431**, 613 (1984); V. Punjabi et al., Phys. Lett. B **350**, 178 (1995); L.S. Azhgirey et al., Phys. Lett. B **391**, 22 (1997); Yad. Fiz. **61**, 494 (1998).
30. Yu.N. Uzikov, V.I. Komarov, Phys. Lett. B **524**, 303 (2002).
31. S.Yashchenko, "Deuteron Breakup $pd \rightarrow (pp)n$ with a Fast Forward Diproton Studied at ANKE-COSY", Ph.D. Thesis, Faculty of Science of Friedrich-Alexander Universität, Erlangen-Nürenberg, 2004.
32. V.I. Kukulin and M.A. Shikhalev, Talk at the Intern. Conference on Nuclear Physics, Rila, Bulgaria, June 25-30, 2005; I.T. Obukhovsky et al., Phys. Rev. C (in press).

# Looking for distinctive signatures of binary gluonic mesons[*]

P. Minkowski[a]

[a] University of Bern, Switzerland

**Abstract.** After the premises, the following topics are discussed: gluon binary bilocal and adjoint string operators; what to learn from octet string breaking. Outlook is given.

## 1 Premises

We face the theoretical abstraction of QCD with $N_{fl} = 6$ , representing strong interactions – adaptable to two or three light flavors (u, d, s) of quarks and anti-quarks.

Quarks: color is counted in $\pi^0 \to \gamma\gamma$; spin and flavor are clearly seen in $q\overline{q}$ and $3q, 3\overline{q}$ spectroscopy.

$$\mathcal{L} = \left[ \overline{q}_{\mathcal{B}f}^{c'} \left\{ \begin{array}{c} \frac{i}{2} \overrightarrow{\partial}_\mu \delta_{c'c} \\ -\nu_\mu^A \left( \frac{1}{2}\lambda^A \right)_{c'c} \end{array} \right\} \gamma_{\mathcal{B}\mathcal{A}}^\mu q_{\mathcal{A}f}^c \\ -m_f \overline{q}_{\mathcal{A}f}^c q_{\mathcal{A}f}^c \right] - \frac{1}{4g^2} F^{\mu\nu A} F_{\mu\nu}^A + \Delta\mathcal{L} \qquad (1)$$

Here $c', c = 1, 2, 3$ (color), $f = 1, \cdots, 6$ (flavor), $\mathcal{B}, \mathcal{A} = 1, \cdots, 4$ (spin), $m_f$ (mass). Gauge bosons:

$$F_{\mu\nu}^A = \partial_\nu \nu_\mu^A - \partial_\mu \nu_\nu^A - f_{ABC} \nu_\nu^B \nu_\mu^C \qquad (2)$$

Here $A, B, C = 1, \cdots, \dim(G = SU3_c) = 8$, and we use Lie algebra labels

$$\left[ \frac{1}{2}\lambda^A, \frac{1}{2}\lambda^B \right] = i f_{ABC} \frac{1}{2}\lambda^C .$$

Perturbative rescaling

$$\nu_\mu^A = g\nu_{\mu\,\text{pert}}^A , \qquad F_{\mu\nu}^A = g F_{\mu\nu\,\text{pert}}^A .$$

Degrees of freedom are seen in jets, in (e.g.) the energy momentum sum rule in deep inelastic scattering, but not clearly in spectroscopy. Completing $\Delta\mathcal{L}$ in Fermi gauges:

$$\Delta\mathcal{L} = \left\{ \begin{array}{c} -\frac{1}{2\eta g^2} \left( \partial_\mu \nu^{\mu A} \right)^2 \\ +\partial^\mu \overline{c}^A (D_\mu c)^A \end{array} \right\} \qquad (3)$$

---

[*] In collaboration with Wolfgang Ochs, earlier work also with Harald Fritzsch.

Here $\eta$ is the gauge parameter, $c$ and $\overline{c}$ are the ghost fermion fields, $(D_\mu c)^A = \partial_\mu c^A - f_{ABD} v_\mu^B c^D$, and $C^A = \partial_\mu v^{\mu A}$ is the gauge fixing constraint.

We first show, in Fig. 1, the $q\overline{q}$ p-wave nonets, discussed in QCD2002. No clear confirmation has been achieved, in particular because of the low mass (large width) scalar candidates $\sigma, \kappa$.
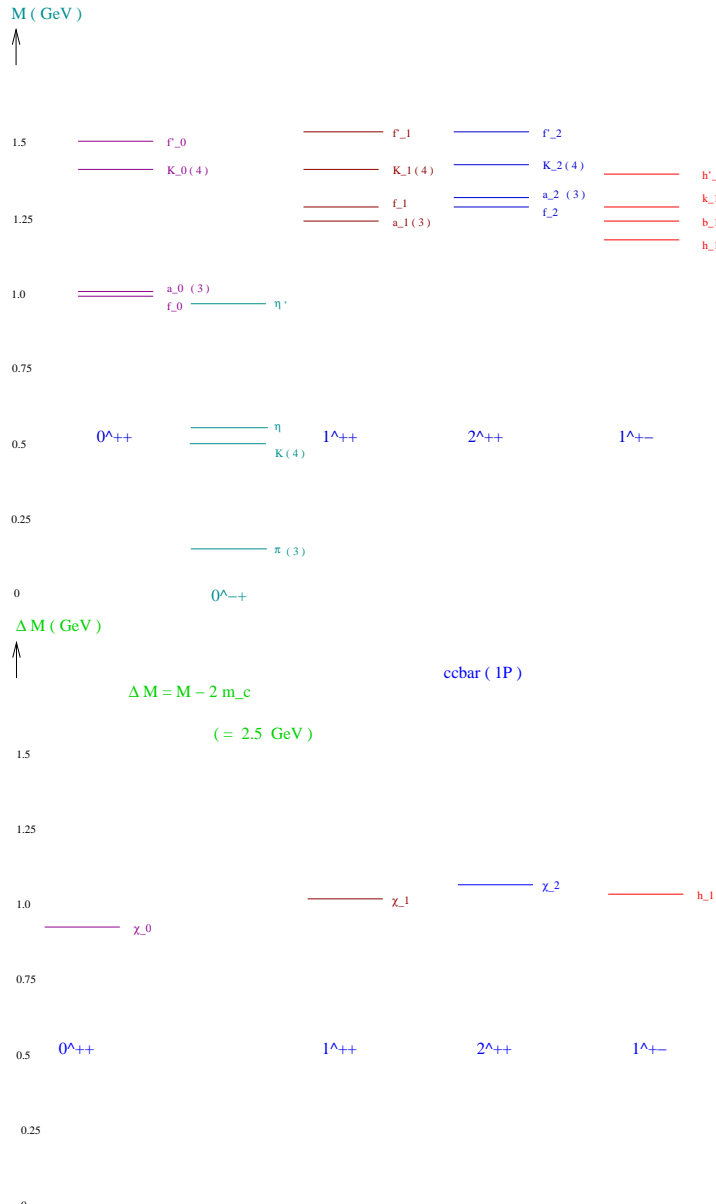


**Fig. 1.** $q\overline{q}$ p-wave nonets $0^{++}$, $1^{+\pm}$, $2^{++}$ (top panel); the pattern can be compared to $c\overline{c}$ p-wave states (bottom panel).

In Fig. 2 (taken from [1]) the charge multiplicity in the fragmentation region of gluon and (anti-)quark jets in three-jet Z decays from the Delphi collaboration is displayed. As a relevant parameter a rapidity gap $\Delta y$ is imposed, $\Delta y = 1.5$. The excess – relative to Monte Carlo results – increases for the gluon jet with increasing $\Delta y$.
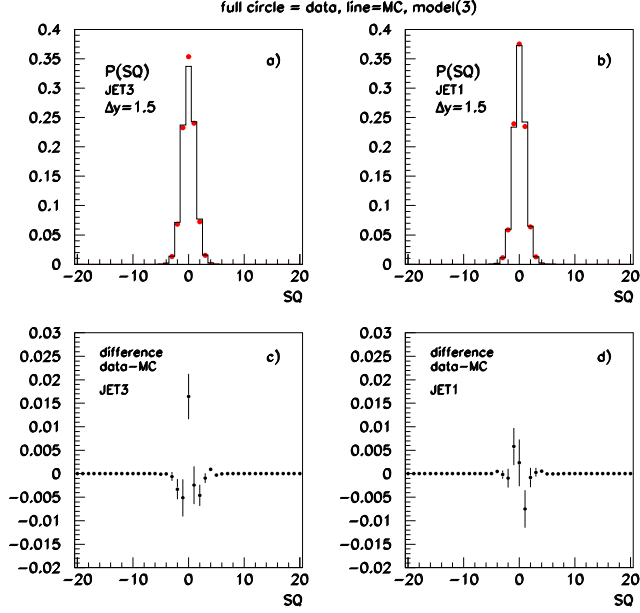


**Fig. 2.** Charge multiplicity in jets (JET3: gluon, JET1: quark).

## 2   Gluon binary bilocal and adjoint string operators

The goal is, to identify – not just some candidate resonance – gluonic mesons, binary and higher modes, and to relate them to the base quantities within QCD.

$$B_{[\mu_1\nu_1],[\mu_2\nu_2]}(x_1, x_2) = F_{[\mu_1\nu_1]}(x_1; A)U(x_1, A; x_2, B)\, F_{[\mu_2\nu_2]}(x_2; B) \qquad (4)$$

Here $A, B, \cdots = 1, \cdots, 8$, and $F_{[\mu\nu]}(x; A)$ denote the color octet of field strengths. The quantity $U(x, A; y, B)$ in Eq. (4) denotes the octet string operator, i.e. the path-ordered exponential over a straight-line path $\mathcal{C}$ from $y$ to $x$.

$$U(x, A; y, B) = P\exp\left(\int_y^x\bigg|_{\mathcal{C}} dz^\mu \frac{1}{i}v_\mu(z, D)\mathcal{F}_D\right)_{AB} \qquad (5)$$

$$(\mathcal{F}_D)_{AB} = if_{ADB}$$

In Eq. (5) $f_{ADB}$ denotes the structure constants of $SU3_c$ and $\mathcal{F}_D$ the generators of its adjoint representation. $v_\mu(z, D) \equiv v_\mu^D(z)$ denote the octet of field potentials.

Properties pertaining to the octet string operators, field strengths and their potentials are discussed in extenso in [2]. The method of QCD sum rules involving correlation functions of local gluon binary operators is "on the way of" identifying gluon binary bilocal and adjoint string operators. This has been pursued – among others – by Stephan Narison [3].

Let me illustrate this goal further, showing "... the abridged ordering in an actual spider web. It follows an abridged double spiral pattern from the center base point and back." The figure (Fig. 3) is adapted from a photograph by Lui Bernard [4].
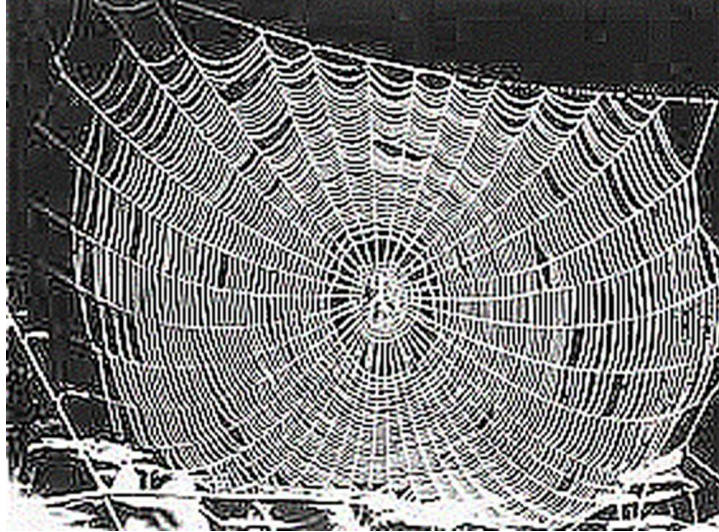


**Fig. 3.** 'Awareness' by the spider of the local spatial rotation group (not $SU3_c$), and associated Riemann normal coordinates, as relevant for the nonabelian Stokes relation.

## 3  What to learn from octet string breaking

Equation (5) defining the octet string operators is repeated below (see Fig. 4).

$$U(x, A; y, B) = P \exp\left( \int_y^x \Big|_{\mathcal{C}} dz^\mu \frac{1}{i} v_\mu(z, D) \mathcal{F}_D \right)_{AB} \tag{6}$$
$$(\mathcal{F}_D)_{AB} = i f_{ADB}$$

Here $U(w, D; v, C)$ and $U(v, B; y, A)$ denote the octet string operators, split apart by the pair of field strengths at the breaking point $v$ (see Fig. 4).
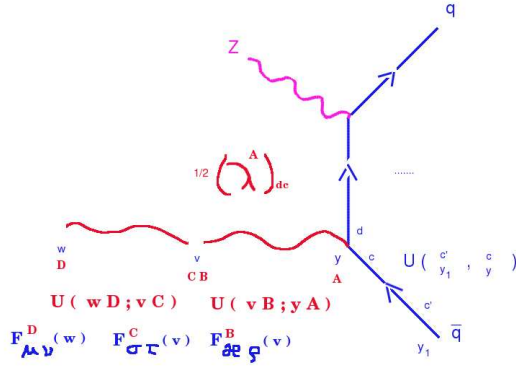
**Fig. 4.** Octet string operators $U(w, D; v, C)$ and $U(v, B; y, A)$ split apart by the pair of field strengths at the breaking point $v$.

The alternative gluon string breaking proceeds also into an octet, but realised by two triplet strings, with each a quark and an antiquark at opposing ends.

It is the final (gluon-gluon) octet breaking, which leads to the hadrons forming the *associated* fragmentation region, which is thought to be dominated by zero (small) electric charge multiplicity [5] , as shown in Fig. 2 [1]. The latter – assuming a dominant (or at least important) octet breaking component in gluon jets – increasingly so with an increasing rapidity gap imposed, evolve in a gluon enriched environment – and thus our suggestion, that gluonic mesons as well as hybrids may be prominent there.

In the analysis of Buschbeck, Mandl and Siebel [1] of the Delphi events $Z \rightarrow$ 3 jets it was however impossible, due to low statistics, aggravated by the rapidity gap requirement, to resolve the invariant mass distribution of the hadrons forming the gluon jet fragments.

I look forward to ensuing experiments at the Tevatron and the LHC.

## 4   Outlook

1) While the candidate assignments for the lowest lying binary gluonic mesons $J^{PC} = 0^{++}, 0^{-+}, 2^{++}$ remain unchanged, mesonic and baryonic spectroscopy involving u, d, s flavors, mainly in the scalar channel for mesons and exotic (tetra-monoanti-)quark baryons have not helped to clarify the situation.
2) The surprise involving lower than expected masses in the $s\bar{c}$ heavy light system, is uncontroversial experimentally and sheds light on the p-wave $s\bar{c}$ dynamics.
3) The continued study of the charge multiplicity of leading hadrons in gluon relative to (anti-) quark jets, imposing a rapidity gap, has given support to a substantial (gluon-gluon) octet breaking of the gluonic octet string.

4) Even if candidates for binary gluonic mesons are found, new ones or confirming old ones, the identification of their intrinsic gauge boson structure is – theoretically – way inside the domain of nonperturbative field theory.

5) Yet I think they do exist, as cornerstone entities of QCD.

## References

1. M. Siebel, *A study of the charge of leading hadrons in gluon and quark fragmentation*, presented at 40th Rencontres de Moriond on QCD and High Energy Hadronic Interactions, La Thuile, Aosta Valley, Italy, 12-19 March 2005, `hep-ex/0505080`.

2. P. Minkowski, *Central hadron production in crossing of dedicated hadronic beams*, `hep-ph/0405032`.

3. S. Narison, *Scalar mesons in QCD and tests of the gluon content of the sigma*, Contributed to QCD 02: High-Energy Physics International Conference in Quantum Chromodynamics, Montpellier, France, 2-9 July 2002, Nucl. Phys. Proc. Suppl. **121** (2003) 131-134; `hep-ph/0208081`.

4. Lui Bernard, `www.onlinekunst.de/bernard/04.html`.

5. P. Minkowski and W. Ochs, Phys. Lett. B **485** (2000) 139.

# Covariant Description of Baryon Reactions within Constituent Quark Models

W. Plessas

Theoretical Physics, Institute for Physics, University of Graz, Universitätsplatz 5, A-8010 Graz, Austria

**Abstract.** We report on the present status of relativistic studies of various baryon properties within the framework of constituent quark models performed by the Graz group. In particular, we address covariant excitation spectra of light and strange baryons as well as electroweak and hadronic (decay) reactions.

## 1  Poincaré-Invariant Quantum Mechanics

The framework followed for the studies of baryon reactions reported here is relativistic (i.e. Poincaré-invariant) quantum mechanics. It is a theory that relies on a fixed number of particles and is thus qualitatively different from a field-theoretical approach. Nevertheless it might be quite effective, especially in a range of energies where certain degrees of freedom govern the reactions and others are practically frozen. The beauty of such a theory lies in the fact that it can be reliably formulated and solved (on a Hilbert space corresponding to a predetermined number of particles). All of the symmetries of special relativity can be taken care of and one arrives, in particular, at Lorentz-invariant results. The starting point for the calculations is usually an invariant mass operator with interactions, and one solves its eigenvalue problem to deduce spectra and eigenstates. The latter are used to calculate covariant matrix elements of transition operators corresponding to certain reactions.

## 2  Relativistic Constituent Quark Models

We have employed relativistic constituent quark models (RCQMs) with two types of hyperfine interactions. The first one is the one-gluon-exchange (OGE) RCQM parametrized after the Bhaduri-Cohler-Nogami (BCN) model [1] by Theußl et al. [2] and the second one is the Graz Goldstone-boson-exchange (GBE) RCQM [3]. Whenever possible a comparison is given to the instanton-induced (II) RCQM by the Bonn group [4] whose hyperfine forces stem from the 't Hooft interaction. In all cases the confinement interaction is linear with quite similar strengths.

## 3  Baryon Spectroscopy

The detailed light and strange baryon spectra of the OGE, GBE, and II CQMs can be found in the original papers [2–4]. A critical discussion of the qualitative differences between the GBE and OGE hyperfine interactions is presented in ref. [5]. For a critique of some erroneous and misleading results in the literature see also ref. [6]. In the comparison of the GBE, OGE, and II RCQMs some relevant observations have been made specifically with regard to the N and Λ spectra in the Bled Proceedings 2004 [7].

The GBE RCQM has recently been extended to include for the hyperfine interaction additional force components deriving from vector and scalar boson exchanges [8]. The quality of the light and strange baryon spectra is more or less the same as in the case of the GBE RCQM with only pseudoscalar-exchange hyperfine forces.

## 4  Baryon Reactions

For the calculation of baryon reactions we have mostly followed the point-form approach to relativistic quantum mechanics. For the elastic electromagnetic form factors of the nucleons we have also made parallel calculations in instant form. In all cases a spectator model for the transition operator has been employed [9].

## 5  Electroweak Form Factors

Here, I am not addressing the electromagnetic and weak reactions. Rather, I refer to the contribution of R. Wagenbrunn at this Workshop [10]. He has dealt with elastic and inelastic electromagnetic as well as axial form factors both in the point and instant forms.

I only mention that a comprehensive study of the electric radii and magnetic moments of all octet and decuplet baryon ground states has recently been completed by K. Berger [11]. Some of the results have already been published in ref. [12].

## 6  Mesonic Decays of Baryon Resonances

So far we have considered $\pi$ and $\eta$ decay modes of $N^*$ and $\Delta^*$ resonances. Only covariant point-form results are available up till now. They have recently been published in ref. [13]. This paper also contains a critical discussion of the decay widths comparing predictions of the OGE, GBE, and II RCQMs. While the results are rather similar for all of these RCQMs - but usually rather far away from experimental data - one finds in all instances considerable relativistic effects. This puts considerable doubt on previous nonrelativistic or relativized calculations.

A comprehensive study of all mesonic decay modes of baryon resonances, including the strange sector, is presently under way [14].

# References

1. R. K. Bhaduri, L. E. Cohler, and Y. Nogami, Nuovo Cim. **A65**, 376 (1981).
2. L. Theussl, R. F. Wagenbrunn, B. Desplanques, and W. Plessas, Eur. Phys. J. **A12**, 91 (2001).
3. L. Y. Glozman, W. Plessas, K. Varga, and R. F. Wagenbrunn, Phys. Rev. D **58**, 094030 (1998).
4. U. Loering, K. Kretzschmar, B. C. Metsch, and H. R. Petry, Eur. Phys. J. **A10**, 309 (2001); ibid., 395 (2001).
5. L. Ya. Glozman, Z. Papp, W. Plessas, K. Varga, and R. F. Wagenbrunn, Phys. Rev. C **57**, 3406 (1998).
6. W. Plessas, Few-Body Syst. Suppl. **15**, 139 (2003).
7. W. Plessas, In: Proceedings of the Workshop on Quark Dynamics, Bled, 2004. Ed. by B. Golli, M. Rosina, and S. Sirca, Ljubljana Univ., Ljubljana, 2004, p. 49. http://www-f1.ijs.si/Bled2004/
8. K. Glantschnig, R. Kainhofer, W. Plessas, and R. F. Wagenbrunn, Eur. Phys. J. A **23**, 507 (2005).
9. T. Melde, L. Canton, W. Plessas, and R. F. Wagenbrunn, Eur. Phys. J. A **25**, 97 (2005).
10. R. F. Wagenbrunn, Contribution to this Workshop.
11. K. Berger, Doctoral Thesis, University of Graz, 2005.
12. K. Berger, R. F. Wagenbrunn, and W. Plessas, Phys. Rev. D **70**, 094027 (2004).
13. T. Melde, W. Plessas and R. F. Wagenbrunn, Phys. Rev. C **72**, 015207 (2005).
14. B. Sengl, Doctoral Thesis, University of Graz, in preparation.

# Double charm hadrons revisited $^\star$

J.-M. Richard[a] and Fl. Stancu[b]

[a] Laboratoire de Physique Subatomique et Cosmologie, Université Joseph Fourier–IN2P3-CNRS, 53, avenue des Martyrs, 38026 Grenoble cedex, France
[b] Institute of Physics, B.5, University of Liege, Sart Tilman, 4000 Liege 1,Belgium

**Abstract.** The dynamics of two heavy quarks inside the same hadron is probed against the double charm baryon results seen at SELEX. This can be seen as a part of the mechanism to bind tetraquarks with two heavy quarks and two light antiquarks. In the framework of potential models, it is possible to test the role of different effects: relativistic corrections, confinement, hyperfine forces, etc. It is conjectured that an additional interaction rescaled from the nucleon–nucleon system and acting between light quarks only, can help in bringing extra, possibly required, binding in tetraquarks.

## 1 Introduction

The observation of double charmed baryons, $(ccq)$, by the SELEX collaboration [1,2] has brought new incentive to study hadrons containing heavy quarks. The discovery by Belle and BaBar of the $D_{s,J}$ states [3], of the anomalously narrow $X(3872)$ meson [4], and of the other hidden-charm states $X(3940)$ [5] and $Y(4260)$ [6] also stimulated much activity in this field. Some of these states might be interpreted as meson–meson molecules or as multiquark states.

Regarding double-charm baryons, several uncertainties are left in the SELEX results: only the $(ccd)^+(3520)$ is confirmed, as being seen in two different weak-decay modes. Unfortunately, other peaks, which are candidates for isospin partner, spin or orbital excitation, are far from being established [7]. There is hope that the final analysis of SELEX data and future experiments could clarify the situation. In particular, the double charm production seen in B-factories to detect charmonium states recoiling against other charmonium states, could possibly lead to final states with double charm hadrons recoiling against double anticharm systems.

The purpose of the present study is to investigate whether or not charmonium $(c\bar{c})$, charmed mesons $(c\bar{q})$ and baryons $(cqq)$ can be described in a simple unified picture and lead to predictions for double-charm baryons $(ccq)$ and for hidden-charm $(cq\bar{c}\bar{q})$ and double-charm $(cc\bar{q}\bar{q})$ tetraquarks.

We believe that mixing heavy and light quarks or antiquarks in the same system sometimes favours multiquark binding below the threshold for spontaneous dissociation into simpler hadrons. Some attractive effects between two

---

$^\star$ Talk delivered by Fl. Stancu

heavy quarks, or between two light quarks, might lower the mass of a multiquark system without acting on the threshold energy.

The structure of this paper is a follows. In the next section, we present the main dynamical ingredients that play a role in multiquark binding. In Secs. 3 and 4, we briefly review some of the theoretical approaches to double charm baryons. Section 5 is devoted to an analysis of the latest results on open charm tetraquarks. The last section raises several questions on the role of various dynamical effects and, in particular, of the light quark dynamics in the binding of tetraquarks.

## 2  Aspects of quark dynamics

### 2.1  The heavy–heavy effect

Flavour independence is one of the appealing features of quark models, directly linked to QCD. Potentials have been designed, for instance, to describe simultaneously the $(c\bar{c})$ and $(b\bar{b})$ spectra. In a flavour-independent potential used in the context of the Schrödinger, or an improved equation, with relativistic kinematics, one automatically gets a *heavy–heavy* effect: a subsystem with large reduced mass takes better benefit of the attraction. This is illustrated by the following inequalities [8].

$$(Q\overline{Q}) + (q\bar{q}) \leq 2(Q\bar{q}) , \tag{1}$$

$$(QQq) + (qqq) \leq 2(Qqq) , \tag{2}$$

$$(QQ\bar{q}\bar{q}) \leq 2(Q\bar{q}) . \tag{3}$$

While (1) and (2) are valid for any value of the heavy-to-light mass ratio $x = M/m$, (3) requires a minimal value of $x$ for a bound state to occur. In atomic physics, a sort of flavour independence is also present, inasmuch as the same Coulomb potential acts on light and heavy charges. There the inequality (1) means that a system of a protonium and a positronium is lighter than the hydrogen plus the antihydrogen. The inequality (3) is also observed: while the positronium molecule is marginally bound, the hydrogen molecule lies well below the threshold of dissociation into two hydrogen atoms.

### 2.2  The light–light effect

In quark physics, one also encounters a *light–light* effect, which is not explicitly included in simple potential models and thus should be added by hand. Two hadrons, containing at least one light quark each, have a long-range strong interaction which is sometimes attractive and might contribute to binding. The best known example is the deuteron. The $(D\overline{D}^* + c.c.)$ is another possibility, which has perhaps been seen in the Belle data [4]. This light–light effect also contributes to the inner dynamics of hadrons with two or more light quarks.

In Sec. 5, we shall speculate about the role of an additional meson exchange interaction at the quark level, as in Ref. [9,10]. Only the residual interaction between light-flavour quarks is admitted to be significant. Accordingly, such an interaction, rescaled from the nucleon–nucleon interaction can increase the binding the two interacting mesons.

## 3   Phenomenological models

Several attempts have been made to build potentials that describe simultane-
ously meson and baryon masses, with a suitable ansatz for going from the quark–
antiquark to the quark–quark case [11]. Some models were even extended from
the heavy to the light quark sector [12] and can be applied to systems such as
charmed mesons and double charm baryons and tetraquarks.

For the sake of the discussion, we consider explicitly the potential of Bhaduri
et al. [12] and the AL1 potential [13], the parameters of which include constituent-
quark masses, the string tension of a linear confinement, the strength of the Cou-
lomb interaction, and the strength and size parameters of the hyperfine interac-
tion which is a smeared contact term. The Hamiltonian reads

$$H = \sum_i m_i + \sum_i \frac{\mathbf{p}_i^2}{2m_i} - \frac{(\sum_i \mathbf{p}_i)^2}{2\sum_i m_i} + \sum_{i<j} [V_\ell(r_{ij}) + V_c(r_{ij}) + V_h(r_{ij})] \,,$$

$$V_\ell(r_{ij}) = -\frac{3}{16} \lambda_i^c \cdot \lambda_j^c \, (a r_{ij} - b)\,, \quad V_c(r_{ij}) = -\frac{3}{16} \lambda_i^c \cdot \lambda_j^c \, \frac{\kappa}{r_{ij}}\,, \qquad (4)$$

$$V_h(r_{ij}) = -\frac{3}{16} \frac{\kappa}{m_i m_j r_0^2} \frac{\exp(-r_{ij}/r_0)}{r_{ij}} \lambda_i^c \cdot \lambda_j^c \, \sigma_i \cdot \sigma_j \,.$$

In the case of AL1, the smearing parameter $r_0$ depends on the reduced mass of
the quark pair.

## 4   Double charm baryons

An extensive study of the double-charm baryons has been performed by Fleck
and Richard [14] and a review of the situation at that time can be found in Refs.
[15,16]. This has been followed by other potential model studies, as for example,
Ref. [13]. These studies suggest that the ground state $\Xi_{cc}^{++}$ (ccu) and $\Xi_{cc}^{+}$ (ccd) have
a mass around 3.6 GeV (for more examples, see Ref. [17]). In a more recent work
[18] an effective scale-dependent strong-coupling constant which distinguishes
between qq, cq and cc pairs has been used to calculate the spectrum of double
charmed baryons, but the ground state of $\Xi_{cc}^{+}$ (ccd) was fitted to the SELEX data
[1,2] at 3520 MeV. Double-charm baryons have also been investigated in lattice
QCD. Predictions for masses and spin splittings were made in lattice nonrela-
tivistic quenched QCD calculations [19,20] prior to the SELEX experiment. Re-
cently, quenched lattice calculations with exact chiral symmetry [21] showed an
agreement with the published SELEX data [1,2]. There are also studies based on
an effective field theory Lagrangian approach adequate for heavy quarks [22].

In Table 1, preliminary estimates of the masses from the Bhaduri et al. po-
tential [12] are compared with the experimentally known masses. The results are
shown without and with hyperfine interaction. For single charm baryons we use
PDG data [23] and for the confirmed double charm baryon the SELEX data [1].
Note that the spin and parity are quark model predictions, not determined ex-
perimentally so far, even for single charm baryons. Our estimate is made with

**Table 1.** The baryon masses (in MeV) obtained obtained from the Bhaduri et al. [12] model, without and with hyperfine interaction $V_h$, compared to the experimental values, from PDG [23] for single charm and from SELEX data [1] for double charm baryons.

| Content | without $V_h$ | with $V_h$ | Exp. |
|---------|---------------|------------|------|
| cqq | 2500 | 2332 $(1/2^+)$ | $\Lambda_c$ (2285) |
|  |  | 2500 $(1/2^+)$ | $\Sigma_c$ (2455) |
|  |  | 2568 $(3/2^+)$ | $\Sigma_c$ (2520) |
| ccq | 3693 | 3643 $(1/2^+)$ | $\Xi_{cc}^+$(3520) |
|  |  | 3724 $(3/2^+)$ | ? |

the powerful method of Kamimura et al. [24]. So far, we have used a small number of terms in the Gaussian expansion. A better calculation with a larger basis will be presented elsewhere.

The mass of $(ccd)(1/2^+)$ is found around 3.6 GeV, consistent with several previous constituent quark model calculations [17] and lattice results [19,20]. Note that the hyperfine splitting of $(1/2)^+$ and $(3/2)^+$ states is about 80 MeV, similar to most quark model studies and lattice calculation results, but at variance with the 24 MeV splitting of Ref. [18], which seems to be anomalously small.

## 5    Tetraquarks

An understanding of baryons with two heavy quarks could make it possible to better extrapolate towards tetraquarks with double heavy flavour [25,26]. Let us consider the tetraquarks with open charm $cc\bar{q}\bar{q}$ which have been extensively studied in the framework of the Bhaduri et al. potential [12] or in some of its improved versions [13].

Table 2 displays the binding energy $\Delta E = M(cc\bar{q}\bar{q}) - M_{th}$ of the lowest state having spin $S = 1$ and isospin $I = 0$ calculated with the Bhaduri et al. potential and with the AL1 potential. The masses were obtained with two different numerical methods. The threshold mass is $M_{th} = M(D) + M(D^*)$.

**Table 2.** The $I = 0$, $S = 1$ tetraquark binding energy (in MeV) $\Delta E = M(cc\bar{q}\bar{q}) - M_{th}$, where the threshold mass $M_{th}$ is calculated with the same model.

| Potential | Bhaduri et al. | AL1 |
|-----------|----------------|-----|
| Silvestre-Brac & Semay [27] | 19 | 11 |
| Janc & Rosina [28] | −0.6 | −2.7 |

The tetraquark with spin $S = 1$ and isospin $I = 0$ appears unbound in Ref. [27], where the four-body problem is solved by an expansion in a harmonic-oscillator basis up to $N = 8$ quanta. However, it is bound in the calculations by Janc and Rosina [28], who used a multi-channel variational basis, as presented in

Ref. [29], by including, in particular, meson–meson type of asymptotic channels. It was already noted in Ref. [30] that the meson–meson configurations are important when the stability limit is approached. On the other hand, using the mass of 3520 MeV for ccu/ccd from SELEX the mass of the tetraquark $cc\bar{u}\bar{d}$ becomes about 3905 MeV i. e. some 35 MeV above the $D + D^*$ threshold [26], consistent with earlier estimates [25].

The picture of a "two-meson" state in tetraquarks also emerges from recent SU(3) lattice QCD calculations [31]. There it is seen as a flux-tube recombination, known as "flip-flop", when a quark and antiquark are near each other. The extension to pentaquarks has been considered in a more recent calculation [32].

There are several ways to increase the binding, all related to long-range forces. One concerns the confinement potential. The common assumption is that the confinement is two-body, although this is too a simplified picture in the light of lattice calculations [31]. It has been suggested that a three-body confinement interaction can be introduced as a colour operator via the cubic invariant of SU(3) [33]. This is a pure algebraic approach, without an underlying physical picture, so far. It can produce an increase of the binding, depending on the sign and strength of the three-body interaction [28].

## 6   Perspectives

It is remarkable that stable tetraquarks are predicted from Hamiltonians adjusted to 2- and 3-body systems and applied to 4-body systems. If the $(cc\bar{q}\bar{q})$ state exits, it will be accessible to ongoing and future experiments.

The prediction deserves further investigation and the natural question is whether or not the stability survives changes in the basic assumptions. This is the aim of our present and future study. Several questions can be raised, for instance:

- are the relativistic effects important, are they more important in tetraquarks than in mesons and baryons?
- is the interaction between quarks pairwise?
- in the case of a two-body interaction is the $\lambda_i^c \cdot \lambda_j^c$ operator appropriate to describe the colour dependence?
- is the linear parametrisation of the confinement adequate?
- do we need to introduce asymptotic-freedom type of correction to the strength $\kappa$ of the Coulomb term?
- is the chromomagnetic interaction $V_h \propto \lambda_i^c \cdot \lambda_j^c \, \sigma_i \cdot \sigma_j$ realistic enough to describe hyperfine effects?
- do results on stability depend strongly on the assumed regularisation of the hyperfine interaction?
- does a tensor type interaction increase the binding in tetraquarks?

In addition to these questions, it seems crucial to us to investigate the role of the light–light effect mentioned in the introduction. This is required by chiral dynamics as well as by empirical evidence. An observation is that in simple quark models, it is difficult to accommodate simultaneously light and heavy

hadrons. Also a long-range hadron–hadron exists, if both hadrons contain light quarks. This suggests to introduce a residual interaction of meson-exchange type, admitted to be significant only between light quarks. This pedestrian way of implementing chiral symmetry at the quark level leads to interesting predictions. According to Refs. [9,10], the contribution of light pairs represents a fraction of the nucleon-nucleon interaction, so it can be obtained by rescaling the nucleon-nucleon interaction to the corresponding hadron–hadron system. In particular, the $\Xi_{cc} - \Xi_{cc}$ interaction includes a pion exchange component. Although its strength is only a fraction of the nucleon–nucleon interaction, [1] a deuteron-like bound state is likely to exist between double charm baryons because the kinetic energy has a less repulsive effect in $\Xi_{cc} - \Xi_{cc}$ than in NN, as a consequence of the large mass of $\Xi_{cc}$.

By analogy, we expect that in a $(cc\bar{q}\bar{q})$ system the $\bar{q}\bar{q}$ pair should bring an extra attraction like in $\Xi_{cc}$ - $\Xi_{cc}$, and possibly lead to stable tetraquarks against strong decays.

In the future we plan to estimate the contribution of the light pairs of quarks to the mass of $cc\bar{q}\bar{q}$ from a realistic nucleon-nucleon interaction, as for example the Paris potential [34].

The $(cc\bar{q}\bar{q})$ state has the unique feature to combine the heavy–heavy and light–light effects which are absent in its dissociation products, and hence offers the best possibility for multiquark binding.

# References

1. M. Mattson *et al.* [SELEX Collaboration], Phys. Rev. Lett. **89** (2002) 112001 [arXiv:hep-ex/0208014].
2. A. Ocherashvili *et al.* [SELEX Collaboration], Phys. Lett. B **628** (2005) 18 [arXiv:hep-ex/0406033].
3. B. Aubert *et al.* [BABAR Collaboration], Phys. Rev. Lett. **90** (2003) 242001 [arXiv:hep-ex/0304021].
4. S. K. Choi *et al.* [Belle Collaboration], Phys. Rev. Lett. **91**, 262001 (2003) [arXiv:hep-ex/0309032].
5. K. Abe *et al.* [Belle Collaboration], Phys. Rev. Lett. **94** (2005) 182002 [arXiv:hep-ex/0408126].
6. B. Aubert *et al.* [BABAR Collaboration], Phys. Rev. Lett. **95**, 142001 (2005) [arXiv:hep-ex/0506081].
7. J. Engelfried [SELEX Collaboration], Nucl. Phys. A **752** (2005) 121.
8. S. Nussinov and M. A. Lampert, Phys. Rept. **362** (2002) 193 [arXiv:hep-ph/9911532].
9. F. Froemel, B. Julia-Diaz and D. O. Riska, Nucl. Phys. A **750** (2005) 337 [arXiv:nucl-th/0410034].
10. B. Julia-Diaz and D. O. Riska, Nucl. Phys. A **755** (2005) 431 [arXiv:nucl-th/0405061].
11. D. P. Stanley and D. Robson, Phys. Rev. Lett. **45** (1980) 235.
12. R. K. Bhaduri, L. E. Cohler and Y. Nogami, Nuovo Cim. A **65** (1981) 376.
13. B. Silvestre-Brac, Few Body Syst. **20** (1996) 1.
14. S. Fleck and J.-M. Richard, Prog. Theor. Phys. **82** (1989) 760.

---

[1] For example, the light quark fraction of the central part and of the spin-isospin part of the long range interaction are 1/9 and 1/25 respectively [10].

15. M. J. Savage and R. P. Springer, Int. J. Mod. Phys. A **6** (1991) 1701.
16. S. Fleck and J.-M. Richard, Part. World **1** (1990) 67.
17. V. V. Kiselev, A. K. Likhoded, O. N. Pakhomova and V. A. Saleev, Phys. Rev. D **66**, 034030 (2002) [arXiv:hep-ph/0206140], and references therein.
18. J. Vijande, H. Garcilazo, A. Valcarce and F. Fernandez, Phys. Rev. D **70**, 054022 (2004) [arXiv:hep-ph/0408274].
19. R. Lewis, N. Mathur and R. M. Woloshyn, Phys. Rev. D **64** (2001) 094509 [arXiv:hep-ph/0107037].
20. N. Mathur, R. Lewis and R. M. Woloshyn, Phys. Rev. D **66**, 014502 (2002) [arXiv:hep-ph/0203253].
21. T. W. Chiu and T. H. Hsieh, Nucl. Phys. A **755**, 471 (2005) [arXiv:hep-lat/0501021].
22. N. Brambilla, A. Vairo and T. Rosch, Phys. Rev. D **72**, 034021 (2005) [arXiv:hep-ph/0506065].
23. S. Eidelman *et al.* [Particle Data Group], Phys. Lett. B **592** (2004) 1.
24. M. Kamimura , Phys. Rev. **A 38** (1988) 621; H. Kameyama, M. Kamimura and Y. Fukushima, Phys. Rev. **C 40** (1989) 974; E. Hiyama, Y. Kino and M. Kamimura, Prog. Part. Nucl. Phys. **51** (2003) 223.
25. M. Rosina and D. Janc, Eur. Phys. J. A **19**, 43 (2004) [arXiv:hep-ph/0311051].
26. B. A. Gelman and S. Nussinov, Phys. Lett. B **551** (2003) 296 [arXiv:hep-ph/0209095].
27. B. Silvestre-Brac and C. Semay, Z. Phys. C **57** (1993) 273; **61** (1994) 271; **59** (1993) 457.
28. D. Janc and M. Rosina, Few Body Syst. **35** (2004) 175 [arXiv:hep-ph/0405208].
29. D. M. Brink and F. Stancu, Phys. Rev. D **57** (1998) 6778.
30. S. Zouzou, B. Silvestre-Brac, C. Gignoux and J. M. Richard, Z. Phys. C **30** (1986) 457.
31. F. Okiharu, H. Suganuma and T. T. Takahashi, Phys. Rev. D **72** (2005) 014505 [arXiv:hep-lat/0412012].
32. F. Okiharu *et al.*, arXiv:hep-ph/0507187.
33. V. Dmitrasinovic, Phys. Lett. B **499** (2001) 135 [arXiv:hep-ph/0101007].
34. M. Lacombe, B. Loiseau, J. M. Richard, R. Vinh Mau, J. Cote, P. Pires and R. De Tourreil, Phys. Rev. C **21** (1980) 861.

# Point-Form and Instant-Form Calculations of Electroweak Elastic and Inelastic Form Factors

R.F. Wagenbrunn

Institut für Physik, Fachbereich Theoretische Physik, Karl-Franzens-Universität Graz,
Universitätsplatz 5, A-8010 Austria

**Abstract.** In this contribution we address the calculation of electromagnetic and axial nucleon form factors within a relativistic constituent quark model. We show and discuss results for elastic form factors obtained in the point and instant forms within a spectator model for the current operator.

## 1  Introduction

Quantum chromodynamics (QCD) is nowadays accepted as the fundamental theory of strong interactions. However, it still cannot (yet) be solved — accurately enough — in the low-energy domain. Therefore, for the description of low-energy hadron properties one has developed effective (field) theories and/or effective models. A promising approach is offered by constituent quark models (CQMs). These can be constructed so as to take into account the relevant properties of QCD in the low-energy regime, notably the consequences of the spontaneous breaking of chiral symmetry. At the same time the requirements of special relativity are incorporated by adhering to the framework of Poincaré-invariant quantum mechanics [1].

It relies on a relativistically invariant mass operator with the interactions included according to the Bakamjian-Thomas construction [2], thereby fulfilling all the required symmetries of special relativity. That means that a representation of the Poincaré-group on the Hilbert-space with a finite number of degrees of freedom is established. There are three main different forms of dynamics [3] which are specified through the interaction going into different sets of generators. The other generators which are not affected by the interaction are called kinematic and generate a subgroup of the Poincaré-group, the so-called stability group. In this contribution we only consider the point and instant forms. In the point form the stability group is the Lorentz group, i.e., all rotations and boosts, while all four components of the momentum operator (generating the translations in space-time) are dynamical. In the instant form the stability group is the three-dimensional Euclidean group, i.e., all spatial rotations and translations, while the generators of the boosts and the 0-component of the momentum operator are dynamical. The Bakamjian-Thomas construction must therefore be different for point form and instant form. For both cases we can, however, adopt the same invariant mass operator, leading to the same spectrum.

In this contribution we consider a constituent quark model where the interaction relies on the exchange of Goldstone bosons between the constituent quarks [4]. Its dynamics was motivated by the idea that at low energies the dominant QCD degrees of freedom are furnished by constituent quarks and Goldstone bosons. The so-called Goldstone-boson-exchange (GBE) CQM for baryons relies thus on the mass operator

$$\sum_{i=1}^{3} \sqrt{\mathbf{k}_i{}^2 + m_i^2} + \sum_{i<j=1}^{3} [V_{conf}(ij) + V_{hf}(ij)] .$$ (1)

The first term represents the free mass operator of three particles, where $\mathbf{k}_i$ and $m_i$ are the three-momenta (fulfilling the restriction $\sum \mathbf{k}_i = 0$) and masses of the constituent quarks, respectively. The confinement potential $V_{conf}(ij)$ is taken in linear form. The hyperfine interaction $V_{hf}(ij)$ consists of the spin-spin part of the exchange of octet and singlet pseudoscalar bosons (mesons). The spectra for light and strange baryons are found by solving the eigenvalue problem

$$M|\Psi_B\rangle = m_B|\Psi_B\rangle,$$ (2)

where $|\Psi_B\rangle$ is the eigenstate of all 4 components of the momentum operator $P^\mu$ with eigenvalues $p_B^\mu$ and $m_B = \sqrt{p_B^\mu p_{B\,\mu}}$ is the mass eigenvalue of a baryon B.

Electromagnetic and axial form factors are obtained from matrix elements of current operators

$$\langle\Psi'_{B'}|J^\mu(0)|\Psi_B\rangle, \qquad \langle\Psi'_{B'}|A^\mu(0)|\Psi_B\rangle.$$ (3)

Here B and B′ can be the same for elastic form factors or different for inelastic form factors. The meaning of $\Psi'$ is that for B = B′ the momenta, spin projections and isospin-projections can be different. For all explicit calculations one must find a representation of the eigenstates in basis states

$$|p_1, \sigma_1; p_2, \sigma_2; p_3, \sigma_3\rangle = |p_i, \sigma_i\rangle$$ (4)

of the Hilbert space where for a moving baryon $\sum \mathbf{p}_i \neq 0$. Due to the different character of boosts in point and instant forms these representations are different. We do not go into the details here but sketch only the crucial point. In both cases a separation of the internal motion and the motion of the total baryon is possible. In the point form all four components of the momentum operator are dynamical but the four-velocity operator $V^\mu = P^\mu/M$ is kinematic and both, the baryon states and the basis states, are eigenstates of $V^\mu$. Thus the representation of the baryon state in point form is given by

$$\langle p_i, \sigma_i|\Psi_B\rangle \sim \delta(\mathbf{v} - \mathbf{v}_B)\psi_B,$$ (5)

with $v^\mu = \sum p_i^\mu / \sqrt{(\sum p_i)^\mu (\sum p_i)_\mu}$ and $v_B^\mu = p_B^\mu/m_B$. In the instant form, on the other hand, the baryon states and the basis states are eigenstates of the spatial components of the momentum operator. Thus the representation of the baryon state in instant form is given by

$$\langle p_i, \sigma_i|\Psi_B\rangle \sim \delta\left(\sum \mathbf{p}_i - \mathbf{p}_B\right)\psi_B.$$ (6)

In both cases $\psi_B$ is the internal wave function depending on the restricted momenta $\mathbf{k}_i$ which is found by solving the mass eigenvalue equation. Due to the different $\delta$-functions, however, the relations between the $\mathbf{k}_i$ and the $p_i$ are different in point and instant form.

For the current operator we employ a spectator model where two constituent quarks are spectators (here two and three, the two other cases are taken into account by a factor three, noting the total symmetry of the wave function)

$$\langle p_i', \sigma_i' | J^\mu(0) | p_i, \sigma_i \rangle = 3\mathcal{N}\langle p_1', \sigma_1' | J_{[1]}^\mu(0) | p_1, \sigma_1 \rangle 2E_2 \delta(\mathbf{p}_2' - \mathbf{p}_2) 2E_3 \delta(\mathbf{p}_3' - \mathbf{p}_3) \quad (7)$$

and analogously for the axial current. The electromagnetic current for the struck quark can be defined as

$$\langle p_1', \sigma_1' | J_{[1]}^\mu(0) | p_1, \sigma_1 \rangle = e_1 \bar{u}(p_1', \sigma_1') \left[ f_1(Q^2)\gamma^\mu + i\frac{f_2(Q^2)}{2m_1}\sigma^{\mu\nu}q_\nu \right] u(p_1, \sigma_1). \quad (8)$$

Here $e_1$ is the charge and the functions $f_{1,2}$ are the Dirac and Pauli form factors of the constituent quark. They depend on $Q^2 = -q^\mu q_\mu$ with the momentum transfer $q^\mu = p'^\mu_B{}_{,} - p^\mu_B$ on the baryon. It is important to notice that $q^\mu \neq p'^\mu_1 - p^\mu_1 = \tilde{q}$ in either of the forms at least for one of the components $\mu = 0, 1, 2$ or $3$. The axial current for the struck quark can be defined as

$$\langle p_1', \sigma_1' | A_a^\mu | p_1, \sigma_1 \rangle = \bar{u}(p_1', \sigma_i') \left[ g_A(Q^2)\gamma^\mu + \frac{2f_\pi}{Q^2 + m_\pi^2} g_{\pi q}(Q^2)q^\mu \right] \gamma_5 \frac{\tau_a}{2} u(p_i, \sigma_i). \quad (9)$$

Here $a$ indicates the isospin component, $f_\pi$ and $m_\pi$ are the pion decay constant and mass, and the functions $g_A$ and $g_{\pi q}$ are the axial form factor of the constituent quark and the $Q^2$-dependent pion-quark coupling strength. The factor $\mathcal{N}$ has to be introduced in the point form only in order to reproduce the correct charge of the proton. We chose the form

$$\mathcal{N} = \left( \frac{m_{B'}m_B}{\sum \omega_i' \sum \omega_i} \right)^{\frac{3}{2}}, \quad (10)$$

where $\omega_i = \sqrt{\mathbf{k}_i^2 + m_i^2}$ and $\omega_i' = \sqrt{\mathbf{k}_i'^2 + m_i^2}$. Some discussion on this factor will be given later, see also [5,6].

In the calculations in the point form spectator model (PFSM) [40–42] we assumed $f_1(Q^2) = 1$, $f_2(Q^2) = 0$, $g_A(Q^2) = 1$, and $g_{\pi q}^2(Q^2)/(4\pi) = 0.67$, i.e., there are no explicit constituent quark form factors or anomalous magnetic moments. The value for $g_{\pi q}(Q^2)$ was taken according to the parametrization of the pion-exchange potential in the mass operator of the GBE CQM. In that respect the results were obtained as direct predictions, i.e., without further parameters beyond those of the constituent quark model fixed already for the description of the baryon spectra. In figure 1 we show results for the electromagnetic form factors of proton and neutron and the axial form factor of the nucleon. The PFSM results are represented by the dashed lines. In contrast to the definition above in the pion-pole term of the axial current $\tilde{q}$ and $\tilde{Q}^2 = -\tilde{q}^\mu \tilde{q}_\mu$ instead of $q^\mu$ and $Q^2$
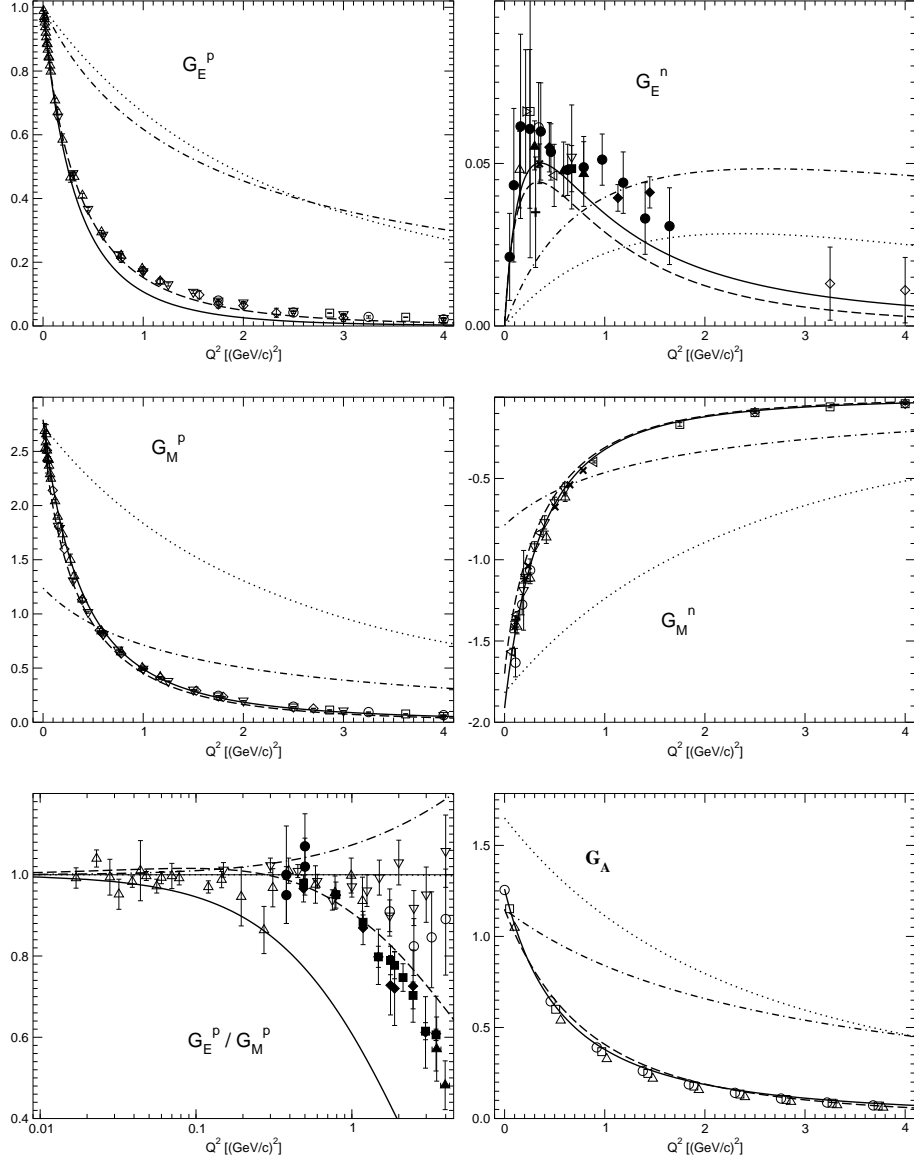
**Fig. 1.** Electromagnetic and axial form factors for the GBE CQM. In the top and central plots we show the electric and magnetic form factors of the proton (left) and the neutron (right), and in the bottom plots the ratio $G_E^p(Q^2)/G_M^p(Q^2)$ (left) and the axial nucleon form factor (right). The dashed lines are the PFSM results and the solid and dash-dotted lines are the IFSM results with and without constituent quark form factors and anomalous magnetic moments, respectively. For comparison the results for a nonrelativistic impulse approximation are also shown by the dotted lines. Data for electromagnetic form factors are from [7]–[37], for the axial form factor dipole shapes according to [38,39] are assumed.

was used in ref. [42]. The pion pole term only affects the induced pseudoscalar form factor, which we do not discuss in this contribution. For all form factors a rather reasonable agreement with the data is achieved within the PFSM. The PFSM results are very different from those obtained within a completely non-relativistic impulse approximation (NRIA), which is represented by the dotted lines in figure 1. The dash-dotted lines in figure 1 are the Breit frame IFSM results obtained as for the PFSM without constituent quark form factors or anomalous magnetic moments [43]. For the electric form factors they are closer to the NRIA than to the PFSM results. For the magnetic form factors the $Q^2$ dependence is also similar as for the NRIA but the values at $Q^2 = 0$, i.e., the magnetic moments, differ considerably from the values obtained in the PFSM and the NRIA and are about half of the size of the experimental values. The IFSM result for ratio of the electric to the magnetic proton form factor becomes greater than one opposite to the experimental findings. The axial charge in the IFSM is exactly the same as for the PFSM since it does not depend on the boosts but again the $Q^2$ dependence of the axial form factor is similar to the NRIA. The only way of describing the data within the IFSM is to introduce electromagnetic and axial form factors of the constituent quarks themselves (as was alos done in other models [44,45]). The solid lines in figure 1 show results with a simple parametrization

$$f_1^u(Q^2) = \left(1 + \frac{Q^2}{0.465 \text{ GeV}^2}\right)^{-1}, \tag{11}$$

$$f_2^u(Q^2) = 0.656 \left(1 + \frac{Q^2}{1.155 \text{ GeV}^2}\right)^{-2}, \tag{12}$$

$$f_1^d(Q^2) = \left(1 + \frac{Q^2}{0.384 \text{ GeV}^2}\right)^{-1}, \tag{13}$$

$$f_2^d(Q^2) = 0.767 \left(1 + \frac{Q^2}{1.022 \text{ GeV}^2}\right)^{-2}, \tag{14}$$

$$g_A^q(Q^2) = 1.1 \left(1 + \frac{Q^2}{0.49 \text{ GeV}^2}\right)^{-1}. \tag{15}$$

These form factors introduce also anomalous magnetic moments and an axial charge different from one for the constituent quarks. In that way an agreement with the data of similar quality as for the PFSM can be achieved for the IFSM. In particular the parameters have been chosen such that the experimental values for charge radii and magnetic moments of proton and neutron, as well as for the nucleon axial charge and radius are reproduced. On the other hand the result for the electric proton form factor falls off a little too fast with this parametrization. By introducing more fit parameters an even better agreement with the data could be found.

In the PFSM model the role of the normalization factor (10) has to be clarified. It is connected to momentum conservation or equivalently to translational invariance [5]. The momentum conservation of the total system gives rise to a δ-function of the difference of the sums of momenta of all incoming and of all outgoing particles in the corresponding transition amplitude. On the level of the

constituents the momentum conservation is violated, however. One could introduce a new δ-function depending on some effective momenta (called q̃). The relation between the two δ-functions must then somehow lead to the appearance of the normalization factor. We can reasonably motivate a normalization factor in the PFSM for elastic processes at zero momentum transfer of the form

$$\mathcal{N} = \left( \frac{m_B}{\sum \omega_i} \right)^3 . \tag{16}$$

For inelastic processes and/or nonzero momentum transfers we keep this expression but symmetrize with respect to incoming and outgoing states which yields just eq. (10). It turns out that the electromagnetic PFSM current does not explicitly violate current conservation for elastic form factors with a symmetric choice, i.e., it fulfills

$$q_\mu \langle \Psi'_B | J^\mu(0) | \Psi_B \rangle = 0 \tag{17}$$

in all frames. In the Breit frame eq. (17) requires $\langle \Psi'_B(\text{Breit}) | J^3(0) | \Psi_B(\text{Breit}) \rangle = 0$, which is also demanded by time reversal properties of the electromagnetic current (see for example [46]). However, we stress that eq. (17) is a necessary but not a sufficient condition for current conservation. Indeed it turns out that for electromagnetic transitions current conservation is violated with the PFSM current as defined above. The electromagnetic PFSM current operator must therefore be supplemented with some additional many-body current. It is important to notice, however, that the PFSM current cannot be a pure one-body current but has a many-body character by itself since q̃ and the normalization factor $\mathcal{N}$ depend on the momenta of all three constituent quarks of the incoming and outgoing baryons. This means also that it could effect some $Q^2$-dependence in the baryon form factor taking the role of constituent quark form factors. All together we emphasize that the PFSM current must not be interpreted as a one-body current of point-like constituents. How it can be furnished with additional terms to become a conserved conserved current operator requires further studies.

   The IFSM results have been calculated in the Breit frame. Since in the instant form the boosts are dynamical, the results for the form factors in the respective IFSM are frame dependent. The matrix elements for the elastic electromagnetic form factors in the Breit frame are consistent with current conservation (i.e., $\langle \Psi'_B(\text{Breit}) | J^3(0) | \Psi_B(\text{Breit}) \rangle = 0$) while in any other frame the IFSM current explicitly violates current conservation. Thus in such a frame one must add some additional current to restore current conservation. As long as there is no unique way how to do this the electric form factors which are related to the longitudinal components of the current cannot be extracted uniquely in that case. Thus it is reasonable to calculate elastic form factors in the Breit frame. We have not yet studied transition form factors in the IFSM. Maybe it is always possible to find a unique frame where the spectator current is consistent with current conservation which then can be taken for the most reasonable determination of the form factors. Since there is no normalization factor necessary in the IFSM the current can be closer related to the microscopic picture of a one-body current. However, also in the instant form the zero component of the momentum delivered to struck quark differs from that delivered to the baryon as a whole, i.e., $q_0 \neq \tilde{q}_0$.

The very different results of PFSM and IFSM with seemingly analogous currents for point-like constituent quarks may come due to the normalization factor in the PFSM. A concrete physical picture of this factor is required in order to understand the PFSM results and to judge whether their surprisingly close agreement with the data for the elastic electromagnetic and axial nucleon form factors is by chance or has some physical meaning. Furthermore only when one understands the starting point one can seriously think about adding additional many-body currents (like meson exchange currents in the GBE CQM) to the spectator current.

## Acknowledgment

## References

1. B. D. Keister and W. N. Polyzou, Adv. Nucl. Phys. **20**, 225 (1991).
2. B. Bakamjian and L. H. Thomas, Phys. Rev. **92**, 1300 (1953).
3. P. A. M. Dirac, Rev. Mod. Phys. **21**, 392 (1949).
4. L. Y. Glozman, W. Plessas, K. Varga, and R. F. Wagenbrunn, Phys. Rev. D **58**, 094030 (1998).
5. T. Melde, L. Canton, W. Plessas, and R. F. Wagenbrunn, Eur. Phys. J. A **25**, 97 (2005).
6. R. F. Wagenbrunn, T. Melde, and W. Plessas, arXiv e-Print hep-ph/0509047.
7. L. Andivahis *et al.*, Phys. Rev. D **50**, 5491 (1994).
8. R. C. Walker *et al.*, Phys. Lett. **B224**, 353 (1989).
9. A. F. Sill *et al.*, Phys. Rev. D **48**, 29 (1993).
10. G. Höhler *et al.*, Nucl. Phys. **B114**, 505 (1976).
11. W. Bartel *et al.*, Nucl. Phys. **B58**, 429 (1973).
12. T. Eden *et al.*, Phys. Rev. C **50**, R1749 (1994).
13. M. Meyerhoff *et al.*, Phys. Lett. **B327**, 201 (1994).
14. A. Lung *et al.*, Phys. Rev. Lett. **70**, 718 (1993).
15. C. Herberg *et al.*, Eur. Phys. J. A **5**, 131 (1999).
16. D. Rohe *et al.*, Phys. Rev. Lett. **83**, 4257 (1999).
17. M. Ostrick *et al.*, Phys. Rev. Lett. **83**, 276 (1999).
18. J. Becker *et al.*, Eur. Phys. J. A **6**, 329 (1999) with FSI corrections calculated by J. Golak *et al.*, Phys. Rev. C **63**, 034006 (2001).
19. I. Passchier *et al.*, Phys. Rev. Lett. **82**, 4988 (1999).
20. H. Zhu *et al.*, Phys. Rev. Lett. **87**, 081801 (2001).
21. R. Schiavilla and I. Sick, Phys. Rev. C **64**, 041002 (2001).
22. J. Bermuth *et al.*, Phys. Lett. **B564**, 199 (2003).
23. R. Madey *et al.*, Phys. Rev. Lett. **91**, 122002 (2003).
24. D. I. Glazier *et al.*, Eur. Phys. J. A **24**, 101 (2005).
25. P. Markowitz *et al.*, Phys. Rev. C **48**, R5 (1993).
26. S. Rock *et al.*, Phys. Rev. Lett. **49**, 1139 (1982).
27. E. E. W. Bruins *et al.*, Phys. Rev. Lett. **75**, 21 (1995).
28. H. Gao *et al.*, Phys. Rev. C **50**, R546 (1994).

29. H. Anklin *et al.*, Phys. Lett. **B336**, 313 (1994).
30. H. Anklin *et al.*, Phys. Lett. **B428**, 248 (1998).
31. W. Xu *et al.*, Phys. Rev. Lett. **85**, 2900 (2000).
32. G. Kubon *et al.*, Phys. Lett. **B524**, 26 (2002).
33. W. Xu *et al.*, Phys. Rev. C **67**, 012201 (2003).
34. B. D. Milbrath *et al.*, Phys. Rev. Lett. **80**, 452 (1998); *erratum*: Phys. Rev. Lett. **82**, 2221 (1999).
35. M. K. Jones *et al.*, Phys. Rev. Lett. **84**, 1398 (2000).
36. O. Gayou *et al.*, Phys. Rev. Lett. **88**, 092301 (2002).
37. V. Punjabi *et al.*, Phys. Rev. C **71**, 055202 (2005).
38. A. Liesenfeld *et al.*, Phys. Lett. **B468**, 20 (1999).
39. T. Kitagaki *et al.*, Phys. Rev. D **28**, 436 (1983).
40. R. F. Wagenbrunn *et al.*, Phys. Lett. B **511**, 33 (2001).
41. L. Y. Glozman *et al.*, Phys. Lett. B **516**, 183 (2001).
42. S. Boffi *et al.*, Eur. Phys. J. A **14**, 17 (2002).
43. K. Berger, Ph.D. thesis, University of Graz, 2005.
44. F. Cardarelli, E. Pace, G. Salmè, and S. Simula, Phys. Lett. B **357**, 267 (1995).
45. M. De Sanctis, M. M. Giannini, E. Santopinto, and A. Vassallo, arXiv e-Print nucl-th/0506033.
46. L. Durand, III, P. C. DeCelles, and R. B. Marr, Phys. Rev. **126**, 1882 (1962).

# Soliton picture for pentaquarks

Herbert Weigel

Fachbereich Physik, Siegen University, Walter–Flex–Straße 3, D–57068 Siegen, Germany

**Abstract.** In this talk I report on a thorough comparison between the bound state and rigid rotator approaches to generate baryon states with non–zero strangeness in chiral soliton models. This comparison shows that the two approaches are equivalent in the large $N_C$ limit and that the prediction of pentaquark states is not an artifact of the rigid rotator approach. The comparison also paves the way to unambiguously compute the width of the $\Theta^+$ pentaquark in chiral soliton models.

## 1   Introduction

In this talk I have discussed two issues regarding pentaquarks in chiral soliton models. First I have reviewed the relation between exotic five–quark states and radial excitations. In particular I have explained that the wave–functions of the crypto–exotic partners of the pentaquarks have significant admixture of radial excitations of the ordinary baryons and that this may have significant impact on transition magnetic moments. I have extensively described that issue before [1] and will abstain from repeating it in these proceedings. Rather, I will focus on the second topic of my talk which deals with potential differences between the bound state and rigid rotator approaches (BSA and RRA, respectively) to generate baryon states with non–zero strangeness from the classical soliton; two seemingly different treatments of the *same* model. It has previously been argued that the prediction of pentaquarks, *i.e.* exotic baryons with strangeness $S = +1$, would be a mere artifact of the RRA [2]. A major result of the investigation presented in this talk is that pentaquark states do indeed emerge in both approaches. This comparison furthermore shows how to unambiguously compute the width of pentaquarks. That computation differs substantially from previous approaches based on assuming pertinent transition operators for $\Theta^+ \to KN$ [3,4]. Details of these studies and an exhaustive list of relevant references are contained in the recent paper [5] in collaboration with Hans Walliser.

The qualitative results, on which I focus, are *model independent* while quantitative results may be quite sensitive to the model parameters and/or the actual form of the chiral Lagrangian. For simplicity, our calculations in ref. [5] have been performed in the Skyrme model Lagrangian augmented by the Wess–Zumino and the simplest flavor symmetry breaking terms. The latter parameterizes the kaon–pion mass difference. Chiral soliton calculations are organized in powers of $N_C$, the number of colors and hidden expansion parameter of QCD. The leading

contribution is the classical soliton energy, $E_{cl} = \mathcal{O}(N_C)$. The reported calculation is complete to $\mathcal{O}(N_C^0)$, allows to separate the resonance contribution in the kaon–nucleon scattering amplitude and provides insight in $1/N_C$ corrections.

## 2    Small amplitude vs. collective coordinate quantization

I start with phrasing the problem by briefly reviewing the two popular approaches to generate baryon states with strangeness $S = \pm 1$ from a soliton configuration. Chiral soliton models are in general functionals of the chiral field, $U$, the non–linear realization of the pseudoscalar fields. Starting point in these considerations is the classical soliton, *i.e.* the hedgehog embedded in the isospin subgroup of flavor $SU(3)$,

$$U_0(\boldsymbol{x}) = \exp\left[i\boldsymbol{\tau} \cdot \hat{x}F(r)\right] , \quad r = |\boldsymbol{x}| \tag{1}$$

parameterized by the three Pauli matrices $\tau_i$. The essential issue, however, is the treatment of the strange degrees of freedom, the kaons.

The *ansatz* for small amplitude quantization of kaon modes, known as BSA, reads

$$U(\boldsymbol{x},t) = A_2(t)\sqrt{U_0(\boldsymbol{x})} \exp\left[\frac{i}{f_\pi} \sum_{\alpha=4}^{7} \lambda_\alpha \eta_\alpha(\boldsymbol{x},t)\right] \sqrt{U_0(\boldsymbol{x})}\, A_2^\dagger(t) , \tag{2}$$

where $\lambda_\alpha$ are Gell–Mann matrices of $SU(3)$. The fluctuations $\eta_\alpha$ are treated as small amplitude fluctuations in harmonic approximation. The pion decay constant, $f_\pi$ is $\mathcal{O}(\sqrt{N_C})$. Hence this harmonic expansion is complete at $\mathcal{O}(N_C^0)$. Subleading contributions may be substantial but they are not under control in the BSA. The dynamical treatment of the collective coordinates, $A_2 \in SU(2)$ for the spin–isospin orientation of the soliton adds some of them. Quantization of both $\eta$ and $A_2$ results in the mass formula

$$M_S = E_{cl} + \omega_S + \frac{1}{2\Theta_\pi}\left[c_S J(J+1) + (1 - c_S) I(I+1)\right] + \mathcal{O}\left(\eta^4\right) . \tag{3}$$

for strangeness $S = \pm 1$ baryons. Here $J$ and $I$ are the spin and isospin quantum numbers of the considered baryon, respectively. The parameters in eq. (3) can be approximated as functionals of the chiral angle, $F(r)$ and are conveniently described by defining $\omega_0 = \frac{N_C}{4\Theta_K}$,

$$\omega_\pm = \frac{1}{2}\left[\sqrt{\omega_0^2 + \frac{3\Gamma}{2\Theta_K}} \pm \omega_0\right] \quad \text{and} \quad c_\pm = 1 - \frac{4\Theta_\pi \omega_\pm}{8\Theta_K \omega_\pm \mp N_C} . \tag{4}$$

The difference between $\omega_+$ and $\omega_-$ originates from the Wess–Zumino term. Explicit expressions for the moments of inertia $\Theta_\pi$ (rotation in coordinate space) and $\Theta_K$ (rotations in $SU(3)$ flavor space) as well as the symmetry breaking parameter $\Gamma$ (proportional to $m_K^2 - m_\pi^2$) may be traced from the literature [5]. They are all $\mathcal{O}(N_C)$.

The second approach treats the kaon modes purely as collective excitations of the classical soliton, eq. (1). These collective modes are maintained to all orders

and quantized canonically. The *ansatz* for this so–called rigid rotator approach (RRA) reads

$$U(\boldsymbol{x},t) = A_3(t)U_0(\boldsymbol{x})A_3^\dagger(t) \quad \text{with} \quad A_3(t) \in SU(3). \tag{5}$$

This parameterization describes only a limited number of soliton excitations, those that arise as a rigid rotation of the classical soliton. Though generating contributions of $\mathcal{O}(N_C^0)$ to baryon masses it is not complete at this order, *e.g.* S–wave excitations are not accessible. However, since the rigid rotations are treated to any order, they may account for significant subleading effects on the low–lying P–wave baryons. From the *ansatz*, eq. (5) the Hamiltonian for the collective coordinates is straightforwardly derived. The corresponding baryon spectrum is the solution to the eigenvalue problem ($D_{ab} = \frac{1}{2}\text{tr}[\tilde{A}\lambda_a A^\dagger \lambda_b]$)

$$\left\{ \left( \frac{1}{2\Theta_\pi} - \frac{1}{2\Theta_K} \right) J(J+1) + \sum_{a=1}^{7} \frac{R_a^2}{2\Theta_K} + \frac{\Gamma}{2}(1 - D_{88}) \right\} \Psi = \mathcal{E}\Psi, \quad R_8\Psi = \frac{N_C}{2\sqrt{3}}\Psi, \tag{6}$$

in each spin–isospin channel. The $R_a$ denote the (intrinsic) $SU(3)$ generators conjugate to the collective rotations $A_3 \in SU(3)$. This eigenvalue problem is (numerically) exactly solved for arbitrary (odd) $N_C$ and symmetry breaking $\Gamma$ by generalizing the techniques of ref. [6]. The spectrum is then determined by the eigenvalues $\mathcal{E}$. In the flavor symmetric case the eigenstates are members of $SU(3)$ representations. For $N_C = 3$ those are the octet and the decuplet for the low–lying $J = \frac{1}{2}$ and $J = \frac{3}{2}$ baryons, respectively. Also low–lying are states in the anti–decuplet. The probably lowest mass state in the anti–decuplet is the $\Theta^+$ pentaquark. For arbitrary $N_C$ the condition on $R_8$ alters the allowed $SU(3)$ representations and the inclusion of flavor symmetry breaking leads to mixing of states from different representations. These effects are incorporated in the numerical solution. In figures 1 and 2 I compare the spectra for the low–lying P–wave baryons obtained from eqs. (3) and (6) as functions of $N_C$.

Obviously the two approaches yield identical results as $N_C \to \infty$, as they should. This is the case for the ordinary hyperons and the pentaquarks. Figure 2 also shows that even with flavor symmetry breaking included, the $\Delta$–nucleon mass difference is $\mathcal{O}(1/N_C)$ in contrast to what is stated in ref. [7].

## 3   Constrained fluctuations and $\Theta^+$ width

The above observed identity between BSA and RRA in the large $N_C$ limit has a caveat. Though $\omega_- < m_K$ corresponds to a true bound state, $\omega_+$ is a continuum state. Thus, a pronounced resonance structure is expected in the corresponding phase shift. However, that is not the case, as indicated in the left panel of figure 3. The computed phase shift hardly reaches $\pi/2$ rather then quickly passing through this value. This has been used to argue that pentaquarks are a mere artifact of the RRA [2]. However, the ultimate comparison requires to generalize the RRA to the rotation–vibration approach (RVA)

$$U(\boldsymbol{x},t) = A_3(t)\sqrt{U_0(\boldsymbol{x})}\exp\left[\frac{i}{f_\pi}\sum_{\alpha=4}^{7}\lambda_\alpha\tilde{\eta}_\alpha(\boldsymbol{x},t)\right]\sqrt{U_0(\boldsymbol{x})}A_3(t)^\dagger. \tag{7}$$
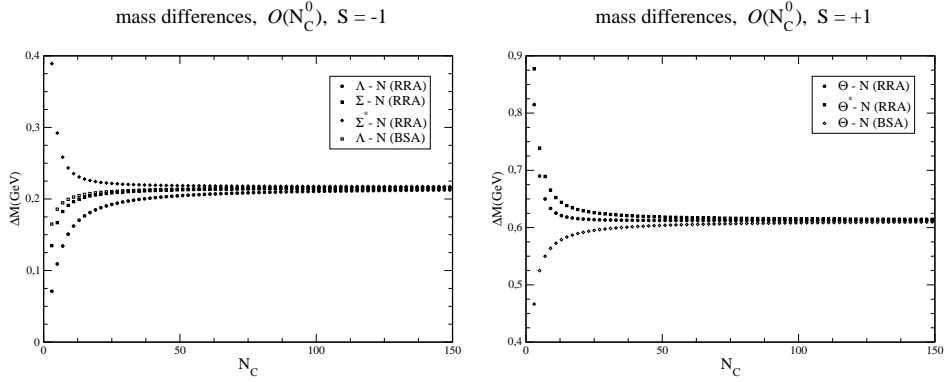
**Fig. 1.** Mass differences at $\mathcal{O}(N_C^0)$ computed within the bound state and rigid rotator approaches (BSA and RRA, respectively) in the Skyrme model as functions of $N_C$. In the RRA they are the corresponding differences of the eigenvalues in eq. (6) while in the BSA they are extracted from eq. (3). Left panel $\Delta S = -1$; right panel $\Delta S = +1$.
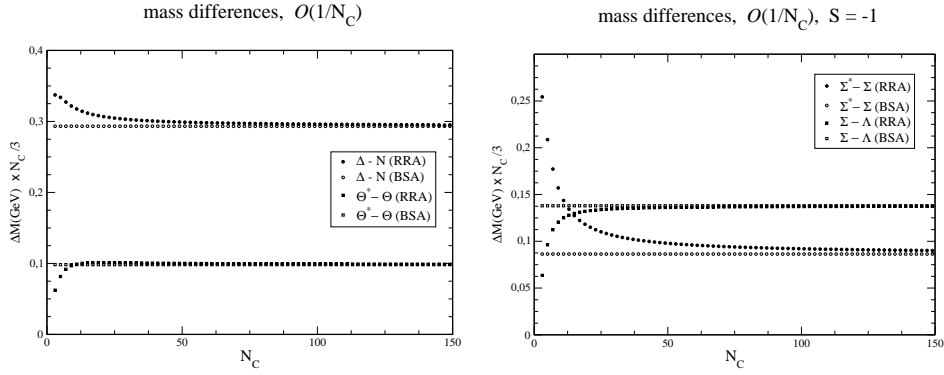


**Fig. 2.** Mass differences at $\mathcal{O}(1/N_C)$ computed in the Skyrme model as functions of $N_C$. Left panel: baryons with strangeness $S = 0, 1$; right panel $S = -1$. See also caption of figure 1.

Modes that correspond to the collective rotations must be excluded from the fluctuations $\widetilde{\eta}$, *i.e.* the fluctuations must be orthogonal to the zero–mode $z(r) \sim \sin\left(\frac{F(r)}{2}\right)$. Imposing the corresponding constraints for these fluctuations (and their conjugate momenta) yields integro–differential equations listed in ref. [5]. For the moment let's omit those effects on $\widetilde{\eta}$ that originate from the exchanges of collective excitations. This truncation defines the background wave–function $\overline{\eta}$ (also orthogonal to the zero mode). Treating $\overline{\eta}$ as an harmonic fluctuation provides the background phase shift shown as the blue curve in the right panel of figure 3. Remarkably, the difference between the phase shifts of $\overline{\eta}$ and $\eta$ exhibits a clear resonance structure. It is the resonance phase shift to be associated with the $\Theta^+$ pentaquark in the limit $N_C \to \infty$.

There is actually an even more convincing computation of this resonance phase shift. In contrast to the parameterization, eq. (2) the *ansatz*, eq. (7) yields an interaction Hamiltonian that is linear in the fluctuations, generating Yukawa couplings between the collective soliton excitations (eigenstates of eq. (6)) and the background fluctuations ($\overline{\eta}$). In ref. [5] we have derived this Hamiltonian keeping all contributions that survive as $N_C \to \infty$. The corresponding Yukawa exchanges extend the integro–differential equations for $\overline{\eta}$ by a separable potential, therewith providing the equations of motion for $\widetilde{\eta}$ [5]. When treated in an R–matrix formalism on top of the constrained fluctuations $\overline{\eta}$, this separable potential *exactly* yields the resonance phase shift shown in figure 3 when the Yukawa coupling is computed for $N_C \to \infty$. Moreover, in that limit the equation of motion for $\widetilde{\eta}$ is solved by $\widetilde{\eta} = \eta - az$ with $a = \langle z|\eta \rangle$ [5]. Here $\eta$ is the unconstrained small amplitude fluctuation of the BSA, eq. (2). The phase shifts extracted from $\eta$ and $\widetilde{\eta}$ are identical because $z(r)$ is localized in space.
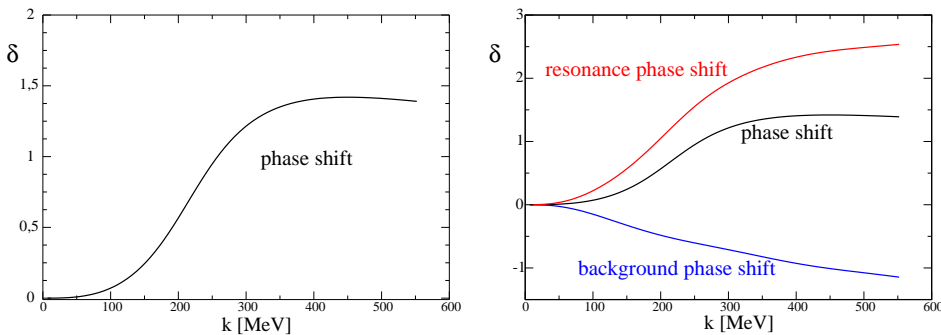


**Fig. 3.** Phase shift computed in the BSA (left panel) and resonance phase shift after removal of the background contribution in the RVA (right panel). Note the different scales.

Thus the BSA and RVA yield the same spectrum and are indeed equivalent in the large $N_C$ limit. But, the RVA provides a distinction between resonance and background contributions ($\widetilde{\eta}$ vs. $\overline{\eta}$) to the scattering amplitude. Hence pentaquarks are no artifacts of the collective coordinate approach. They are also predicted by the BSA; just well hidden. On top of that, the RVA is suitable to obtain finite $N_C$ corrections to the BSA for the properties of $\Theta^+$.

Though these general results are model independent, the numerical results for the masses and the widths of pentaquarks are not. The predictions may suffer from subleading $1/N_C$ contributions that can only be roughly estimated. For example, in the case $m_K = m_\pi$ the mass difference with respect to the nucleon increases by a factor two from $\omega_0$ to $(N_C+3)/4\Theta_K$ for $N_C = 3$. In the realistic case with $m_K \neq m_\pi$ this mass difference is obtained from solving the eigenvalue problem, eq. (6). Furthermore, the resonance (extracted from the comparison between $\widetilde{\eta}$ and $\overline{\eta}$) becomes sharper as $N_C < \infty$ [5].

The above mentioned separable potential provides the general expression for the width as a function of the kaon energy $\omega_k = \sqrt{k^2 + m_K^2}$ from the R-matrix formalism [5]

$$\Gamma(\omega_k) = 2k\omega_0 \left| X_\Theta \int_0^\infty r^2 dr\, z(r) 2\lambda(r)\overline{\eta}_{\omega_k}(r) \right.$$
$$\left. + \frac{Y_\Theta}{\omega_0} \left(m_K^2 - m_\pi^2\right) \int_0^\infty r^2 dr\, z(r)\overline{\eta}_{\omega_k}(r) \right|^2. \qquad (8)$$

Here $\overline{\eta}_{\omega_k}(r)$ is the P–wave projection of the background wave–function $\overline{\eta}$ for a prescribed energy $\omega_k = \sqrt{k^2 + m_K^2}$. Furthermore $\lambda(r)$ is a radial function that stems from the Wess–Zumino term. The matrix elements of the collective coordinate operators that enter in eq. (8) ($D_{\pm a} = D_{4a} \pm iD_{5a}$)

$$X_\Theta := \sqrt{\frac{32}{N_C}} \langle \Theta^+ | \sum_{\alpha,\beta=4}^{7} d_{3\alpha\beta} D_{+\alpha} R_\beta |n\rangle \,, \qquad (9)$$

$$Y_\Theta := \sqrt{\frac{8N_C}{3}} \langle \Theta^+ | \sum_{\alpha,\beta=4}^{7} d_{3\alpha\beta} D_{+\alpha} D_{8\beta} |n\rangle \qquad (10)$$

approach unity as $N_C \to \infty$ in the flavor symmetric case. In general they are computed from the eigenstates of the collective coordinate Hamiltonian, eq. (6). The resulting width is shown for $N_C = 3$ in figure 4 for the flavor symmetric case and the physical kaon–pion mass difference.
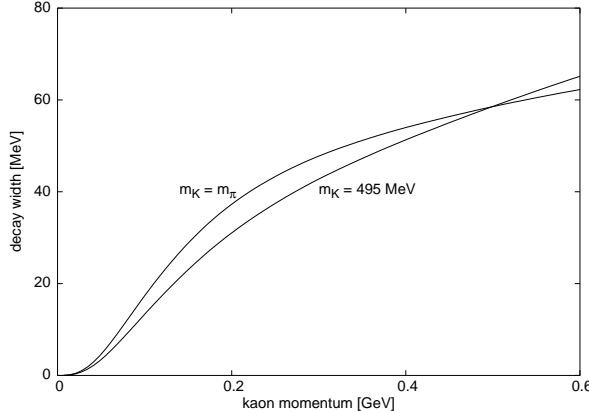


**Fig. 4.** Model prediction for the decay width, $\Gamma(\omega)$ of $\Theta^+$ for $N_C = 3$ as function of the kaon momentum $k = \sqrt{\omega^2 - m_K^2}$, *cf.* eq. (8). Top: $m_K = m_\pi$, bottom: $m_K \neq m_\pi$.

As function of momentum, there are only minor differences between these two cases. Assuming the observed resonance to be the (disputed [8]) $\Theta^+(1540)$ a width of roughly 40MeV is read off from figure 4 [5].

## 4   Conclusion

In this talk I have presented a thorough comparison [5] between the bound state (BSA) and rigid rotator approaches (RRA) to chiral soliton models in flavor $SU(3)$. For definiteness I have only considered the simplest version of the Skyrme model augmented by the Wess–Zumino and symmetry breaking terms. However, this analysis merely concerns the treatment of kaon degrees of freedom. Therefore the qualitative results are valid for *any* chiral soliton model.

A sensible comparison with the BSA requires the consideration of harmonic oscillations in the RRA as well. They can indeed be combined to the rotation–vibration approach (RVA), however constraints must be implemented to ensure that the introduction of such fluctuations does not double–count any degrees of freedom. The RVA then clearly shows that the prediction of pentaquarks is not an artifact of the RRA, pentaquarks are genuine within chiral soliton models. Only within the RVA chiral soliton models generate interactions for hadronic decays. Technically the derivation of this Hamiltonian is quite involved, however, the result is as simple as convincing: In the limit $N_C \to \infty$, in which the BSA is undoubtedly correct, the RVA and BSA yield identical results for both the baryon spectrum as well as the kaon–nucleon S-matrix. This equivalence also holds when flavor symmetry breaking is included. This result is very encouraging as it clearly demonstrates that collective coordinate quantization is valid regardless of whether or not the respective modes are zero–modes. Though the large $N_C$ limit is helpful for testing the results of the RVA, taking only leading terms in the respective matrix elements is not trustworthy.

In the flavor symmetric case the interaction Hamiltonian contains only a single structure ($X_\Theta$) of $SU(3)$ matrix elements for the $\Theta^+ \to KN$ transition. Any additional $SU(3)$ structure only enters via flavor symmetry breaking. This proves earlier approaches [3,4] incorrect that adopted any possible structure that would contribute in the large $N_C$ limit and fitted coefficients from a variety of hadronic decays under the assumption of $SU(3)$ relations. That treatment yielded a potentially small $\Theta^+$ width from cancellations between different such structures even in the flavor symmetric case. The study presented in this talk thus clearly shows that it is not worthwhile to bother about the obvious arithmetic error in ref. [3] that was discovered earlier [1,9] because the conceptual deficiencies in such width calculations are more severe. Assuming $SU(3)$ relations among hadronic decays is not a valid procedure in chiral soliton models. The embedding of the classical soliton breaks $SU(3)$ and thus yields different structures for different hadronic transitions. Especially strangeness conserving and changing processes are not related to each other in chiral soliton model treatments.

Even in case pentaquarks turn out not to be what recent experiments have indicated, they have definitely been very beneficial in combining the bound state and rigid rotator approaches and solving the Yukawa problem in the kaon sector; both long standing puzzles in chiral soliton models.

# References

1. H. Weigel, Eur. Phys. J. A **2** (1998) 391;  AIP Conf. Proc. **549** (2002) 271;  Eur. Phys. J. A **21** (2004) 133; `arXiv:hep-ph/0410066`.

2. N. Itzhaki, I. R. Klebanov, P. Ouyang and L. Rastelli, Nucl. Phys. B **684** (2004) 264.
   T. D. Cohen, Phys. Lett. B **581** (2004) 175; `arXiv:hep-ph/0312191`.
   A. Cherman, T. D. Cohen, T. R. Dulaney and E. M. Lynch, `arXiv:hep-ph/0509129`.

3. D. Diakonov, V. Petrov, M. Polyakov, Z. Phys. A **359** (1997) 305.

4. J. R. Ellis, M. Karliner, M. Praszałowicz, JHEP **05** (2004) 002;
   M. Praszałowicz, Acta Phys. Polon. B **35** (2004) 1625;
   M. Praszałowicz and K. Goeke, Acta Phys. Polon. B **36** (2005) 2255;
   `arXiv:hep-ph/0506041`.

5. H. Walliser, H. Weigel, `arXiv:hep-ph/0510055`.

6. H. Yabu and K. Ando, Nucl. Phys. B **301** (1988) 601.

7. M. Praszałowicz, Phys. Lett. B **583** (2004) 96.

8. K. Hicks, J. Phys. Conf. Ser. **9** (2005) 183;
   S. Kabana,  AIP Conf. Proc. **756** (2005) 195.

9. R. L. Jaffe, Eur. Phys. J. C **35** (2004) 221.

# Hadron spectroscopy of possible non-standard hadrons and pentaquark search at Belle

Ilija Bizjak[a], for the Belle Collaboration

[a]J. Stefan Institute, Ljubljana, Slovenia

**Abstract.** The record performance of the KEKB factory is currently supplying Belle with about 1 million $B\overline{B}$ meson pairs per day. The vast amounts of accumulated data have helped Belle Collaboration to discover new particle states in the charm sector. Two years ago a resonance X(3872) was discovered by Belle that does not seem to correspond to any conventional $c\bar{c}$ meson. Current analysis examined possible $J^{PC}$ quantum number assignments for the X(3872). After exhaustive and detailed investigations of its properties, it seems feasible that X(3872) could represent a first known example of a two-meson molecule. This year Belle reported observation of another possible non-conventional hadron, Y(3940). All that is known about it to date hints at the possibility that it may not be a standard quark-antiquark particle, but, instead, an example of a so-called "hybrid meson," which is a particle that is conjectured to be comprised of a quark, an antiquark and a gluon. Search for pentaquarks was also performed at Belle using kaon secondary interactions in the detector material, where the inclusive production of the $\Theta(1540)^+$ was examined. Upper limit was set on the ratio of the $\Theta(1540)^+$ to $\Lambda(1520)$ inclusive production cross-sections.

## 1 Introduction

The Belle detector [1] is situated at the KEKB $e^+e^-$ collider with asymmetric beam energies tuned to the energy of the $\Upsilon(4S)$ resonance [2]. Its main purpose is to explore CP violation in the decays of B mesons, but its very clean environment with small number of particles in events due to colliding leptons, and specially its record luminosity performance in collecting events, makes it suitable also for other types of analysis.

One of the active sidelines of the Belle detector is also a search for new possible non-standard resonances. Such a search enables us to test the predictions of QCD at low energies (bound states) where the running coupling constant $\alpha_s$ is large and QCD is in its non-perturbative regime.

Search for pentaquarks is also performed with Belle detector data. Since it was argued that the production mechanisms for pentaquark production might be different at different energies, we perform the search both in the B decays and in the events where charged kaons, with typical energies of $0.5\,\mathrm{GeV}$, interacted with the detector material.

## 1.1   Belle detector

The Belle detector is situated at the interaction region of the $e^+e^-$ beams, covering 92% of the solid angle. Several detector sub-parts enable reconstruction of tracks and identification of particles that were produced in the collision.

The sub-detector closest to the interaction point is the Silicon Vertex Detector (SVD) and it is used to measure the primary and secondary vertices of the produced tracks. The particle momenta are measured using the main tracking device of the detector, the Central Drift Chamber (CDC), which is enclosed in a superconducting solenoid, providing a homogeneous 1.5 T magnetic field. The identification of charged particles is performed with the help of the Time of Flight detector (TOF) and the Aerogel Cherenkov Counter (ACC), where particle velocities are measured through the Cherenkov effect. Combined information on momentum and velocity of the particle determines its mass; the efficiency for identification of charged kaons is about 85%, where the probability of mis-identification of a pion as a kaon is less than 10%, exact performance depending on the momentum and the direction of charged tracks. Electrons and photons are identified in the Electromagnetic Calorimeter (EC), where their energy is measured. Muons and $K_L$ candidates are detected using the $K_L$ and Muon detector (KLM).

## 1.2   Reconstruction of events with B mesons

The collisions of $e^+e^-$ produce a $q\bar{q}$ meson, where q can be any of the quarks u, d, s, c or b. A smaller sample of data is recorded at about 60 MeV below the mass of the $\Upsilon(4S)$, called continuum data, to study the effect of this continuum (non-$\Upsilon(4S)$) background on the B meson reconstruction.

The reconstruction of B decays needs to differentiate between events where $\Upsilon(4S)$ was produced and events where $q\bar{q}$ mesons with other quarks were produced. This is achieved by combining several observables separating the more spherical B meson decays (B mesons are produced almost at rest in the center-of-mass system of $e^+e^-$ (cms)) from the jet-like annihilation events [3].

The quality of B meson reconstruction is assessed based on the beam-constrained mass, $M_{bc} = \sqrt{E^{*2}_{beam}/c^4 - p^{*2}_B/c^2}$, and the energy difference, $\Delta E = E^*_B - E^*_{beam}$. Here $E^*_{beam} = \sqrt{s}/2 \simeq 5.290\,\text{GeV}$ is the beam energy in the cms, and $p^*_B$ and $E^*_B$ are the cms momentum and energy of the reconstructed B meson. These two variables are used instead of the invariant mass of the B meson, due to better resolution. For genuine decays of the B meson the $M_{bc}$ distribution has a peak at about $5.28\,\text{GeV}/c^2$, the mass of the meson, and $\Delta E$ peaks at zero.

To observe a resonance, such as the ones discussed in the following sections, a significant peaking component is searched for in the distributions of the beam-constrained mass near $5.28\,\text{GeV}/c^2$ and energy difference around zero, and the number of events reconstructed in the resonance is obtained by fitting the $M_{bc}$ and $\Delta E$ distributions to the sum of an empirical parametrization of the background plus a signal shape.

## 2    What kind of resonances are X(3872) and Y(3940)?

### 2.1   X(3872)

The resonance called X(3872) was discovered by the Belle collaboration in 2003 as an enhancement in the $B \rightarrow K\pi^+\pi^- J/\psi$ decays [4] and was soon after confirmed by three other experimental groups [5]. It was seen as a narrow peak in decays $B \rightarrow \pi^+\pi^- J/\psi K$, where the particle $J/\psi$ is reconstructed in the decays to two leptons: $J/\psi \rightarrow \ell^+\ell^-$. There are many difficulties in identifying X(3872) as a $c\bar{c}$ resonance. For example, the distribution of the invariant mass of the pion pair has a broad enhancement near the nominal $\rho$ mass that cannot be described well by the predicted phase space distribution, and seems to be consistent with a $\rho$ meson. The decay of a $c\bar{c}$ meson into $\rho J/\psi$ is isospin-violating and should be highly suppressed, indicating that the resonance X(3872) might not be one of the of the yet unidentified $c\bar{c}$ mesons. Belle collaboration therefore performed several tests [6,7] to determine X(3872) quantum numbers J, P and C, enabling it to make further interpretation. The observation of radiative $X(3872) \rightarrow \gamma J/\psi$ decays and
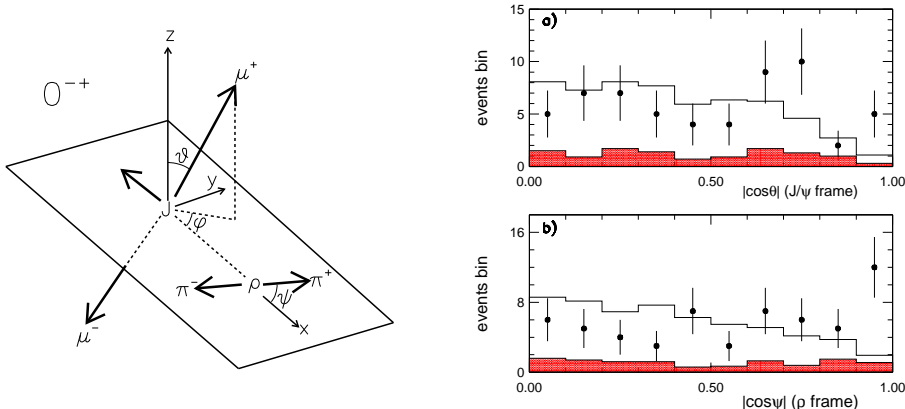


**Fig. 1.** $X(3872) \rightarrow \pi^+\pi^- J/\psi$ angular distributions for data (points), and for the $J^{PC} = 0^{-+}$ hypothesis (histogram), including background estimated from the mass sidebands (shaded). The definition of the angles is shown in the sketch on the left. The $\chi^2$ of the fits are (a) 17.7 and (b) 34.2 for 9 degrees of freedom, disfavoring $0^{-+}$. Note the concentration of events in the final bins, contrary to expectation.

subtreshold decays to $\omega^* J/\psi$ in $X(3872) \rightarrow \pi^+\pi^-\pi^0 J/\psi$ decays [6] indicate that the C-parity of X(3872) is even.

The analysis of angular correlations of X(3872) decays [7] was used to test different $J^{PC}$ hypotheses, exploiting the comparison of predicted distributions to data in the region where the predicted distribution has zeroes [8] (an example of such analysis is shown in Fig. 1). Such an analysis disfavored $0^{++}$ and $0^{+-}$, while showing good agreement with the $1^{++}$ assumption. The fits to the invariant mass distribution of the two charged pions in $X(3872) \rightarrow \pi^+\pi^- J/\psi$ decays favor $J^{++}$
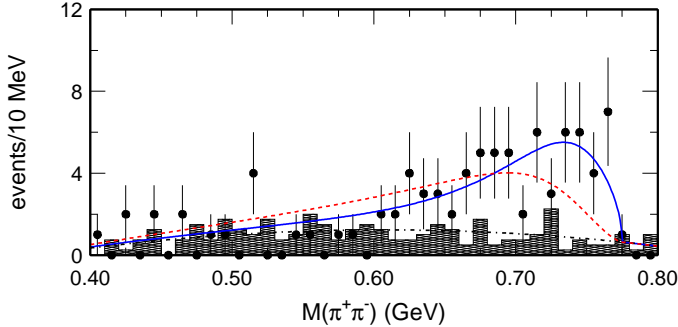
**Fig. 2.** The distribution of $M(\pi^+\pi^-)$ for events in the X(3872) signal region (points) and sideband (shaded). Fits for S-wave (solid) and P-wave (dashed) hypotheses are also shown, showing the preference for the S-wave hypothesis.

assignment (Fig. 2). The roll-off near the kinematical boundary has a different $q^*_{J/\psi}$ dependence for an S wave ($q^*_{J/\psi}$) compared to a P wave (($q^*_{J/\psi})^3$), yielding a better agreement for the S wave.

To compare the $1^{++}$ and $2^{++}$ assignments, the search of decays X(3872) $\rightarrow$ $D^0\overline{D}^0\pi^0$ was performed. The preliminary evidence of such decays disfavors $J^{PC} = 2^{++}$.

We conclude that the assignment for X(3872), corresponding best to our data, is $J^{PC} = 1^{++}$; it is unlikely, though, that X(3872) be the charmonium $1^{++}$ state $\chi'_{c1}$. Our conclusion rests on the following facts: The $\chi'_{c1}$ mass is predicted to be about $100\,\mathrm{MeV}/c^2$ higher than observed, the isospin-violating decays $\chi'_{c1} \rightarrow \pi^+\pi^- J/\psi$ should have a very small partial width, contradictory to the measurement, and the low ratio of radiative to dipion partial widths $\Gamma(X \rightarrow \gamma J/\psi)/\Gamma(X \rightarrow \pi^+\pi^- J/\psi) = 0.14 \pm 0.05$ [6], all disfavoring the $\chi'_{c1}$ interpretation.

The observed properties of X(3872) agree well with the molecular $D^0 - \overline{D}^{*0}$ model proposed by Swanson [9]. The mass of the resonance is within errors consistent to the sum of the masses of $D^0$ and $\overline{D}^{*0}$ mesons: $M(D^0) + M(\overline{D}^{*0}) - M(X) = 0.6 \pm 1.1\,\mathrm{MeV}/c^2$. Since the mass difference of $M(D^+D^{*-}) - M(D^0\overline{D}^{*0}) = 8.1\,\mathrm{MeV}/c^2$ is large compared to it, the isospin violation is natural for such a state, explaining the observation of nearly equally common decays of X to $2\pi J/\psi$ and $3\pi J/\psi$. The small value of $\Gamma(X \rightarrow \gamma J/\psi)/\Gamma(X \rightarrow \pi^+\pi^- J/\psi)$ is also predicted by the same model.

### 2.2 Y(3940)

It is natural to ask if the X(3872) resonance is the only non-standard meson candidate in this mass region or is there a new set of resonances with similar non-standard properties like X(3872). A search was performed for enhancements in the spectra of $\rho J/\psi$, $\eta J/\psi$ and $\omega J/\psi$. While the search in the first two modes was unsuccessful, we have observed [10] an enhancement in the spectrum of $\omega J/\psi$ just above the threshold (Fig. 3).
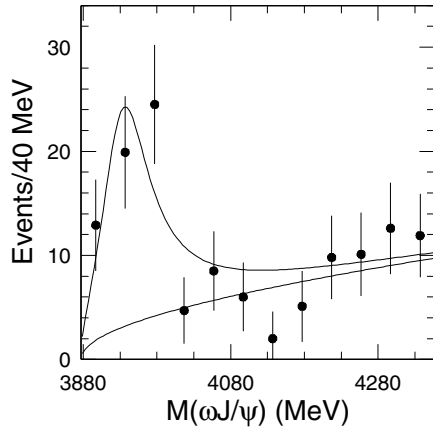
**Fig. 3.** The invariant mass distribution of $\pi^+\pi^-\pi^0 J/\psi$ just above the threshold for $\omega J/\psi$, from the $B^+ \to K^+\pi^+\pi^-\pi^0 J/\psi$ decays.

The B meson yield was obtained by a simultaneous fit to the $M_{bc}$ and $\Delta E$ distributions in bins of $25\,\mathrm{MeV}/c^2$ in $M(\omega J/\psi)$. The obtained yields are plotted in Fig. 3, where the lower curve shows the expectation for the pure phase space distribution, while the enhancement of events, present near the threshold, is fitted using an additional Breit-Wigner function. The Breit-Wigner signal yield is found to be $58 \pm 11$ events (with statistical significance above $8\sigma$) and was interpreted as a particle ($Y(3940)$) with mass $M = (3943 \pm 11 \pm 13)\,\mathrm{MeV}/c^2$ and decay width $\Gamma = (87 \pm 22 \pm 26)\,\mathrm{MeV}$.

Since the mass of $Y(3940)$ is above the $D\overline{D}^{(*)}$ mass threshold, if this is a standard $c\bar{c}$ resonance, its dominant decay should be to $D\overline{D}^{(*)}$, while the first observation of an enhancement in a decay channel other than $D\overline{D}$ is surprising. While its width makes it unlikely to be a tetraquark, it is a possible candidate for a $c\bar{c} - gluon$ hybrid, for which the decays to open charm are expected to be suppressed or forbidden. Further analysis, determining its quantum numbers, will help resolve its identity.

## 3   Pentaquark search

Belle has performed dedicated searches of some exotic states interpreted as pentaquarks, that were claimed to be observed in last few years [11,12]. Search was performed in both B decays, and, to mimic the production mechanism of some of the detectors observing pentaquarks [11], in the events where a kaon interacted with detector material.

The search for $\Theta^+$, $\Theta^{*++}$, $\Theta_c^0$ and $\Theta_c^{*+}$ was performed [13] in B decays to proton, anti-proton and a D meson or kaon, setting upper limits to ratios of branching fractions for decays proceeding over the searched exotic state to all decays with same decay products.

For example, for the search of $B^0 \to \bar{p}\pi^+\Theta_c^0 \to \bar{p}\pi^+D^-p$ the reconstructed $\Delta E$ distribution is shown in Fig.4 (left). For events in the signal region (consisting of $303\pm21$ signal events) the mass of the $D^-p$ is presented in Fig.4 (right). This distribution is fitted with a phenomenological function describing the background and a Gaussian signal, positioned at the mass of $3099\,MeV/c^2$, corresponding to the mass of the claimed $\Theta_c^0$ pentaquark [12]. Since the peak of the expected pentaquark should be narrower than the detector resolution, the width of the signal part was fixed at 3.5 MeV, the estimated detector resolution. No statistically significant signal was found and the corresponding 90% C.L. upper limit on the production of $\Theta_c^0$ relative to the $B^0 \to \bar{p}\pi^+D^-p$ branching ratio is placed at

$$Br(B^0 \to \Theta_c^0\bar{p}\pi^+) \cdot Br(\Theta_c^0 \to D^-p)/Br(B^0 \to \bar{p}\pi^+D^-p) < 1.2\% \ .$$
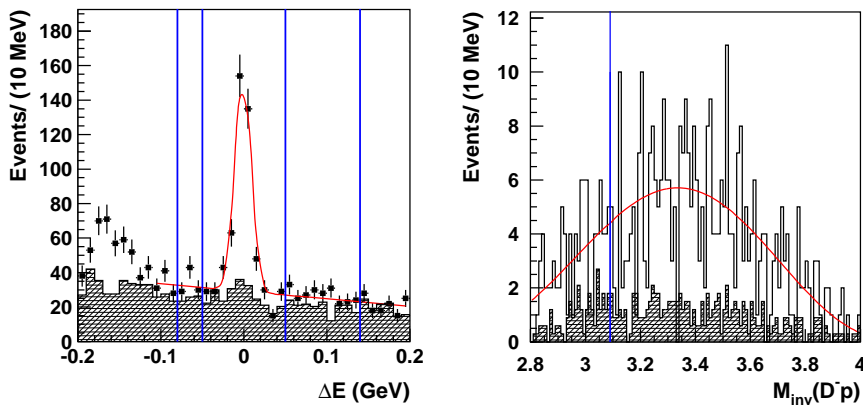


**Fig. 4.** Left: $\Delta E$ distribution of $B^0 \to \bar{p}\pi^+D^-p$ decays, the vertical lines flag the $\Delta E$ sideband. Right: Invariant mass of $D^-p$ pairs for events in $\Delta E$ signal region, the background (shaded) is estimated from the $\Delta E$ sideband. The result of the fit with a phenomenological model function is also shown (dotted/red), while the vertical line indicates $3099\,MeV/c^2$.

In the search using interactions of charged and neutral kaons in the material of the detector [14] the average energy of kaons is $0.5\,GeV$, creating "low energy" conditions of pentaquark search similar to that of the HERMES detector [11].

The coordinates of the common vertices of identified $K_s p$ and $K^\pm p$ pairs produce a "tomographic" picture of the detector (Fig. 5, left), where the distribution of the material in the beam pipe, ladders of SVD and the support structure of the CDC are clearly visible), showing that such pairs correspond to secondary reactions with the detector material.

The search is performed in $M(pK_S)$, the invariant mass of the $pK_S$ pair, by comparing the possible signal in $M(pK_S)$ to the large signal of $\Lambda(1520)$ in the $M(pK^-)$ distribution (Fig. 5, right).
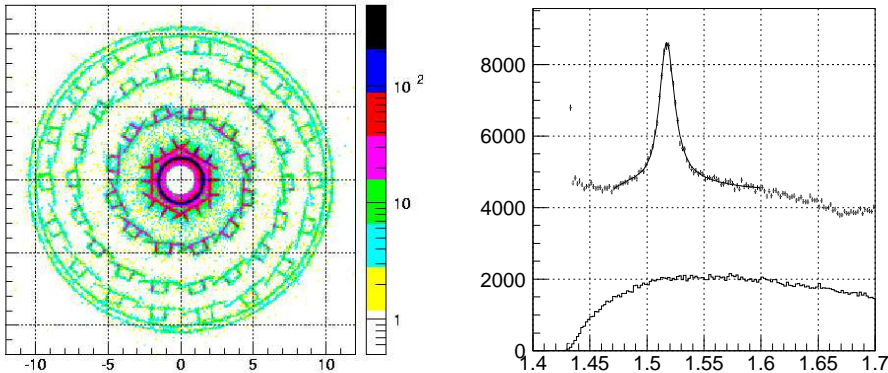
**Fig. 5.** Left: Scatter plot of pK vertices in the plane perpendicular to the beam, where various elements of the detector can be seen. Right: the invariant mass distributions for the $pK^-$ (top, with $\Lambda(1520)$ peak) and $pK_S$ pairs. (bottom).

In the $M(pK^-)$ distribution the $\Lambda(1520)$ peak in the $M(pK^-)$ is fitted with a threshold function and a D-wave Breit-Wigner term, convolved with the experimental resolution (2 MeV/c$^2$). The obtained parameters of $\Lambda(1520)$ are in agreement with the world average values [15]. The distribution for the $pK_S$ pairs is fitted with a third order polynomial and a narrow signal, positioned at different values of $M(pK_S)$. For $M(pK_S) = 1540\,\text{MeV/c}^2$, the mass of the claimed $\Theta^+$ pentaquark [11], the resulting signal yield is $58 \pm 129$ events. Assuming $\text{Br}(\theta^+ \to pK_S) = 25\%$, $\text{Br}(\Lambda(1520) \to pK^-) = 1/2\,\text{Br}(\Lambda(1520) \to N\overline{K})$, and evaluating the ratio of efficiencies for $\theta^+ \to pK_S$ and $\Lambda(1520) \to pK^-$ from MC, one arrives at the upper limit for $\theta^+$ production using Feldman-cousins method [16]:

$$\frac{\sigma(KN \to \theta^+ X)}{\sigma(\overline{K}N \to \Lambda(1520)X)} < 2.5\% \ \text{ at } \ 90\%\text{C.L.}$$

This result is two orders of magnitude lower than the value reported by the HERMES Collaboration [11].

## 4   Conclusion

Recent analyses show that the Belle detector is suitable also for searches of possible new exotic particles, which can test our understanding of QCD. The determination of quantum numbers of $X(3872)$ and the observation $Y(3940)$ opens a new page in exotic particle spectroscopy with exciting possibilities.

The search for pentaquarks puts Belle among the experiments with negative search results, which seem to outnumber those claiming to have detected pentaquarks. The puzzle is nevertheless far from resolved yet, and Belle will try to contribute to increasing the understanding in this field.

# References

1. A. Abashian et al. (Belle Collaboration), Nucl. Instrum. Meth. **A 479** (2002) 117.
2. S. Kurokawa, E. Kitakani, Nucl. Instr. Meth. A **A499** (2003) 1.
3. K. Abe *et al.* (Belle Collaboration), Phys. Rev. Lett. **87** (2001) 101801, and references therein.
4. S. K. Choi, S. L. Olsen et al. (Belle Collaboration), Phys. Rev. Lett. **91**, 262001 (2003).
5. D. Acosta et al. (CDF-II), Phys. Rev. Lett. **93** (2004) 072001;
   V. M. Abazov et al. (D0), Phys. Rev. Lett. **93** (2004) 162002;
   B. Aubert et al. (BaBar), Phys. Rev. D **71** (2005) 071103.
6. K. Abe et al. (Belle Collaboration), BELLE–CONF–0540, `arXiv:hep-ex/0505037`.
7. K. Abe et al. (Belle Collaboration), BELLE–CONF–0541, `arXiv:hep-ex/0505038`.
8. J. Rosner, Phys. Rev. D **70**, 094023 (2004).
9. E. S. Swanson, Phys. Lett. B **588** (2004) 189; Phys. Lett. B **598** (2004) 197.
10. S. K. Choi, S. L. Olsen et al. (Belle Collaboration), Phys. Rev. Lett. **94** (2005) 182002.
11. HERMES Collaboration, A. Airapetian et al., Phys. Lett. B **585** (2004) 213.
12. H1 Collaboration, A. Aktas et al., Phys. Lett. B **588** (2004) 17.
13. R. Mizuk (for the Belle Collaboration), `arXiv:hep-ex/0411005`.
14. K. Abe et al. (Belle Collaboration), BELLE–CONF–0518, submitted to Phys. Lett. B, `hep-ex/0507014`.
15. S. Eidelman et al. (Particle Data Group), Phys. Lett. B **592** (2004) 1.
16. G. J. Feldman and R. D. Cousins, Phys. Rev. D **57** (1998) 3873.

# Chiral models for exciting baryons[*]

B. Golli[a,b] and S. Širca[b,c]

[a] Faculty of Education, University of Ljubljana, 1000 Ljubljana, Slovenia
[b] Jožef Stefan Institute, 1000 Ljubljana, Slovenia
[c] Faculty of Mathematics and Physics, University of Ljubljana, 1000 Ljubljana, Slovenia

**Abstract.** We study low lying resonances in models in which the pions linearly couple to the quark core. We derive the coupled channel equations for pion scattering, and discuss preliminary results for pion scattering in the Roper channel.

## 1 Introduction

In our previous work [1–3] we have presented a method to calculate the K-matrix for pion scattering and electro-production in quark models with chiral mesons. The method has several advantages over more standard methods because it allows for a clear separation of the resonant part of the amplitude from the background. We have successfully applied it to the calculation of the phase shift and electro-production amplitudes in the P33 channel.

In the present work we extend the method to cover the cases where it is necessary to include two or more channels. This allows us to attack perhaps the most intriguing among the low lying resonances – the Roper resonance. In this contribution we develop the coupled channel formalism for scattering and present some preliminary results.

## 2 K matrix in chiral quark models

We consider quark models in which p-wave pions couple linearly to the three-quark core. Assuming a pseudo-scalar quark-pion interaction, the part of the Hamiltonian referring to pions can be written as

$$H_\pi = \int dk \sum_{mt} \left\{ \omega_k\, a^\dagger_{mt}(k) a_{mt}(k) + \left[ V_{mt}(k) a_{mt}(k) + V^\dagger_{mt}(k)\, a^\dagger_{mt}(k) \right] \right\}, \quad (1)$$

where $a^\dagger_{mt}(k)$ is the creation operator for a p-wave pion with the third components of spin $m$ and isospin $t$, and

$$V_{mt}(k) = -v(k) \sum_{i=1}^{3} \sigma^i_m \tau^i_t \qquad (2)$$

---

[*] Talk delivered by B. Golli

is the general form of the pion source, with $v(k)$ depending on the model.

In the basis with good total angular momentum $J$ and isospin $T$, in which the K and T matrices are diagonal, it is possible to express the K matrix in the form[3][1]

$$K^{JT}(k, k_0) = -\pi \sqrt{\frac{\omega_k}{k}} \langle \Psi_{JT}^P(W) \| V(k) \| \Phi_N \rangle \,. \tag{3}$$

The corresponding principal-value state[4] obeys

$$|\Psi_{JT}^P(W)\rangle = \sqrt{\frac{\omega_0}{k_0}} \left\{ \left[ a^\dagger(k_0)|\Phi_N\rangle \right]^{JT} - \frac{\mathcal{P}}{H-W} \left[ V(k_0)|\Phi_N\rangle \right]^{JT} \right\}, \tag{4}$$

where $[\;]^{JT}$ denotes coupling to good $J$ and $T$, and $k_0$ and $\omega_0$ the pion mementum and energy.

We assume that the operator $V$, acting on the ground state $\Phi_N$, does not only flip the quark spin and isospin but also excites quarks to higher spatial states. As an example let us mention the state with the flipped spins (the bare delta) which plays a crucial role in the formation of the $\Delta(1232)$ resonance, and the excitation of one quark to the 2s state which is believed to be the main mechanism in the formation of the Roper resonance.

The general form (4) therefore suggests the following ansatz in which the states with excited quark core, $\Phi_B$, are separated from the state corresponding to pion scattering on the nucleon. Neglecting the two-pion states we can write

$$|\Psi_{JT}(W)\rangle = \sqrt{\frac{\omega_0}{k_0}} \left\{ \left[ a^\dagger(k_0)|\Phi_N\rangle \right]^{JT} \right.$$
$$\left. + \int dk \, \frac{\chi(k, k_0)}{\omega_k - \omega_0} \left[ a^\dagger(k)|\Phi_N\rangle \right]^{JT} + \sum_B c_B(W)|\Phi_B\rangle \right\}. \tag{5}$$

The pion amplitude is related to the K matrix by

$$\chi(k_0, k_0) = \frac{k_0}{\pi \omega_0} K(k_0, k_0) \,. \tag{6}$$

## 3   Coupled channels

We have shown [3] that the above ansatz successfully describes scattering as well as electro-production of pions in the P33 channel at lower energies. At higher energies, the two pion decay channel becomes important and cannot be neglected. In most cases, the two pion decay proceeds through an intermediate resonance; in the P11 channel as well as in the P33 channel this is the $\Delta(1232)$ which accounts for 30 %–40 % of the width in the region of the Roper resonance and even 40 %–70 % in the region of the $\Delta(1600)$ resonance.

---

[1] In the static approximation, $k_0$ is uniquely related to the energy $W = E_N + \omega_0$, so one can use either $k_0$ or $W$ to label the states; for the on-shell K matrix we write $K(k_0, k_0) = K(W)$.

In the simplest extension of the model we therefore include an additional channel representing the pion scattering on the $\Delta(1232)$. The corresponding principle-value state takes the form:

$$|\Psi_{JT}^\Delta(W,E)\rangle = \sqrt{\frac{\omega_0}{k_0}}\left\{\left[a^\dagger(k_E)|\Psi_\Delta(E)\rangle\right]^{JT}\right.$$
$$\left. + \int dk\, \frac{\chi_\Delta(k,k_E)}{\omega_k - \omega_E}\left[a^\dagger(k)|\Psi_\Delta(E)\rangle\right]^{JT} + \sum_B c_B(W,E)|\Phi_B\rangle\right\}. \quad (7)$$

The key point in the above ansatz is that the energy of the delta state, $E$, is not fixed (e.g. to 1232 MeV) but is varied from the threshold value $E_N + m_\pi$ to the maximum allowed value $W - m_\pi$. (Obviously, this channel opens at the two-pion threshold, i.e at $W = E_N + 2m_\pi$.) For simplicity we work in the static limit in which the pion energy and momentum can be written as $\omega_E = W - E$, $k_E = \left(\omega_E^2 - m_\pi^2\right)^{1/2}$. The delta state in (7) is given by (5) except that it is now normalized to $\delta(E - E')$ rather than to $(1 + K_\Delta(E)^2)\delta(E - E')$:

$$|\Psi_\Delta(E)\rangle = \frac{1}{\sqrt{1 + K_\Delta(E)^2}}\sqrt{\frac{\omega_0}{k_0}}\left\{\left[a^\dagger(k_0)|\Phi_N\rangle\right]^{\frac{3}{2}\frac{3}{2}}\right.$$
$$\left. + \int dk\, \frac{\chi(k,k_0)}{\omega_k - \omega_0}\left[a^\dagger(k)|\Phi_N(k)\rangle\right]^{\frac{3}{2}\frac{3}{2}} + c_\Delta(E)|\Phi_\Delta\rangle\right\}. \quad (8)$$

with $\omega_0 = E - E_N$ and $k_0 = \left(\omega_0^2 - m_\pi^2\right)^{1/2}$.

By a straightforward extension of the formula (3) we can now write down the K-matrix, which has two discrete indexes and one continuous index $E$, as

$$K_{NN}(W) = -\pi\sqrt{\frac{\omega_0}{k_0}}\,\langle\Phi_N\|V^\dagger(k_0)\|\Psi_{JT}(W)\rangle, \quad (9)$$

$$K_{N\Delta}(W,E) = -\pi\sqrt{\frac{\omega_E}{k_E}}\,\langle\Psi_\Delta(E)\|V^\dagger(k_E)\|\Psi_{JT}(W)\rangle, \quad (10)$$

$$K_{\Delta N}(W,E) = -\pi\sqrt{\frac{\omega_0}{k_0}}\,\langle\Phi_N\|V^\dagger(k_0)\|\Psi_{JT}^\Delta(W,E)\rangle, \quad (11)$$

$$K_{\Delta\Delta}(W,E,E') = -\pi\sqrt{\frac{\omega_E}{k_E}}\,\langle\Psi_\Delta(E')\|V^\dagger(k_{E'})\|\Psi_{JT}^\Delta(W,E)\rangle. \quad (12)$$

The full and the partial widths are related to the T matrix, and the phase shift and the inelasticity to the S matrix. The T matrix is obtained from $T = -K/(1 - iK)$

or $T = -K + iKT$ which yields the following set of integral equations:

$$T_{NN}(W) = -K_{NN}(W) + i\left[ K_{NN}(W)T_{NN}(W) \right.$$
$$\left. + \int_{E_N + m_\pi}^{W - m\pi} dE \, K_{N\Delta}(W, E)T_{\Delta N}(W, E) \right], \qquad (13)$$

$$T_{N\Delta}(W, E) = -K_{N\Delta}(W, E) + i\left[ K_{NN}(W)T_{N\Delta}(W, E) \right.$$
$$\left. + \int_{E_N + m_\pi}^{W - m\pi} dE' \, K_{N\Delta}(W, E')T_{\Delta\Delta}(W, E', E) \right], \qquad (14)$$

$$T_{\Delta N}(W, E) = -K_{\Delta N}(W, E) + i\left[ K_{\Delta N}(W, E)T_{NN}(W, E) \right.$$
$$\left. + \int_{E_N + m_\pi}^{W - m\pi} dE' \, K_{\Delta\Delta}(W, E, E')T_{\Delta N}(W, E') \right], \qquad (15)$$

$$T_{\Delta\Delta}(W, E, E') = -K_{\Delta\Delta}(W, E, E') + i\left[ K_{\Delta N}(W, E)T_{N\Delta}(W, E') \right.$$
$$\left. + \int_{E_N + m_\pi}^{W - m\pi} dE'' \, K_{\Delta\Delta}(W, E, E'')T_{\Delta\Delta}(W, E'', E') \right]. \qquad (16)$$

From the first T matrix we deduce the phase shift $\delta$ and the elasticity $\eta$ thought the relation

$$S = 1 - 2iT_{NN}(W) = \eta(W)e^{2i\delta(W)}. \qquad (17)$$

## 4   Solution of the coupled equations in a simplified model

To get more insight in the method let us consider a simplified case in which we assume that the bare states dominate the channel states $\Psi_{JT}$ and $\Psi_{JT}^\Delta$ as well as the states $\Phi_N$ and $\Psi_\Delta$. Then, to evaluate the matrix elements of the K matrix (12) we use

$$|\Psi_{JT}(W)\rangle \approx \sqrt{\frac{\omega_0}{k_0}} \left[ c_B(W)|B\rangle + \delta_{J\frac{1}{2}}\delta_{T\frac{1}{2}}c_N(W)|N\rangle \right] \qquad (18)$$

$$|\Psi_{JT}^\Delta(W, E)\rangle \approx \sqrt{\frac{\omega_E}{k_E}} \left[ c_{B'}(W, E)|B'\rangle + \delta_{J\frac{1}{2}}\delta_{T\frac{1}{2}}c_\Delta^N(W, E)|N\rangle + \delta_{J\frac{3}{2}}\delta_{T\frac{3}{2}}c_\Delta^\Delta(W, E)|\Delta\rangle \right] \qquad (19)$$

where for the P11 channel $B = B' = R$ (i.e. $N^*(1440)$) while for the P33 channel we use $B = \Delta(1232)$ and $B' = \Delta(1600)$.[2] The second terms in the above expressions ensure the mutual orthogonality of the channel states and the ground state. The intermediate state appearing in $\Psi_{JT}^\Delta$ can be approximated as

$$|\Psi_\Delta(E)\rangle \approx \sqrt{\frac{\omega}{k}} \frac{\Psi_{JT}^\Delta}{\sqrt{1 + K_\Delta(E)^2}} |\Delta\rangle \approx \frac{2\sin\delta_\Delta(E)}{\sqrt{2\pi\Gamma_\Delta}} |\Delta\rangle, \qquad (20)$$

---

[2] Note that we have not included the $\Delta(1600)$ in the first channel because of the relatively small $\pi N$ branching ratio.

where $\omega = E - E_N$, $k = \sqrt{\omega^2 - m_\pi^2}$, $\Gamma_\Delta = 2\pi\omega|\langle N\|V\|\Delta\rangle|^2/k$, $K_\Delta(E) = \frac{1}{2}\Gamma_\Delta/(E_\Delta - E)$. The coefficients $c_B$ and $c_{B'}$ are most easily determined from

$$(H - W)|\Psi_{ST}(W)\rangle = 0 \quad \text{and} \quad (H - W)|\Psi_{ST}^\Delta(W, E)\rangle = 0\,, \tag{21}$$

which, after multiplying by $\langle B|$, yields

$$(E_B - W)c_B(W) = -\langle B\|V(k_0)\|N\rangle\,, \tag{22}$$

$$(E_{B'} - W)c_{B'}^\Delta(W, E) = -\frac{2\sin\delta_\Delta(E)}{\sqrt{2\pi\Gamma_\Delta}}\,\langle B'\|V(k_E)\|\Delta\rangle\,. \tag{23}$$

Here $E_B$ and $E_{B'}$ include the self-energy. For the coefficients $c_N$ and $c_\Delta$ we get

$$c_N^N(W) = -\langle\Phi_N\|a^\dagger(k_0)\|\Phi_N\rangle \approx \frac{\langle N\|V(k_0)\|N\rangle}{W - E_N}\,, \tag{24}$$

$$c_\Delta^N(W, E) = -\langle\Phi_N\|a^\dagger(k_E)\|\Psi_\Delta(E)\rangle \approx \frac{2\sin\delta_\Delta(E)}{\sqrt{2\pi\Gamma_\Delta}}\,\frac{\langle N\|V(k_E)\|\Delta\rangle}{W - E_N}\,, \tag{25}$$

and similarly for $c_\Delta^\Delta$

We immediately notice that the K matrices can be written in a separable form; in the P11 channel we find

$$K_{i,j} = \frac{a_i a_j}{E_R - W} - \frac{b_i b_j}{\omega_0}\,, \qquad i = N, \Delta;\ j = N, \Delta \tag{26}$$

with

$$a_N(W) = \sqrt{\frac{\pi\omega_0}{k_0}}\,\langle B\|V(k_0)\|N\rangle\,, \quad a_\Delta(W, E) = \sqrt{\frac{\pi\omega_E}{k_E}}\,\frac{2\sin\delta_\Delta(E)}{\sqrt{2\pi\Gamma_\Delta}}\,\langle B'\|V(k_E)\|\Delta\rangle\,, \tag{27}$$

$$b_N(W) = \sqrt{\frac{\pi\omega_0}{k_0}}\,\langle N\|V(k_0)\|N\rangle\,, \quad b_\Delta(W, E) = \sqrt{\frac{\pi\omega_E}{k_E}}\,\frac{2\sin\delta_\Delta(E)}{\sqrt{2\pi\Gamma_\Delta}}\,\langle N\|V(k_E)\|\Delta\rangle\,. \tag{28}$$

The coefficients $b_N$ and $b_\Delta$ strongly influence the phase shift close to the threshold but in the vicinity of the resonance we can neglect them. In this in case it is possible to find the solution for the T matrices in a simple form:

$$T_{ij} = -\frac{a_i a_j}{E_R - W - i\left[a_N^2 + \int_{E_N + m_\pi}^{W - m_\pi} dE\, a_\Delta(E)^2\right]}\,. \tag{29}$$

The partial widths read

$$\Gamma_{NN}(W) = 2a_N(W)^2 = \frac{2\pi\omega_0}{k_0}\,\langle B\|V(k_0)\|N\rangle^2\,, \tag{30}$$

$$\Gamma_{N\Delta}(W) = 2\int dE\, a_\Delta(W, E)^2 \approx \frac{2\pi\omega_E}{k_E}\langle B'\|V(k)\|\Delta\rangle^2\,. \tag{31}$$

To get the latter expression we have assumed that $a_\Delta(W, E)$ is sufficiently strongly peaked around $E = E_\Delta$. The phase shift for $\pi N \to \pi N$ is obtained from (17):

$$\tan 2\delta(W) = \frac{\Gamma_{NN}(W)(E_R - W)}{(E_R - W)^2 - \frac{1}{4}\left(\Gamma_{NN}(W)^2 - \Gamma_{N\Delta}(W)^2\right)}\,. \tag{32}$$

The inelasticity is expressed as

$$\text{Im}T^{\text{in}} = -\text{Im}T_{\text{NN}} - |T_{\text{NN}}|^2 = \frac{\frac{1}{4}\Gamma_{\text{NN}}(W)\Gamma_{\text{N}\Delta}(W)}{(E_{\text{R}} - W)^2 + \frac{1}{4}\left(\Gamma_{\text{NN}}(W) + \Gamma_{\text{N}\Delta}(W)\right)^2} \, . \tag{33}$$

## 5   Preliminary results for the Roper in the Cloudy Bag Model

We shall illustrate the method using the simplified approach presented in the previous section by calculating scattering in the P11 channel which is dominated by the Roper resonance. Though the above expressions are general and can be applied to any model in which the pions linearly couple to the quark core we choose here the Cloudy Bag Model, primarily because of its simplicity. The Hamiltonian of the model has the form (1) and (2) with

$$v(k) = \frac{1}{2f_\pi} \frac{k^2}{\sqrt{12\pi^2\omega_k}} \frac{\omega_{\text{MIT}}^0}{\omega_{\text{MIT}}^0 - 1} \frac{j_1(kR)}{kR} \, , \tag{34}$$

when no radial excitation of of the core takes place, and

$$v^*(k) = r_\omega v(k) \, , \qquad r_\omega = \frac{1}{\sqrt{3}} \left[ \frac{\omega_{\text{MIT}}^1(\omega_{\text{MIT}}^0 - 1)}{\omega_{\text{MIT}}^0(\omega_{\text{MIT}}^1 - 1)} \right]^{1/2} \, , \tag{35}$$

when one quark is excited from the 1s state to the 2s state. Here $\omega_{\text{MIT}}^0 = 2.04$ and $\omega_{\text{MIT}}^1 = 5.40$ The free parameter is the bag radius R. Though the bare values of different 3-quark configurations are in principle calculable in the model, the model lacks a mechanism that would account for large hyperfine splitting between certain states, e.g. the nucleon and the delta. For each R, we therefore adjust the splitting between the bare states such that the experimental position of the resonance is reproduced. Furthermore, using the experimental value of $f_\pi$ in (34) leads to too small coupling constants irrespectively of the bag radius; in our calculation we have therefore decreased this value by 10 %.

Preliminary results for the phase shift and inelasticity in the P11 channel have been calculated using the simplified model of the previous section. We have used the parameters with which the P33 phase shift is reproduced in the region of the delta resonance, i.e. the bag radius in the range 0.8 fm $<$ R $<$ 1.1 fm and $f_\pi = 81$ MeV.
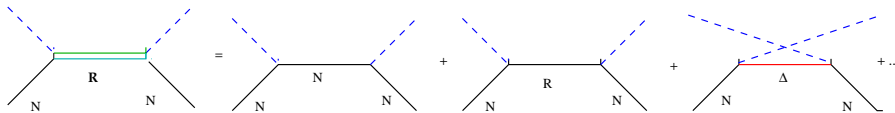


**Fig. 1.** Processes dominating scattering in the P11 channel: the nucleon pole term, the direct term and the crossed term with the delta intermediate state.

The experimental phase shift (Fig. 2 can be reasonable well reproduced by the the direct term only (see Fig. 1) provided we use a smaller value of the bag

radius. (Larger values yield too small the resonance width.). Yet, close to the threshold the phase shift exhibits a wrong behavior; it should be negative with the strength dictated by the πNN coupling constant. The proper behavior at low
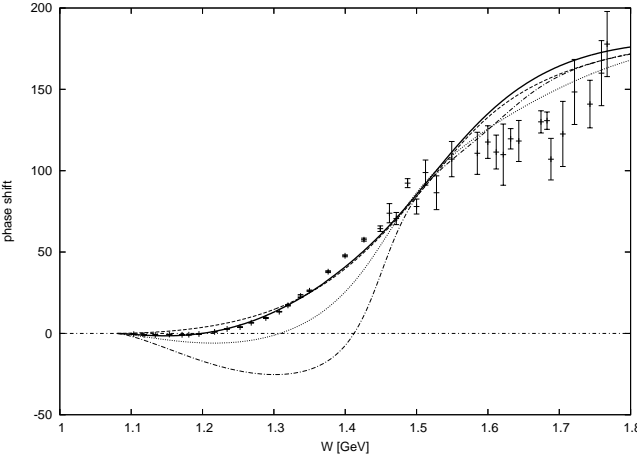


**Fig. 2.** Different contribution to the phase shift in the P11 channel: the direct term (dashed line), the inclusion of the nucleon pole (dotted line), the inclusion of the crossed term with the $\Delta(1232)$ (dashed and dotted line), the inclusion of the second $\Delta(1600)$ (full line). The bag radius $R = 0.83$ fm is used. The data points are from [7].

energies is established through the inclusion of the nucleon pole term. The nucleon pole term is in our model generated by requiring the orthogonality of the channel state vector to the ground state; including this term provides a consistent behavior at small energies (and in particular in the limit $\omega_0 \to 0$). However, at intermediate energies the agreement is strongly deteriorated. Since the strength of this term is fixed by the $\pi NN$ coupling constant which is well reproduced in the model, additional, non-resonant, terms are needed to cure this behavior. The important contribution that increases the phase shift comes from the crossed terms, and in particular from the term with the intermediate delta states (see the last term in Fig. 1), as noted already in [6]. To the leading order it contributes the term

$$K^{\Delta}_{NN} = \pi \frac{\omega_0}{k_0} \frac{4}{9} \frac{\langle N||V||\Delta\rangle^2}{\omega_0 + E_\Delta - E_N} \tag{36}$$

to the K matrix in the $\pi N$ channel. But even if we increase the model value of the $\pi N\Delta$ vertex such that the experimental width of $\Delta(1232)$ is reproduced, the phase shift at lower energies remain still too negative. Another intermediate state that has a relatively strong coupling to the $\pi N$ channel is the excited delta state, $\Delta(1600)$. If we include the corresponding term in our calculation we obtain an almost perfect agreement with the experiment at lower energies; which, taking into account the crudeness of our model, should not be considered as a proof of a great predictive power of our approach but rather as an indication of the important role that other resonances may play in the formation of the Roper resonance.

Fig. 3 shows that the calculated inelasticity in the resonance region qualitatively agrees with the experimental one. It does, however, not reproduce the large inelasticity above the resonance energy which approaches the unitarity limit. From our formula (33) such an behavior can be explained by assuming that the partial widths, $\Gamma_{N\Delta}$ and $\Gamma_{NN}$, remain almost equal over a relatively large interval of energies. This could again be attributed to the interplay of different processes involving neighboring resonances not included in the present calculation.
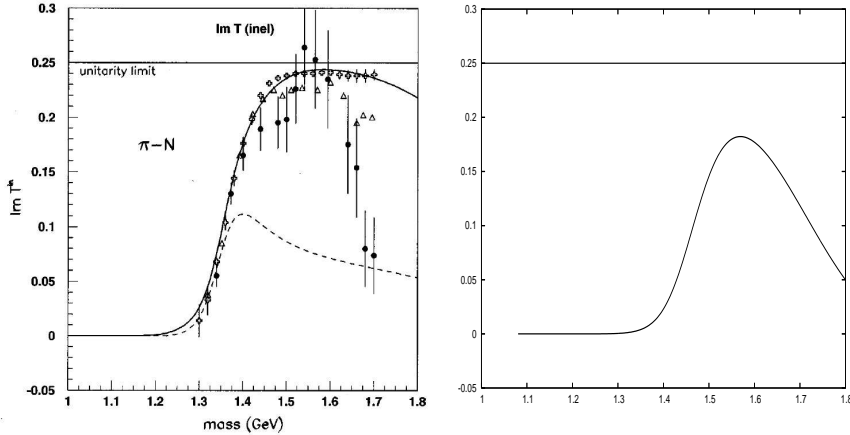


**Fig. 3.** The inelasticity in the P11 channel. The left figure is from [8], the right figure is our calculation with the direct terms only.

To conclude, our very preliminary calculation points out the importance of including different contributions stemming from the neighboring resonances to explain the rather peculiar properties of the Roper resonance. We believe that such conventional mechanisms have to be carefully exploited before making any conclusion about possible necessity of exotic degrees of freedom.

# References

1. B. Golli, in: B. Golli, M. Rosina, S. Širca (eds.), *Proceedings of the Mini-Workshop "Effective Quark-Quark Interaction"*, July 7–14, 2003, Bled, Slovenia, p. 83.
2. B. Golli, P. Alberto, L. Amoreira, M. Fiolhais and S. Širca in: B. Golli, M. Rosina, S. Širca (eds.), *Proceedings of the Mini-Workshop "Quark dynamics"*, July 12–19, 2004, Bled, Slovenia, p. 62.
3. P. Alberto, L. Amoreira, M. Fiolhais, B. Golli, and S. Širca, Eur. Phys. J. A **26** (2005) 99.
4. R. G. Newton, *Scattering Theory of Waves and Particles*, Dover Publications, New York 1982.
5. A. S. Rinat, Nucl. Phys. A **372** (1982) 341.
6. A. Suzuki, Y. Nogami, N. Ohtsuka, Nucl. Phys. A **395** (1983) 301.
7. R. A. Arndt, W. J. Briscoe, R. L. Workman, I. I. Strakovsky, SAID Partial-Wave Analysis, http://gwdac.phys.gwu.edu/.
8. H. P. Morsch and P. Zupranski, Phys. Rev. C **61** (2000) 024002.

# Computational problems with the tetraquark X(3872)

Damijan Janc*

Jožef Stefan Institute, 1000 Ljubljana, Slovenia

Constituent quark models predict a weak binding of the two heavy mesons D and $D^*$ into tetraquark [1]. In Ref. [1] the wave function was expanded in terms of Gaussians of different sets of Jaccobi coordinates. The structure of this state turned out to be molecular with the mean distance of 2 fm between the two heavy c quarks.

It is tempting to use the same method for the $D + \bar{D}^*$ tetraquarks speculating that the recently discovered X(3872) resonance [2] which lies just above the $D\bar{D}^*$ threshold at 3.872 MeV might be interpreted as the weakly bound state of these two heavy mesons, in analogy to the $DD^*$ molecular state.

However, the situation in the $D\bar{D}^*$ systems is rather different. The calculation poses serious computational difficulties which are a real challenge!

1. *Large isospin violation*
   The channel
   $D^0 + \bar{D}^{*0} = 3871.2$ MeV is **open**, and
   $D^+ + D^{*-} = 3879.3$ MeV is **closed**.
   Therefore an isospin violating term should be added to the interaction. Most model parameters should be refitted to account well for the important isospin multiplets. This would require a careful understanding of isospin multiplets. For a reliable prediction, the effective quark-quark interaction should give a unified description of light and heavy mesons and baryon (at least in ground and some low-lying states). For that reason we used in the study of the $DD^*$ tetraquark the nonrelativistic constituent quark model with the Bhaduri or Grenoble (AL1) gluon exchange interactions since they at least partially satisfy these criteria. However, they do not contain an isospin breaking term and it would be a major effort to refit them for our delicate purpose.

2. *Open channels*
   In addition to $D^0 + \bar{D}^{*0}$ there are also two more open channels:
   $J/\psi + \rho = 3867$ MeV is **open**,
   $J/\psi + \omega = 3879$ MeV is **closed**,
   $J/\psi + \eta = 3644$ MeV is **open**.
   The last one is especially important since this is the channel in which the X(3872) state was discovered [2]. Therefore a coupled channel calculation is needed.

---

* Present address: Ultra (Telargo), V. Otona Župančiča 23a, 1410 Zagorje, Slovenia

3. *Low-lying open channel*

Such a coupled channel calculation would be very difficult since the last open channel is way below the threshold. Therefore the relative wavefunction oscillates strongly and needs a large and reliable basis for expansion. The usual expansion in Gaussians with different width or different position or in harmonic oscillator function would require a large basis and high precision.

A promising approximation seems to be available, to artificially close the low-lying decay channel, assuming that it does not influence much the resonance near the threshold. The simplest way to do this is to restrict the four-body basis to singlet colour meson-singlet colour meson states. However, in this subspace no color · color interaction between (anti)quark of the first D meson and the (anti)quark of the second $\bar{D}$ meson is present, thus some additional interaction would be needed to produce the binding between two heavy mesons, e.g. a three-body interaction or an instanton generated interaction between light quarks. To produce binding, these additional interactions should be quite strong or long-ranged. Such modifications of the Bhaduri or AL1 constituent quark model would then require the refitting model parameters. If, on the other hand, the binding of D and $\bar{D}^*$ is a result of a significant admixture of the color octet-octet configuration as in the case of the $DD^*$ tetraquark [1], where the small component of the atomic-like configuration (similar to $\Lambda_b$ with cc diquark instead of b) produces just enough attractive force between heavy mesons to bind them, then one must solve the Hamiltonian in full color space. Since the total mass of the two mesons is so close to the energy of the newly discovered state in the charmonium spectra this calls for very accurate calculations where also the presence of the $J/\psi + \eta$ open channel must be taken into the account.

Other tricks to artificially close the low-lying decay channel seem risky due to its low energy. A simple variational calculation with partially restricted Hilbert space is likely to give a random resonance energy anywhere in between the $D + \bar{D}^*$ threshold and the asymptotic $J/\psi + \eta$ value, depending how far one goes with the optimisation. In [3] where this four quark system was essentially artificially enclosed inside the harmonic oscillator, they obtained strong binding more than 400 MeV below the D and $\bar{D}^*$ threshold but still almost 200 MeV above the energy of the free $J/\psi + \eta$.

# References

1. D. Janc and M. Rosina, Few-Body Systems **35** (2004) 175,
2. Choi et al. (Belle Collaboration), Phys.Rev.Lett. **91** (2003) 262001,
3. B. Silvestre-Brac and C. Semay, Z. Phys. **57** (1993) 273.

# Scalar mesons on the lattice

Saša Prelovšek

Department of Physics, University of Ljubljana, Ljubljana, Slovenia, and
Jožef Stefan Institute, Ljubljana, Slovenia

**Abstract.** The simulations of the light scalar mesons on the lattice are presented at the introductory level. The methods for determining the scalar meson masses are described. The problems related to some of these methods are presented and their solutions discussed.

## 1  Introduction

The observed spectrum of the light scalar resonances below 2 GeV is shown in Fig. 1. The existence of flavor singlet $\sigma$ and strange iso-doublet $\kappa$ are still very controversial [1]. Irrespective of their existence, it is difficult to describe all the observed resonances by one or two $SU(3)$ flavor nontes of $\bar{q}q$ states:

- If $\sigma$ and $\kappa$ do not exist, than $K_0(1430)$ has to be strange partner of $a_0(980)$, but the mass difference appears to big. Also there are to many states to be described by one nonet.
- If $\sigma$ and $\kappa$ exist, then all these states could represent two $\bar{q}q$ nonets and one glueball, where the largest glueball component is commonly attributed to $f_0(1500)$. However, most of the models and lattice simulations have difficulties in relating the observed properties of states below 1 GeV to the $\bar{q}q$ states.

This situation is in contrast to the spectrum of light pseudoscalar, vector and axial-vector resonances, where $\bar{q}q$ assignment works well. It raises a question whether the scalar resonances below 1 GeV are conventional $\bar{q}q$ states or perhaps exotic states such as tetraquarks [2].

This issues could be settled if the mass of the lightest $\bar{q}q$ states could be reliably determined on the lattice and identified with the observed resonances. In lattice QCD, the hadron masses are conventionally extracted from the correlation functions that are computed on the discretized space-time.

In the next section we present how the scalar correlator is calculated on the lattice. The relation between the scalar correlator and the scalar meson mass is derived in Section 3. A result for the mass of $I = 1$ scalar meson is presented in Section 4. In Section 5 we point out the problems which arise due to the unphysical approximations that are often used in the lattice simulations and we discuss the proposed solutions. We close with Conclusions.

This article follows the introductory spirit of the talk given at the Workshop *Exciting hadrons* and many technical details are omitted.

| I=0 | I=0 | I=1/2 | I=1/2 | I=1 | |
|-----|-----|-------|-------|-----|-|
| uu,dd | ss | us | ds | ud | |

2 GeV

f0(1710)

f0(1500)                                        a0(1450)

f0(1370)              K0(1430)

1 GeV

f0(980)              $\kappa$ ?              a0(980)

f0(600) or $\sigma$ ?
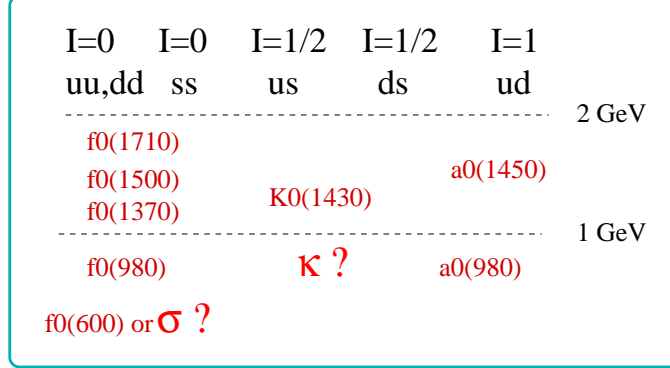
**Fig. 1.** The spectrum of observed light scalar resonances below 2 GeV [1]. The existence of σ and κ are still very controversial experimentally.

## 2  Calculation of the scalar correlator

Let us consider the correlation function for a *flavor non-singlet scalar meson* $\bar{q}_1 q_2$ first. In a lattice simulation it is calculated using the Feynman functional integral on a discretized space-time of finite volume and finite lattice spacing. The correlation function represents a creation of a pair $\bar{q}_1 q_2$ with $J^P = 0^+$ at time zero and annihilation of the same pair at some later Euclidean time t

$$C(t) = \sum_{\mathbf{x}} \langle 0| \bar{q}_1(\mathbf{x}, t) q_2(\mathbf{x}, t) \; \bar{q}_2(\mathbf{0}, 0) q_1(\mathbf{0}, 0)|0\rangle \,, \tag{1}$$

where both quarks are created (annihilated) at the same spatial point for definiteness here[1]. Wick contraction relates this to the product of two quark propagators shown by the connected diagram in Fig. 2b

$$C(t) = \left\langle C_G(t) \right\rangle_G \tag{2}$$

$$C_G(t) = \sum_{\mathbf{x}} \mathrm{Tr}_{s,c} \left[ \mathrm{Prop}^2_{0,0 \to \mathbf{x},t} \, \mathrm{Prop}^1_{\mathbf{x},t \to 0,0} \right]$$

$$= \sum_{\mathbf{x}} \mathrm{Tr}_{s,c} \left[ \mathrm{Prop}^2_{0,0 \to \mathbf{x},t} \gamma_5 \mathrm{Prop}^{1\,\dagger}_{0,0 \to \mathbf{x},t} \gamma_5 \right] \,.$$

The quark propagator in the gluon field G and Euclidean space-time [3]

$$\mathrm{Prop}^i_{\mathbf{x},x_0 \to \mathbf{y},y_0} = \left( \frac{1}{\slashed{D}_E + m_i} \right)_{\mathbf{x},x_0 \to \mathbf{y},y_0} \tag{3}$$

is the inverse of the discretized Dirac operator $\slashed{D}_E + m_i$ , which is a matrix in coordinate space and depends on the gluon field G [2]. The inversion of a large Dirac matrix is numerically costly, but the calculation of correlator (2) is feasible

---

[1] Different shapes of creation and annihilation operators in spatial direction can be used.
[2] $\slashed{D} = \gamma^\mu (\partial_\mu + \frac{i}{2}\lambda_a G^a_\mu)$ in continuum Minkowski space-time.

since it depends only on two propagators from a certain point $(0,0)$ to all points $(\mathbf{x}, t)$. Both of these are obtained by solving the equation $(\not{D}_E + m_i)V' = V$ for a single[3] source vector $V$ which is non-zero only at $(0,0)$. The expectation value over the gluon fields in (2) is computed based on the Feynman functional integral

$$C(t) = \frac{\int \mathcal{D}G\, C_G(t) \int \mathcal{D}q \int \mathcal{D}\bar{q}\, e^{-S_{QCD}}}{\int \mathcal{D}G \int \mathcal{D}q \int \mathcal{D}\bar{q}\, e^{-S_{QCD}}} = \frac{\int \mathcal{D}G\, C_G(t)\, \Pi_i \det[\not{D}_E + m_i]\, e^{-S_G}}{\int \mathcal{D}G\, \Pi_i \det[\not{D}_E + m_i]\, e^{-S_G}}\,. \tag{4}$$

A finite ensemble of N gluon field configurations is generated in the lattice simulations. Each configuration is generated with a probability $\Pi_i \det[\not{D}_E + m_i]\, e^{-S_G}$ for a given discretized gauge action $S_G$ and Dirac operator $\not{D}_E$. The functional integral (4) is calculated as a sum over the ensemble

$$C(t) = \frac{1}{N} \sum_{j=1}^{N} C_{G_j}(t)\,. \tag{5}$$
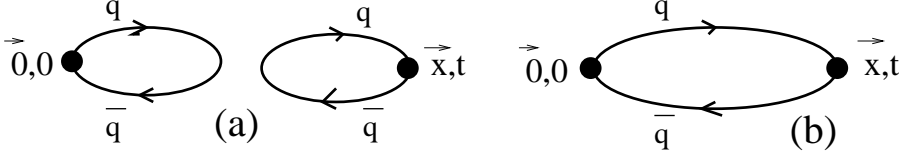


**Fig. 2.** The disconnected (a) and the connected (b) Feynman diagrams that need to be evaluated to compute the correlator. The disconnected diagram is present only for the flavor singlet meson.

The correlator for the *flavor singlet scalar meson* $\bar{q}q$

$$C(t) = \sum_{\mathbf{x}} \langle 0|\bar{q}(\mathbf{x}, t)q(\mathbf{x}, t)\, \bar{q}(0, 0)q(0, 0)|0\rangle \tag{6}$$

requires also the calculation of the disconnected diagram in Fig. 2a

$$\left\langle \mathrm{Tr}_{s,c}\mathrm{Prop}_{0,0 \to 0,0} \sum_{\mathbf{x}} \mathrm{Tr}_{s,c}\mathrm{Prop}_{\mathbf{x},t \to \mathbf{x},t} \right\rangle_G \tag{7}$$

in addition to connected one. The propagator $\mathrm{Prop}_{\mathbf{x},t \to \mathbf{x},t}$ in principle requires the solution of $(\not{D}_E + m_i)V' = V$ for source vector $V$ at any point. Such a number of inversions is normally prohibitively large and one is forced to use approximate methods for evaluating the disconnected part (7) of the singlet correlator. A calculation of the correlator for singlet meson in therefore much more demanding than for non-singlet meson.

---

[3] In fact $(\not{D}_E + m_i)V' = V$ has to be solved for every spin and color of the source vector $V$.

## 3 Relation between correlator and meson mass

In this Section we derive the relation between the scalar correlator and the scalar meson mass. The state $\bar{q}(0)q(0)|0\rangle$ that is created at time zero is not a scalar meson $|S\rangle$, but it is a superposition of the scalar meson and all the other eigenstates of Hamiltonian $|n\rangle$ with the same quantum numbers $J^P = 0^+$ and $I^G$ as $|\bar{q}q\rangle$

$$|\bar{q}q\rangle = \sum_n c_n|n\rangle = c_1|S\rangle + c_2|S^*\rangle + \sum_i c_i \left|\begin{array}{c}\text{multi}\\\text{hadron st.}\end{array}\right\rangle_i + ... \left(+c_0|0\rangle \begin{array}{c}\text{only for}\\\text{singlet}\end{array}\right).$$ 
(8)

Here $|S\rangle$ and $|S^*\rangle$ are ground and excited scalar mesons, while the third term represents the sum over multi-hadron states. The eigenstate $|n\rangle$ evolves as $e^{i\mathbf{p}_n \mathbf{x} - E_n t}$ in Euclidean space-time, so the scalar correlators (1) and (6) evolve as

$$C(t) = \sum_{\mathbf{x}} \langle \bar{q}(\mathbf{x}, t)q(\mathbf{x}, t)\, \bar{q}(0,0)q(0,0)\rangle$$
(9)

$$= \sum_n \sum_{\mathbf{x}} \langle \bar{q}q|n\rangle e^{i\mathbf{p}_n \mathbf{x} - E_n t}\langle n|\bar{q}q\rangle = \sum_n |\langle \bar{q}q|n\rangle|^2\, e^{-E_n t}\big|_{\mathbf{p}=0}$$

$$= |c_1|^2 e^{-m_S t} + |c_2|^2 e^{-m_{S^*} t} + \sum_i |c_i|^2 e^{-E_i^{\text{multi}}_{\text{had.}} t} + ... \left[+|c_0|^2 \begin{array}{c}\text{only for}\\\text{singlet}\end{array}\right]$$ 
(10)

If $|S\rangle$ is the lightest state among $|n\rangle$, than $C(t) \propto e^{-m_S t}$ at large $t$ and $m_S$ and can be extracted simply by fitting the lattice correlator to the exponential time dependence.

In the case of the *flavor singlet* correlator, the lightest state in the sum (8) is the vacuum state. Its corresponding coefficient $c_0$ (8) is the scalar condensate $\langle\bar{q}q\rangle$. Another important light state that contributes at large $t$ is $\pi\pi$, so extraction of $m_\sigma$ requires the fit to

$$C(t) \overset{t\to\infty}{=} |c_\sigma|^2 e^{-m_\sigma t} + \sum_{\mathbf{p}_\pi}\left|c_{\mathbf{p}_\pi}\right|^2 e^{-E_{\mathbf{p}_\pi}^{\pi\pi} t} + \langle\bar{q}q\rangle^2 .$$
(11)

The extraction of $m_\sigma$ is very challenging since $C(t)$ requires the calculation of the disconnected diagram (see previous Section) and since RHS in (11) is largely dominated by $\langle\bar{q}q\rangle^2$.

These two problems do not affect the study of the *flavor non-singlet* meson. However, even in this case there are several multi-hadron states which are light and need to be taken into account in the fit of the correlator (9) at large $t$ in order to extract $m_S$. The lightest multi-hadrons states with $J^P = 0^+$ are two-pseudoscalar states in S-wave. In case of $I = 1$ correlator, the contribution of scalar meson $a_0$ is accompanied by contributions of $\pi\eta$, $\bar{K}K$ and $\pi\eta'$ in three-flavor QCD. Let us note that in nature these three states are lighter than observed resonance $a_0(1450)$; the state $\pi\eta$ is also lighter than observed resonance $a_0(980)$. In two-flavor QCD, the only two-pseudoscalar state $\pi\eta'$ is relatively heavy and not so disturbing for the extraction of $m_{a0}$ from (9).

The above derivation of time-dependence for a correlator was based on QCD, which is a proper unitary field theory. The resulting correlator (9) is positive definite. Let us point out that certain approximations used in lattice simulations

(quenching, partial quenching, staggered fermions, mixed-quark actions) break unitarity and may render negative correlation function. These approximations will be discussed in Section 5 together with the necessary modifications of the fitting formula (9).

## 4   Mass of scalar meson with I=1

A lattice simulation of the scalar meson $a_0$ with $I = 1$ [4] is presented in this section, as an example. It employs two dynamical quarks[4], lattice spacing 0.12 fm, lattice volume $16^3 \times 32$ and ensemble of about 100 gauge configurations [4,5]. The advantage of simulation [4] is that its discretized (Domain-Wall) fermion action has good chiral properties: it is invariant under the chiral transformation for $m_q = 0$ even at finite lattice spacing[5], which is not the case for some of the commonly used discretized fermion actions. Another advantage of the simulation with two dynamical quarks [4] is that the exponential fit of the correlator at large t renders $m_{a0}$. The conventional exponential fit is justified in this case since the only two-pseudoscalar intermediate state in two-flavor QCD is $\pi\eta'$, which is relatively heavy and does not affect the extraction of $m_{a0}$ (see previous Section).

The resulting mass is presented in Fig. 3 for different input masses $m_{u,d}$, where isospin limit $m_u = m_d$ is employed. There are no simulations at physical masses $m_{u,d}$ since the pion cloud around the scalar meson with $\lambda_\pi = \hbar c/140\,\mathrm{MeV} \simeq 9\,\mathrm{fm}$ would be too squeezed on the lattice with extent $16 \times 0.12\,\mathrm{fm} \simeq 2\,\mathrm{fm}$. The u/d quarks and pions are heavier in simulation than in the nature in order to avoid large finite volume effects. The linear extrapolation of $m_{a0}$ to the physical quark mass $m_{u,d} \simeq 4\,\mathrm{MeV}$ in Fig. 3 gives

$$m_{a0} = 1.58 \pm 0.34\,\mathrm{GeV}\ . \tag{12}$$

Although our result for the mass of the lightest $\bar{q}q$ state with $I = 1$ has sizable error-bar, it appears to be closer to the observed resonance $a_0(1450)$ than to $a_0(980)$. It gives preference to the interpretation that $a_0(980)$ is not conventional $\bar{q}q$ state.

Results from other lattice simulations of the light scalar mesons can be found in [6]-[11].

## 5   Problems due to unphysical approximations

The simulation presented in the previous section is a discretized version of two-flavor QCD and does not employ any unphysical approximations except for the discretization of space-time. It renders positive definite correlation function, as expected in proper Quantum Field Theory (9).

---

[4] Fermion determinant in (4) incorporates quarks $i = u, d$.
[5] This is strictly true only when the 5th dimension in Domain-Wall fermion action is infinitely large.
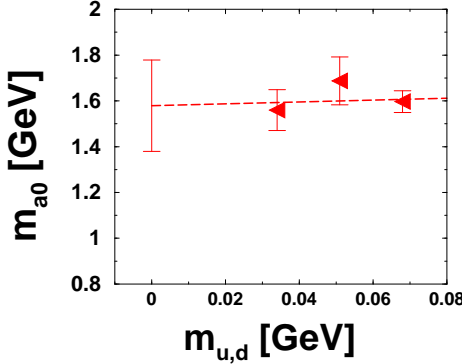
**Fig. 3.** The triangles present resulting $m_{a0}$ for three values of bare quark masses $m_{u,d}$ [4]. The dashed line is the linear extrapolation of $m_{a0}$ to the value of $m_{u,d}$ in nature.

However, lattice simulations often employ unphysical approximations which facilitate numerical evaluation. One of the indications that the simulation does not correspond to a proper QCD is the negative scalar correlator. Another sign of unphysical simulation is when $I = 1$ correlator drops as $e^{-2M_\pi t}$ at large t although the lightest two-pseudoscalar state with $I = 1$ is $\pi\eta$. Both of these unphysical lattice results can occur if the theory that is being simulated is not unitary, which is the case for all the commonly used approximations listed below:

- In *quenched* simulation the fermion determinant in (4) is replaced by a constant. This corresponds to neglecting all the closed sea-quark loops. The $I = 1$ scalar correlator is negative in this case and its negativity was attributed to the intermediate state $\pi\eta'$ in Ref. [6]. The prediction for $\pi\eta'$ intermediate state in quenched version of Chiral Perturbation Theory (ChPT) describes the sign and the magnitude of the lattice correlator at large t well [6,7]. The mass $m_{a0}$ was extracted [6,7] by fitting the quenched $I = 1$ correlator to the sum of $e^{-m_{a0}t}$ term and the contribution of $\pi\eta'$ as predicted by Quenched ChPT.
- In *partially quenched* simulation the mass of the sea quark is different from the mass of the valence quark, although they are the same in nature. The mass of the valence quark is the mass that appears in the propagator of the correlator $C_G$ (2), while the mass of the sea quark is the mass that appears in the fermion determinant (4). The partially quenched scalar correlator with $I = 1$ was found to be negative if $m_{val} < m_{sea}$ [4]. This was attributed to intermediate states with two pseudoscalar mesons and was described well using partially quenched version of ChPT [4]. The mass $m_{a0}$ was extracted by fitting the partially quenched correlator to the sum of $e^{-m_{a0}t}$ term and the contribution of two-pseudoscalar states as predicted by Partially Quenched ChPT [4]. The resulting mass agrees with the mass (12).
- The simulations with *mixed quark actions* employ different discretizations of the Dirac operator for valence and sea quarks. The method of extracting scalar meson mass from a such simulations was proposed in [12,13].

- The simulations with *staggered quarks* use an artificial taste degree of freedom for quarks in order to solve fermion doubling problem [3]. The method of extracting scalar meson mass from simulations with staggered quarks [11] was proposed in [12].

All these approximations modify the contribution of two-pseudoscalar intermediate states with respect to QCD. The effects of these approximations can be therefore determined by predicting the two-pseudoscalar contributions using appropriate versions of ChPT. These analytic predictions [6,4,12,13] allow the extraction of the scalar meson mass from the correlator as long as the contribution of two-pseudoscalar intermediate states does not completely dominate over the $e^{-m_s t}$ term.

## 6  Conclusions

The nature of scalar resonances below 1 GeV is not established yet. A lattice determination of the masses for ground $\bar{q}q$ scalar states would help to resolve the problem.

In principle, the scalar mass can be extracted from the scalar correlator that is computed on the lattice. However, the interesting term $e^{-m_s t}$ in the correlator is accompanied by the contribution of two-pseudoscalar states $e^{-E_{PP} t}$. The problem is that the energy of two-pseudoscalar states is small, so they may dominate the correlator and complicate the extraction of scalar meson mass. On top of that, the contribution of two-pseudoscalar states is significantly affected by the unphysical approximations that are often used in lattice simulations. Luckily, these effects can be predicted using appropriate versions of Chiral Perturbation Theory and they agree with the observed effects on the lattice correlators. We give the list of references, which provide the expressions for extracting $m_S$ from the correlators for various types of simulations.

A simulation, which does not suffer from the problems listed above, gives $1.58 \pm 0.34$ GeV for the mass of the lightest $\bar{q}q$ state with $I = 1$. This supports the interpretation that observed $a0(1450)$ is the lightest $(\bar{q}q)_{I=1}$ state, while $a0(980)$ might be something more exotic.

## References

1. Particle Data Group, *Review of Particle Physics*, Phys. Lett. B **592** (2004) 1.
2. M. G. Alford and R. L. Jaffe, Nucl. Phys. B **578** (2000) 367; L. Maiani et al., Phys. Rev. Lett. **93** (2004) 212002.
3. H. J. Rothe, *Lattice Gauge Theories, An Introduction*, World Scientific.
4. S. Prelovšek et al., RBC Coll., Phys. Rev. D **70** (2004) 094503.
5. Y. Aoki et al., RBC Coll., `hep-lat/0411006`.
6. W. Bardeen et. al, Phys. Rev. D **65** (2002) 014509; W. Bardeen *et. al*, Phys. Rev. D69 (2004) 054502.
7. S. Prelovšek and K. Orginos, RBC Coll., Nucl. Phys. B (Proc. Suppl.) **119** (2003) 822 [`hep-lat/0209132`].

8.  W. Lee and D. Weingarten, Phys. Rev. D **61** (2000) 014015.
9.  T. Kunihiro et al., SCALAR Coll., Phys. Rev. D **70** (2004) 034504.
10. C. McNeile and C. Michael, Phys. Rev. D **63** (2001) 114503;
    A. Hart, C. McNeile and C. Michael, Nucl. Phys. B (Proc. Suppl.) **119** (2003) 266.
11. C. Bernard et al., MILC Coll., Phys. Rev. D **64** (2001) 054506;
    C. Aubin et al., MILC Coll., Phys. Rev. D **70** (2004) 094505;
    A. Irving et al., POS(LAT2005)027 [hep-lat/0510066].
12. S. Prelovšek, hep-lat/0510080.
13. M. Golterman and T. Izubuchi, Phys. Rev. D **71** (2005) 114508.

# What I have learned at BLED 2005

Mitja Rosina[a,b]

[a] Faculty of Mathematics and Physics, University of Ljubljana, 1000 Ljubljana, Slovenia
[b] Jožef Stefan Institute, 1000 Ljubljana, Slovenia

## 1 A short summary

Last year has seen some important discoveries or reconfirmations of tentative multiquark and exotic states. Several surprises appeared regarding their low energies, narrow widths, abundant production etc. On the other hand, the electroexcitation of baryons remains a very promising tool to understand the structure of low-lying excited states. The theoretical trend has been to progress from qualitative to quantitative in describing not only spectra but also the electroweak form factors, transition amplitudes and decay widths.

I shall briefly outline how I have understood the talks and discussion sessions and I apologise for any misinterpretation. For simplicity, I shall follow our timetable chronologically.

Veljko Dmitrašinović presented the t'Hooft interaction supposedly generated by instantons. It plays a noticeable role in the energy shift of mesons and baryons belonging to different representations of flavour SU(3). For some states the agreement between model and experiment is improved significantly. We accepted it as an alternative or as an addition to other effective interactions, for example gluon exchange or Goldstone boson exchange (of Riska, Glozman, Plessas and Wagenbrunn). The effect of the three-body t'Hooft interaction is, however, essential for multiquarks. It can explain the approximate degeneracy of $D^+(2308)$ and $D_s^+(2317)$ mesons which accordingly should be tetraquarks. An interesting attempt for reconciliation between experiments which see and do not see the pentaquark $\Theta(1540)$ was proposed: if this is a weakly bound state of neutron, kaon and pion, it cannot be formed in some experiments.

The Ljubljana group (Bojan Golli, Simon Širca) described their collaboration with experimental groups in MAMI (Mainz) and JLab (USA). as well as their progress in clarifying unexplained features in electroexcitation of the nucleon within the Cloudy Bag Model. The discussion was concentrated on the diversity of facets displayed by the Roper resonance and on plans for its further study. The second group (Mitja Rosina, Damijan Janc) is preparing an attack on the X(3872) resonance assuming that it might be a molecular state of D and $\bar{D}$ mesons, in analogy to the DD molecular state. The difficulties of a model calculation were discussed and are summarized in next section.

Ica Stancu presented the controversial $\Xi = ccu/ccd$ baryons seen by the SE-LEX detector. The presentation triggered lively discussions. Doubts are due to

low statistics, unexpectedly low mass, too large isospin splitting and too high production rate. Her calculations do yield a somewhat higher mass, but it can be lowered by readjustment of model parameters. New experiments are urgently needed. If these states are confirmed, they would lead to interesting consequences regarding our understanding of effective quark interactions, especially the three-body ones.

Herbert Weigel tried to convince us that the controversial pentaquark $\Theta(1540)$ is consistent with the Skyrme soliton model using semiclassical angular momentum projection. The presentation was very instructive. As far as I understand it, the nice agreement between the model and the tentative experimental result has only a qualitative significance and is not conclusive; it is, however, very interesting.

Several important results came from the Belle collaboration (Tsukuba) which includes also a significant Slovenian experimental group. Ilija Bizjak presented several results, in particular he gave an exhaustive documentation about the angular momentum, parity and C-parity assignments of $X(3872)$: $J^{PC} = 1^{++}$. This result is very important for theory since it distinguishes between different models and is relevant also for the work of Janc and Rosina. Bizjak also documented the search for pentaquark: it has not been seen at Belle.

Vladimir Kukulin revived the interest in dibaryons. In his review he admitted that they have not been discovered as usual resonances. He stressed, however, their role as virtual (intermediate) states in nucleon-nucleon collisions and in the disintegration of the deuteron.

Harald Fritzsch presented an interesting model for the spin of the nucleon. From the deep inelastic scattering of polarized electrons it is known that the spin of valence quarks gives only a small contribution to the nucleon spin. In the presented model, the dressed quark is constructed by adding quark-antiquark pairs to the valence quark. The dressed quark then contributes 30% of nucleon spin (25% are suposedly contributed by the orbital motion and 45% by gluons). It will be crucial to measure the contribution of gluons which is one of the programmes of the Compass detector.

Peter Minkowski concentrated on gluonic degrees of freedom. He emphasised that the search for glueballs (as systems of two gluons) is not in vain, since there are too many scalar mesons. Using a nonet classification he pointed out which scalar mesons correspond to the same representation and which meson might be predominantly a glueball. He made an interesting proposal that the glueball appears as a very broad resonance extending from the controversial $\sigma(500)$ up to $f^0(1300)$. He argued that the value of glueball mass above 1600 MeV as given by many authors is too high.

Saša Prelovšek reviewed the lattice QCD calculations of scalar mesons. It was instructive to see the comparison between the static, dynamic and partially dynamic version of the lattice QCD and corresponding techniques to extrapolate the quark mass to a sufficiently low value. The lightest scalar meson comes at least at 1.6 GeV. This result is certainly in disagreement with the interpretation of Minkowski and is expected to heat up the debate for quite some time in the future.

The Graz group (Willi Plessas and Robert Wagenbrunn) developed the relativistic approach to baryon spectroscopy one step further. In addition to the energy spectrum they can calculate consistently electromagnetic and weak form factors as well as some hadronic processes. Some baryonic decay widths agree now well with the experiment and some not yet. A deeper understanding of those cases is still needed and any debate is welcome.

## 2  The future of multiquark states

The search for multiquarks is not just an extravagant sport. They are essential for our understanding of effective quark interactions and limits of validity of the constituent quark model. Can a unified quark model be developed which comprises mesons, baryons, tetraquarks, pentaquarks, hexaquarks and exotics containing gluons?

Some calculations agree with experiment, some do not. Some new states are surprising (possibly false), some predicted states are missing or difficult to find. The moral of the fable is that we should constantly encourage experimentalists to search for our pet states. We should proceed from qualitative to (semi)quantitative in order to give a good guidance to experimentalists. The predicted energies (masses) should be generously commented regarding their reliability, alternative possibilities and possible range of surprises in order not to mislead the experimentalists.

Moreover, dynamical calculations should be improved to supply more reliable production and decay rates, with all their model dependence, however. This might help to invent new promising channels for identification of new multiquarks.

Let me give two examples.

(i) The Belle collaboration has observed an unexpectedly large production rate of double $c\bar{c}$ pairs in $e^+e^-$ collisions (Ref.[1]). Since they used a $J/\psi$ trigger this meant the detection of $J/\psi$ as well as separate $c$ and $\bar{c}$ decay products. Due to the high abundance of two $c$ quarks simultaneously we can expect significant (hopefully measurable) production rates of double-charm baryons and tetraquarks. In order to more reliably calculate these production rates the large production of double $c\bar{c}$ pairs should be better understood (Ref.[2] gives only an estimate). Moreover, suggestions for good detection channels and triggers are welcome.

(ii) The calculation of the X(3872) tetraquark presents serious computational difficulties (Ref.[3]) which are a real challenge!

1. *Large isospin violation.*      The channel $D^0 + \bar{D}^{*0} = 3871.2$ MeV    is open while $D^+ + D^{*-} = 3879.3$ MeV    is closed.
   Therefore an isospin violating term should be added to the interaction. Most model parameters should be refitted to account well for the important isospin multiplets. This would require a careful understanding of isospin multiplets. To my knowledge, no model so far gives a unified description of light and

heavy mesons and baryon (at least in ground and some low-lying states), including isospin effects.

2. *Open channels.*    In addition to $D^0 + \bar{D}^{*0}$, there are two more open channels: $J/\psi + \rho = 3867$ MeV    and $J/\psi + \eta = 3644$ MeV.

   A coupled channel calculation is needed.

3. *Low-lying open channel.*    The last open channel lies much below the threshold. Therefore the relative wavefunction oscillates strongly and needs a large and reliable basis for expansion. The usual expansion in Gaussians with different width or different position, or in harmonic oscillator function would not work.

## References

1. K. Abe et al. (Belle Collaboration), Phys. Rev. Lett. **89** (2002) 142001.
2. D. Janc and M. Rosina, Few-Body Systems **35** (2004) 175.
3. D. Janc, These Proceedings.

# Structure of the Roper resonance
# from pion electro-production experiments

S. Širca[a,b]

[a] Faculty of Mathematics and Physics, University of Ljubljana, 1000 Ljubljana, Slovenia
[b] Jožef Stefan Institute, 1000 Ljubljana, Slovenia

**Abstract.** The $P_{11}(1440)$ (Roper) resonance remains one of the least understood excited states of the nucleon. Relevant open issues of the theoretical and phenomenological analyses of the Roper are identified, and a proposal for a study of the Roper in a pion electro-production experiment with double-polarization observables is given.

## 1  Introduction

The $P_{11}(1440)$ (Roper) resonance [1] is the lowest positive-parity $N^\star$ state. It is visible only indirectly in partial-wave analyses of $\pi N \to \pi N$ and $\pi N \to \pi\pi N$ scattering as a shoulder around 1440 MeV with a large width. The Roper is buried underneath the Born backgrounds and merges with the tails of other neighbouring resonances (in particular the $P_{33}(1232)$, $D_{13}(1520)$, and $S_{11}(1535)$), and thus can not be resolved from the $W$-dependence of the cross-section alone. Furthermore, the methods by which the masses and widths of the Roper have been determined, differ significantly: from $\pi N$ scattering, a Breit-Wigner mass of $\sim 1470$ MeV and width of $\sim 350$ MeV is extracted, while a speed-plot analysis (local maxima of $|dT/dW|$) yields $\sim 1375$ MeV and $\sim 180$ MeV, respectively [2]. In addition, due to its high inelasticity, the Roper resonance has a very atypical behaviour of $\mathrm{Im}T_{\pi N}$ and exhibits multiple T-matrix poles in the complex energy plane on auxiliary Riemann sheets.

Although this four-star resonance is within the energy range of many modern facilities, the experimental analyses so far have not ventured far beyond the determination of its mass, widths, and photon decay amplitudes. Very little is known about its internal structure.

## 2  Two "standard" views of the Roper

The photo-couplings and helicity amplitudes of the Roper resonance have been computed in a multitude of approaches, and have yielded a set of predictions which at this stage can not be conclusively confirmed or ruled out by data. In the SU(6) quark model, the Roper can be understood as a radial excitation of the proton to the $(1s)^2(2s)^1$ configuration. This excitation results in a "breathing

mode" of the proton, implying a sizable Coulomb monopole contribution (C0 or $S_{1-}$). Some models describe the Roper as a gluonic partner of the proton, representing it as a $(q^3g)$ hybrid baryon with three quarks oscillating against explicitly excited configurations of the gluon fields. In this picture, the C0 strength should thus be highly suppressed, implying a predominantly magnetic dipole transition (M1 or $M_{1-}$), in contrast to the concept of "breathing". These two opposing concepts result in rather different predictions for the $Q^2$-dependence of the transverse $(A_{1/2}^P)$ and scalar $(S_{1/2}^P)$ electro-production helicity amplitudes shown in Fig. 1. Of course, numerous other approaches have been suggested (see e.g. [3] for a review).
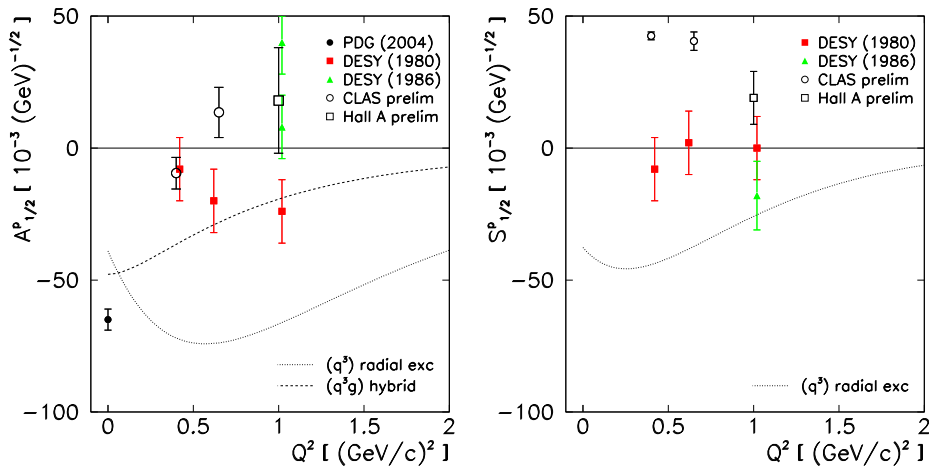


**Fig. 1.** Nucleon-Roper transverse (left) and scalar (right) helicity amplitudes for the charged (proton) state. The curves are for a Roper as a radially excited $(q^3)$ state or a $(q^3g)$ hybrid state.

## 3    Assessment of experimental situation

Experimentally, the $Q^2$-dependence of the helicity amplitudes is not well known (see Fig. 1). A re-analysis of old DESY and NINA electro-production experiments yielded $S_{1/2}^P$ consistent with zero, and gave contradictory results for the $A_{1/2}^P$. The lack of (double)-polarized measurements is, to a great extent, responsible for such large uncertainties. Newer, polarized experiments at Jefferson Lab have yielded more precise values of $S_{1/2}^P$ at $Q^2 = 0.4$ and $0.65\,(GeV/c)^2$. The $A_{1/2}^P$ has also been extracted at $Q^2 = 0.4, 0.65$, and $1.0\,(GeV/c)^2$. It appears to exhibit a zero-crossing in the vicinity of $Q^2 = 0.5\,(GeV/c)^2$, although the situation remains unclear due to limited $Q^2$-coverage and modest error-bars.

Kinematically most extensive data sets on single-pion electro-production in the Roper region come from Hall B of Jefferson Lab. Angular distributions and

*W*-dependence of the electron beam asymmetry $\sigma_{LT'}$ have been measured for both channels in the $P_{33}(1232)$ region at $Q^2 = 0.4$ and $0.65\,(\text{GeV/c})^2$ [4,5]. A complete angular coverage was achieved, and different non-resonant amplitudes were be separated in a partial-wave analysis. The Legendre moments $D_0'$, $D_1'$, and $D_2'$ of the expansion were determined. The $D_1'$ appears to be sensitive to higher resonances, with contributions of about $15-20\,\%$ coming mainly from the $\text{Im}(M_{1-}^* S_{1+})$ interference, pointing to the relevance of the Roper.

Dispersion-relation techniques and unitary isobar models have been applied to analyze the CLAS $\sigma_{LT'}$ data at $Q^2 = 0.4$ and $0.65\,(\text{GeV/c})^2$ spanning also the second resonance region, in order to extract the contributions of the $P_{33}(1232)$, $P_{11}(1440)$, $D_{13}(1520)$, and $S_{11}(1535)$ resonances to single-pion production. Since both the $p\pi^0$ and the $n\pi^+$ channel were measured (facilitating isospin decomposition), the transverse helicity amplitude $A_{1/2}^p$ as well as the scalar $S_{1/2}^p$ could be extracted. The results show a rapid fall-off of $A_{1/2}^p$ and indicate its zero-crossing at $Q^2 \sim 0.5 - 0.6\,(\text{GeV/c})^2$ shown in Fig. 1. It was also shown that $\sigma_{LT'}$ is mainly sensitive to the imaginary part of $P_{11}(1440)$, while the cross-section is sensitive to the real part of the $P_{11}$ multipoles.

In Hall B, further experiments will be devoted to single-pion photo-production in both $p(\gamma, \pi^+)n$ and $p(\gamma, p)\pi^0$ channels, with polarized beam and longitudinally as well as transversely polarized target using the CLAS detector. There is also a competing real-photon experiment of the A2 Collaboration at MAMI devoted to the measurement of polarized asymmetry G.

These uncertainties, in particular the location of the zero-crossing in $Q^2$, are motivating the Hall A study of the Roper by means of double-polarization observables. A measurement over a broad range of *W* and $Q^2$ would provide us with a rich data set on the transition amplitudes in electro-production.

## 4   Lessons learned from E91-011

Polarized electron beam and recoil-polarimetry capability of Hall A allow access to double-polarization observables in single-pion electro-production. Recoil-polarization observables are composed of different combinations of multipole amplitudes than observables accessible in the case of a polarized target. In the sense of experimental method, the measurements of Hall A would be complementary to the efforts with CLAS in Hall B.

A complete angular coverage of the outgoing hadrons to the extent of the CLAS detector in not possible in Hall A due to relatively small angular openings of the Hall A HRS spectrometers *except* at high $Q^2$ where the Lorentz boost from the center-of-mass to lab frame focuses the reaction products into a cone narrow enough to provide a virtually complete out-of-plane acceptance. The E91-011 neutral-pion electro-production experiment in Hall A [6] was performed at sufficiently high $Q^2 = (1.0 \pm 0.2)\,(\text{GeV/c})^2$ and $W = (1.23 \pm 0.02)\,\text{GeV}$ to allow for a measurement of all accessible response functions, even those that vanish for coplanar kinematics. Two Rosenbluth combinations and 14 structure functions were separated, allowing for a restricted partial-wave analysis giving access to

all $l \leq 1$ multipole amplitudes relevant to the $N \rightarrow \Delta$ transition. Both extracted $M_{1-}$ and $S_{1-}$ multipoles [6] in the $p\pi^0$ channel indicate a rising trend approaching the $W \sim 1440\,\text{MeV}$ region, pointing towards the Roper.

Unfortunately, the cross-sections at $W \sim 1440\,\text{MeV}$ (for any $Q^2$) are about an order of magnitude smaller than in the $\Delta$-peak. For high $Q^2 \sim 1\,(\text{GeV/c})^2$, where a large out-of-plane coverage would allow for a decent partial-wave analysis in Hall A, the cross-sections are even smaller. Furthermore, due to the zero-crossing uncertainty of the $M_{1-}$ multipole, it is not clear what value of $Q^2$ to choose in order to have a prominent M1 signal. Furthermore, models indicate that the crucial features of the Roper multipoles (or helicity amplitudes) are visible at relatively small $Q^2$ of a few $0.1\,(\text{GeV/c})^2$, nullifying the boost-advantage of the HRS.

We believe that a measurement in the spirit of the E91-011, attempting a precise extraction of the Roper multipoles from a complete partial-wave analysis at a *single* $Q^2$-point, is not the most effective strategy at this moment. Instead, we believe that a precise measurement of a more restricted set of double-polarization observables, highly sensitive to the Roper multipoles, and spanning a broad range in $Q^2$ and $W$, would yield a more rewarding and critical insight into the structure of the $N \rightarrow R$ transition through comparison with models.

## 5   Options for a Roper experiment in Jefferson Lab Hall A

We believe that an attempt at a large-scale analysis of the Roper multipoles, aiming at a complete partial-wave analysis at a single $Q^2$-point in the spirit of the $N \rightarrow \Delta$ experiment E91-011 [6], presently may not be the most effective approach to study the structure of the $N \rightarrow R$ transition. We are working on designing an experiment that would measure recoil polarization components which exhibit high sensitivities to the Roper resonant multipoles and span a broad range in $Q^2$ and $W$. It is this extended coverage that would allow for a more instructive study of the transition through comparison with models.

In anti-parallel kinematics for the $p(\mathbf{e}, e'\mathbf{p})\pi^0$ process, the polarization components of the ejected proton $P'_x$ and $P_y$ have the following multipole structure:

$$
\begin{aligned}
P'_x \sim R^t_{LT'} = \text{Re}\{\, & L^*_{0+}E_{0+} \\
& + (L^*_{0+} - 4L^*_{1+} - L^*_{1-})M_{1-} + L^*_{1-}(M_{1+} - E_{0+} + 3E_{1+}) \\
& - L^*_{0+}(3E_{1+} + M_{1+}) + L^*_{1+}(4M_{1+} - E_{0+}) + 12L^*_{1+}E_{1+}\,, \quad (1)
\end{aligned}
$$

$$
P_y \sim R^n_{LT} = -\text{Im}\{\cdots\}\,. \tag{2}
$$

The $L^*_{0+}E_{0+}$ interference is relatively large and prominent in all kinematics. The combinations $L^*_{1-}(-E_{0+} + 3E_{1+})$ and $(-4L^*_{1+} - L^*_{1-})M_{1-}$ involving $M_{1-}$ and/or $L_{1-}$ are either relatively small or cancel substantially. The terms largest in magnitude and sensitivity are the $L^*_{0+}M_{1-}$ and the $L^*_{1-}M_{1+}$ each involving one of the relevant Roper multipoles linearly. The contributions of the $M_{1-}$ and $S_{1-}$ multipoles to $P'_x$ and $P_y$ depend strongly on $Q^2$ and $W$, so a measurement of $P'_x$ and $P_y$ in a broad range of $Q^2$ and $W$ would allow us to quantify these dependencies.

We are considering performing two $W$-scans at fixed momentum transfers of $Q^2$ of 0.13 and $0.33\,(\text{GeV/c})^2$ to explore the behaviour on and away from

the resonance position, and a more extensive $Q^2$-scan at the resonance position $W = 1440\,\text{MeV}$, with two overlapping settings. The $W$-scans could be performed at relatively small $Q^2$ because the predicted asymmetries and their sensitivities to the relevant multipoles appear to be largest there. Two beam energies (2 and 3 GeV) could be used. The lower beam energy is needed in order to accommodate the low-$Q^2$ end of the $Q^2$-scan (and the corresponding $W$-scan) without running into the geometrical limits of the HRS spectrometers in Hall A. The proposed kinematics coverage is illustrated in Fig. 2.
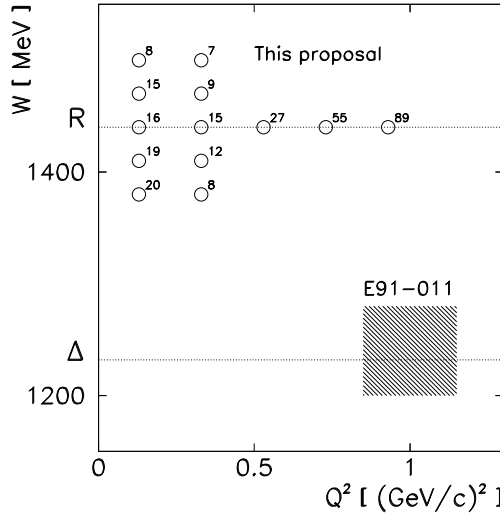


**Fig. 2.** The kinematic coverage in $W$ and $Q^2$ of the E91–011 experiment in Hall A (hatched area) and of the present proposal.

The sensitivity of $P_y$ to the resonant Roper multipoles $M_{1-}$ (proportional to the helicity coupling $A^p_{1/2}$) and $S_{1-}$ (proportional to $S^p_{1/2}$) is different at low and high $Q^2$, and varies through the $W$-range. At $Q^2 = 0.13\,(\text{GeV/c})^2$ (Fig. 3 left), the full prediction for $P_y$ at the resonance position is almost $+100\,\%$, with comparable $M_{1-}$ and $S_{1-}$ contributions, while it is close to zero with the Roper switched off. At $Q^2 = 0.33\,(\text{GeV/c})^2$, $P_y$ drops to about $+40\,\%$ (Fig. 3 right), dropping to about $-40\,\%$ with the Roper switched off, with different roles of $M_{1-}$ and $S_{1-}$. At high $Q^2 = 0.73\,(\text{GeV/c})^2$ and above (not shown), the full $P_y$ is about $-50\,\%$, and only $S_{1-}$ plays an appreciable role.

The role of the resonant multipoles changes very quickly, resulting in dramatic changes in the polarization components on a relatively narrow range in $W$ (about $\pm 60\,\text{MeV}$ away from the resonance position to each side plus some additional coverage due to extended acceptance). The $P_y$ being so large (on the order of several tens of %), a measurement in a broad range of $Q^2$ and $W$ would therefore enable us to study its dependencies quite precisely.

The $W$-dependencies of both $P'_x$ and $P'_z$ become washed out at high $Q^2$. However, the large asymmetries persist in $P_y$ and, to some extent, also in the $P'_x$. A

measurement of the $Q^2$-dependence of $P_y$ and $P'_x$ (see Fig. 4) therefore gives us yet another handle to quantify the role of the individual multipoles, and can be mapped onto the zero-crossing of the $A^P_{1/2}$ helicity amplitude.
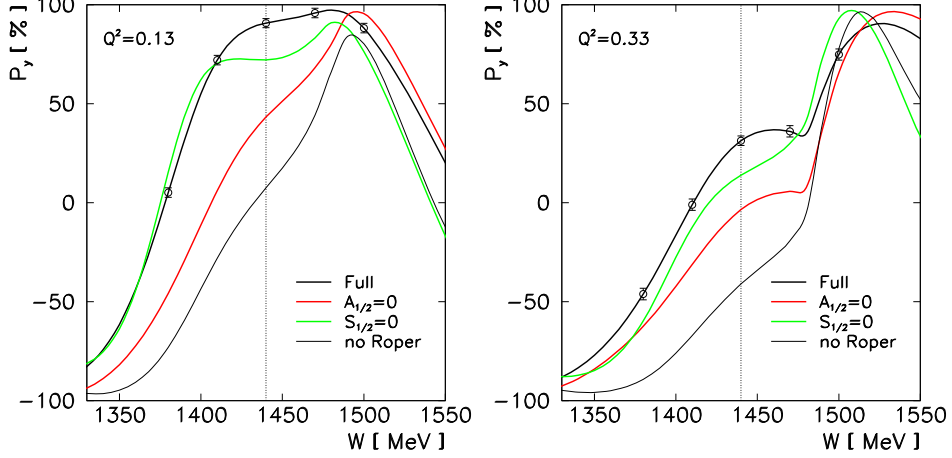


**Fig. 3.** Sensitivity of $P_y$ to the resonant Roper multipoles $M_{1-}$ (helicity amplitude $A^P_{1/2}$) and $S_{1-}$ ($S^P_{1/2}$), as a function of $W$ at $Q^2 = 0.13$ and $0.33\,(\mathrm{GeV}/c)^2$. The expected statistical uncertainties of the proposed measurement are also shown.
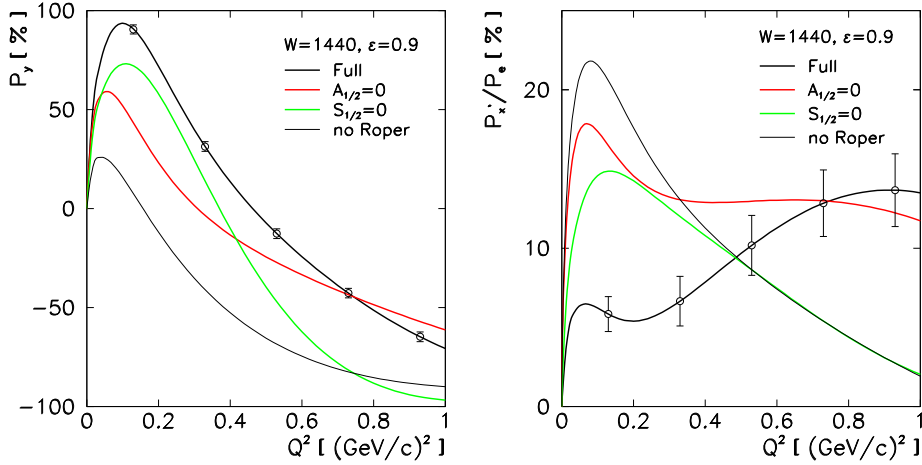


**Fig. 4.** Sensitivity of the normal (induced) recoil polarization component $P_y$ and of the in-plane component $P'_x/P_e$ to the resonant Roper multipoles $M_{1-}$ and $S_{1-}$, as a function of $Q^2$ at $W = 1440\,\mathrm{MeV}$.

# References

1. L. D. Roper, Phys. Rev. Lett. **12** (1964) 340.
2. S. Eidelman et al. (Particle Data Group), Phys. Lett. B **592** (2004) 1.
3. O. Gayou, S. Gilad, S. Širca, A. Sarty (co-spokespersons), Jefferson Lab Proposal PR05-010 (2005).
4. K. Joo et al. (CLAS Collaboration), Phys. Rev. C **68** (2003) 032201(R).
5. K. Joo et al. (CLAS Collaboration), Phys. Rev. C **70** (2004) 042201(R).
6. J. J. Kelly et al. (Hall A Collaboration), Phys. Rev. Lett. **95** (2005) 102001.